Technische Universität Wien
Vienna University of Technology

Diplomarbeit

Calculation and Simulation of Q-switched Laser Ignition Sources

Ausgeführt zum Zwecke des Erlangens des akademischen Grades eines Magisters der Naturwissenschaften (Mag.rer.nat.)

unter der Leitung von

A. o. Univ. Prof. Dr. phil. Ernst Wintner
Institut für Photonik

mit Unterstützung von

Dipl.–Ing. Hannes Tauer
Dipl.–Ing. Heinrich Kofler
Institut für Photonik

Durchgeführt am
Institut für Photonik der Technischen Universität Wien

Eingereicht an der Technischen Universität Wien
Fakultät für Mathematik

von

Franz Trawniczek
Matr. Nr. 0025808
Wolfsgraben 35
3400 Klosterneuburg

Wien, im August 2009

Man darf nicht das, was uns unwahrscheinlich und unnatürlich erscheint, mit dem verwechseln, was absolut unmöglich ist.
Carl Friedrich Gauß.

Acknowledgments

First of all, I would like to thank my supervisor Prof. Ernst Wintner for his great support during the whole time I spent at the Photonics Institute. He enabled me to write my diploma thesis in his research group and over the months I became part of it. His broad knowledge in laser physics and mathematics helped me very often to solve all the problems during the calculation and simulation process. Furthermore we had some very interesting discussions about the whole laser ignition project and also about some other topics besides the diploma thesis.

I am very thankful to Hannes Tauer who introduced me into the laser ignition project and the basics of laser physics. His consolidated knowledge about the field of laser ignition was very important for me over the whole time I spent there. He always had an open ear for all kinds of problems and although he had a lot of work he had enough time to listen to the specific problems. We know each other since our childhood and I am happy that we met at the university again. Besides the topics regarding our work for the thesis we always had a lot of fun together also on the tennis court.

I would like to express my thanks to Heinrich Kofler for all the time we spent together at the pc and during lunch. He has always given me a great deal of advice concerning some programs and for visualisation. He was a great supporter for my arrangements regarding the junior scientist conference 2008.

I am very thankful to Prof. Margarita Deneva who introduced me into the whole simulation process. She explained some of the calculations included in this thesis to me to establish understanding.

I am also grateful to the company GE Jenbacher for its financial support of the whole laser ignition project and my work.

Special thanks are attributed to Prof. Georg Reider, head of the Photonics Institute, for some discussions, support and the agreeable research atmosphere.

I am also thankful to Elisabeth Schwarz, Balthasar Fischer and Ingo Muri for the inspireable atmosphere in the office and the interesting discussions we had about many topics besides the diploma thesis.

I would like to thank Prof. Hellmuth STACHEL, Institute of Discrete Mathematics and Geometry, head of the research group Differential Geometry and Geometric Structures, for the most interesting lectures I attended during my studies at the Vienna University of Technology. I look up to his very high knowledge about the whole field of mathematics, geometry, higher geometry and its applications. He has always been a fair examiner and combined highest knowledge and humor.

I am also grateful to Herbert GAMMEL who has been a very good friend of our family for decades. His suggestions were always very adjuvant for several kinds of problems and decisions in the past. Especially since my father died he became more and more important for me.

I would also thank my mother Eva TRAWNICZEK for her support during my whole life and escpecially during my studies at the Vienna University of Technology. Her mental and financial support were a great help over the last years. She always has an open ear for any kind of problem and she mostly finds a possible solution for the different difficulties.

Last but not least I want to thank my late father Fritz TRAWNICZEK for all the great moments we had together. We always spent a lot of time together and shared the same interests like sports and carambol billard, which we always played together. As a consequence of a tragic incident at the beginning of my studies he died and so it is not possible to share my experiences and successes with him any longer. I will never forget him.

THANK YOU ALL!

Danksagung

Zu Beginn möchte ich mich bei meinem Betreuungsprofessor dieser Diplomarbeit, Prof. Ernst WINTNER bedanken. Er hat mich während meiner Zeit am Institut für Photonik immer ausgezeichnet unterstützt und beraten. Er hat mir ermöglicht diese Arbeit zu verfassen und in seiner Forschungsgruppe mitzuarbeiten. Sein großes Wissen in den Bereichen der Laserphysik und der Mathematik waren für die auftretenden Probleme während dieser Arbeit eine große Hilfe. Wir hatten einige sehr interessante und lehrreiche Diskussionen sowohl über das Projekt der Laserzündung als auch über diverse Themen außerhalb des universitären Alltages.

Mein Dank gebührt auch Hannes TAUER, der mich in das gesamte Projekt der Laserzündung und in das Basiswissen der Laserphysik eingeführt hat. Sein tiefes Wissen über das gesamte Gebiet des Projekts war für den Arbeitsprozess unerlässlich. Er hatte trotz seiner vielen Arbeit immer ein offenes Ohr, wenn Probleme auftraten - ungeachtet ob es um die Arbeit oder andere Dinge ging. Wir kennen uns schon seit unserer Kindheit und ich bin sehr froh darüber, dass wir uns nun an der Universität wieder getroffen haben. Wir haben im letzten Jahr viel Zeit gemeinsam verbracht und oft gemeinsam gelacht, sowohl am Institut als auch am Tennisplatz.

Des weiteren möchte ich mich bei Heinrich KOFLER für all die gemeinsam verbrachte Zeit am PC und während der vielen Mittagspausen bedanken. Er stand immer mit Rat und Tat zur Seite, wenn es um diverse Programme und graphische Umsetzungen ging. Er war mir darüber hinaus eine große Hilfe hinsichtlich meiner Vorbereitungen für die Junior Scientist Conference 2008 an der Technischen Universität Wien.

Mein Dank gilt auch Prof. Margarita DENEVA, sie hat mich in den gesamten Simulationsprozess eingewiesen. Sie hat mir einige Abläufe, welche bei der Berechnung des Lasersystems auftraten ausführlich erklärt, um mein Verständnis dafür zu fördern.

Anschließend möchte ich mich bei GE JENBACHER für die finanzielle Unterstützung des gesamten Projekts der Laserzündung und meiner Arbeit bedanken.

Weiters bedanke ich mich bei Prof. Georg REIDER, Leiter des Instituts für Photonik für manch interessante Diskussion, seine Unterstützung und das angenehme Arbeitsklima innerhalb der Forschungsgruppe.

Mein Dank gilt auch Elisabeth SCHWARZ, Balthasar FISCHER und Ingo MURI für das angenehme Arbeitsklima im gemeinsamen Büro und die vielen interessanten Diskussionen über ganz unterschiedliche Themen und Bereiche des Lebens.

Ich möchte mich auch besonders bei Prof. Hellmuth Stachel vom Institut für Diskrete Mathematik und Geometrie, Leiter der Forschungsgruppe Differentialgeometrie und Geometrische Strukturen für die interessantesten und vielfältigsten Vorlesungen, die ich während meiner Studienzeit an der Technischen Universität Wien besucht habe, bedanken. Ich bewundere sein umfassendes Wissen in den Bereichen Mathematik, Geometrie, höhere Geometrie und ihre Anwendungen. Er war über all die Jahre immer ein fairer und umgänglicher Prüfer und vereinte stets allerhöchstes Wissen mit Humor.

Ich bedanke mich auch bei Herbert Gammel, der seit Jahrzehnten ein sehr guter und treuer Freund unserer Familie ist. Seine Ratschläge zu den unterschiedlichsten Problemen und Entscheidungen waren immer sehr konstruktiv und hilfreich. Speziell seit dem Tod meines Vaters ist er eine sehr wichtige Bezugsperson für mich geworden.

Ich möchte mich auch bei meiner Mutter Eva Trawniczek für ihre Unterstützung über all die Jahre bedanken. Ihre geistige und finanzielle Unterstützung waren immer eine große Stütze in den letzten Jahren. Sie hat immer Zeit wenn Probleme auftreten und findet meist einen guten Weg aus den jeweiligen Schwierigkeiten.

Abschließend möchte ich mich noch bei meinem Vater Fritz Trawniczek für alle tollen gemeinsamen Momente bedanken. Wir haben immer viel Zeit gemeinsam verbracht und teilten sehr viele Interessen, beispielsweise für den Sport im allgemeinen und für Carambol Billard im speziellen. Dieses Spiel hat er mir beigebracht und wir verbrachten dabei viele schöne Stunden. Als Konsequenz eines tragischen Vorfalls zu Beginn meiner Studienzeit verstarb er leider und dadurch ist es mir nicht mehr möglich meine Erfahrungen mit ihm zu teilen. Ich werde ihn stets in bester Erinnerung behalten.

Danke an alle!

Abstract

The scope of this diploma thesis comprises the calculation and simulation of a Q-switched solid-state laser ignition source. This work is part of the development project of an ignition laser which should replace the conventional spark plug in internal combustion engines. The demand for higher efficient and low emission engines for the production of electrical energy increased rapidly due to several environmental aspects. The most important benefit of the new alternative ignition system is the potential for ignition of very lean mixtures which results in lower emissions of nitrous oxides (NO_x) and an increase in efficiency.

A lack of adequate light sources for laser ignition on the market lead to the specific development of an ignition laser whithin our research group which should have a simple and robust configuration, furthermore this system also has to be cheap. Experiments showed, that Nd:YAG (Neodymium-doped Yttrium Aluminium Garnet) is the most promising candidate as a proven solid-state laser material.

The main topic of this diploma thesis is the analysis and the simulation of such a Q-switched laser system. The calculations including all relevant parameters are based on the rate equations for a four-level laser system. The approximation of the pump function, the analysis of the Q-modulator and the detailed overview of one single roundtrip in the laser system are indispensable to obtain all important values of the laser system.

The first step is the simulation of an active Q-switched laser system because there exists a well established theory. The optimum performance of the high peak power Q-switched ignition laser is obtained by the adaption of several important parameters (reflectivities of the two used mirrors, best time for opening of the Q-modulator, transmissions before and after opening of the Q-modulator). The exact analysis of the system of rate equations and the four-level laser system in combination with the parameters of the used active medium Nd:YAG (Neodymium-doped Yttrium Aluminium Garnet) are the background for understanding the laser system. The approximation of the actual pump function as a trapezoid function is essential for obtaining significant results. Applying a code, written in Borland PASCAL, the main behaviour of the laser ignition system is simulated to find the conditions for optimal performance of the high peak power laser and to conform to the needed requirements (one single pulse with high peak power (MW) and a very short duration ($\approx$ 1 ns)).

Kurzfassung

Das Ziel dieser Diplomarbeit ist die Berechung und Simulation eines gütegeschalteten Festkörperlasersystems. Die gesamte Arbeit ist ein Teil der Entwicklung eines alternativen Zündkonzepts für Verbrennungsmotoren. Ziel dieses Konzepts ist die Entwicklung eines Zündlasers, welcher die konventionelle Zündkerze im Verbrennungsmotor ersetzen soll. Im Lauf der letzten Jahre stieg das Interesse an emissionsreduzierten und gleichzeitig effizienteren Motoren für die Produktion von elektrischer Energie infolge ökologischer Aspekte und Überlegungen stark an.

Die Laserzündkerze bringt einige entscheidende Vorteile im Vergleich zur bewährten konventionellen Zündkerze mit sich. Der Funke, der in diesem System das Gas/Luftgemisch zündet ist ein Plasma, welches durch einen kurzen Laserpuls erzeugt wird.

Der dominierendste Vorteil des Zündlasers ist die Möglichkeit äußert magere Gemische zu zünden, was als direkte Konsequenz eine Reduktion der Stickoxide (NO_x) bei gleichzeitigem Anstieg des Wirkungsgrades nach sich zieht. Da am Markt kein adäquates Produkt existierte, war die Eigenentwicklung einer Laserzündkerze notwendig für die Realisierung des neuen Zündkonzepts.

Der Aufbau des Lasers soll einfach, robust und preiswert sein. Nd:YAG (Neodymdotierter Yttrium Aluminium Granat) stellte sich in einer Versuchreihe als das vorteilhafteste Lasermedium heraus.

Diese Diplomarbeit beschäftigt sich mit der Berechnung und der Simulation eines solchen Festkörperlasersystems. Die Berechnungen inklusive aller relevanten Parameter basieren auf den Ratengleichungen eines Vier-Niveau Lasersystems. Die Approximation der Pumpfunktion, die Modellierung des Güteschalters und die detaillierte Analyse eines einzelnen Durchlaufs im Lasersystem sind die Grundlagen um alle erforderlichen Parameter zu erhalten.

Der erste Schritt ist die Simulation eines Systems mit einem aktiven Güteschalter, da hierfür eine fundierte Theorie existiert. Die optimale Konfiguration des gütegeschalteten Festkörperlasersystems kann durch Variation der einzelnen entscheidenden Parameter (Reflektivität der verbauten Spiegel, idealer Zeitpunkt zum Öffnen des Güteschalters, geeignete Anfangs- und Endtransmission) gefunden werden. Die exakte Analyse des Systems von Ratengleichungen in einem Vier-Niveau Lasersystems mit Nd:YAG als aktives Medium sind der theoretische Hintergrund für das Verständnis der Simulation.

Die Approximation der Pumpfunktion als Trapez ist ein entscheidender Faktor für relevante Ergebnisse. Unter Anwendung eines Codes, geschrieben in Borland PASCAL, wird das Laserzündsystem simuliert um die optimale Konfiguration zu finden. Die hohen Anforderungen (ein einzelner Laserpuls mit einer Höchstleistung im Megawatt Bereich bei einer Pulsdauer im Nanosekunden Bereich), die für die Zündung erforderlich sind, müssen vom zu entwickelnden Laser erfüllt werden.

Contents

1 Introduction

A reduction of pollutant emissions and of energy consumption can be achieved by the improvement of internal combustion engines. Such machines are in use for more than one century within a wide range of applications like automotive engines in cars, large stationary gas engines and even lawn mowers. Up till now, gasoline engines are ignited by spark plugs which represents the most used technology. They combine the advantages of an highly advanced development level and the possibility of low cost mass production. The advancement of ignition mechanisms and combustion processes are indispensable to improve engine concepts for the future.

The major objective for new types of ignition systems is to provide development perspectives especially regarding the reduction of exhaust emissions and fuel consumption. One way to increase engine efficiency and to simultaneously reduce the emissions is the combustion of leaner fuel/air mixtures under high ignition pressures. Common spark plugs reach their limits for modern gas engines in the MW range attaining highest ignition pressures due to the required high ignition voltages when burning lean mixtures. A possible solution is the innovative concept of laser-induced ignition. The first ideas of laser ignition were developed during the sixties of the last century [1].

The inflammability limits play a decisive role for this development. The ignition of a leaner fuel/air mixture leads to lower temperatures during the combustion and consequently to lower NO_x emission. As a consequence, it is possible to reduce the NO_x output. Furthermore, the fuel efficiency of the combustion process increases due to the ignition of leaner fuel/air mixtures. Following the new alternative way of ignition, the fuel/air mixture is ignited by a tightly focused ns-pulsed laser beam where the focal spot is in the centre of the combustion chamber. The high intensities around the focus region lead to the formation of a plasma and igniting the mixture.

In contrast to the conventional spark plug ignition, laser ignition offers several advantages:

- Free choice of arbitrary positioning of the ignition plasma in the combustion chamber leads to better engine performance.
- No erosion effects like in case of spark plugs. Consequently, singnificanty longer maintenance - free intervals of a laser ignited system are to be expected.
- Possibility to ignite leaner mixtures than by spark plugs.
- No quenching effects due to the absence of spark plug electrodes.
- The maintenance efforts are reduced when applying diode-pumped solid-state lasers.
- Lower NO_x emissions.
- High load/ignition pressures are possible increase in efficiency.
- Lower combustion temperatures.

The requirements on the laser system were also specified during tests on internal combustion engines in cooperation with GE Jenbacher. The main parameters for the required pulse energy for igniting lean mixtures are pressure, temperature and the fuel/air ratio. For gas engines the required pulse energy is in the order of 8-12 mJ. Certain plasma simulations lead to an optimum pulse duration in the region of 10^{-10} and 10^{-9} seconds.

Customary lasers are, due to their overall size and their high initial costs, only applicable for laboratory tests, but they are not able to fulfil the high requirements (like compactness, robustness, favourable cost-performance ratio) for an ignition laser. For that reason, it was necessary to start with the development of a suitable laser system. An appropriate solution is the longitudinally diode-pumped, passively Q-switched, solid-state laser.

The main topic of this work covers is the analysis and simulation of a Q-switched laser system. First, theoretical aspects of basics of laser physics and a Q-switched laser system were studied in order to derive information about the necessary laser parameters to be chosen. The experimental realisation of the laser system is based on a Nd:YAG (Neodymium-doped Yttrium Aluminium Garnet) gain medium. Afterwards, the calculation and simulation of a Q-switched laser system is presented.

Initially, it is necessary to determine the adequate system of rate equations to analytically describe the whole laser system.

$$\frac{dN_2}{dt} = R_p(t) - BqN_2 - \frac{N_2}{\tau} \tag{1.1}$$

$$\frac{dq}{dt} = BqN_2V_a - \frac{q}{\tau_c} \tag{1.2}$$

where $R_p(t)$ represents the pump function, q is the number of photons, N_2 represents the population number of the upper laser level, τ is the lifetime of the upper laser level, V_a is the active volume and B represents a coefficient of proportionality. The approximation of the pump function and the calculation of one single roundtrip through the whole laser system are inevitable to obtain values for the unknown parameters B and τ_c. The analysis of the threshold conditions is the next step to find the value for N_{th}, which is the minimal threshold inverse population to start laser generation. The comparison of the basic behaviour of the laser system with and without a Q-switch are also very important for the simulation.

The simulation approach starts after obtaining all the important and relevant parameters. The code for the simulation, written in Borland PASCAL, enables the simulation of the laser system with or without introduced Q-switch. The first simulations describe the case of free lasing, where no Q-switch is present. These simulations are very helpful to establish better understanding for the whole laser behaviour.

After detailed analysis of this case, an active Q-switch is added to the system to obtain a very short single pulse in the range of a few nanoseconds with extremely high peak power in the range of megawatt. A sensitivity analysis and the optimisation of the actively Q-switched solid-state laser system play an important role in the simulation process. Finally, computational variation of the important parameters leads to the best solution which is one single pulse with a pulse length of ≈ 4 ns and a peak power of ≈ 4 MW under the set of assumed other parameters.

The aim is the simulation of both, the actively and the passively Q-switched laser system. The actively Q-switched laser system is not economically feasible due to mechanical and constructional restrictions. Most of the actively Q-switched systems require high voltage and this can be avoided in the case of passive Q-switching. The simulation of the actively Q-switched laser system, which is presented in this diploma thesis is the first step of the whole simulation process.

The simulation of the passively Q-switched system is very complicated because it is necessary to calculate at least two-dimensionally. The intensity of the light is radially distributed according to a Gaussian profile as illustrated in Figure 3.10 and this is indispensable to incorporate for the simulation of such a laser system. The next step for the future is the calculation and simulation of a passively Q-switched laser system in order to compare the results of the simulation with the experimental conditions of the laboratory.

2 Basics of Laser Ignition

2.1 Principle and advantages of laser ignition

The ignition process converts a combustible mixture of gases from an unreactive state to a reactive state whereby energy is released. During the last century, the ignition process was mainly initiated by electric spark plugs [5]. The electrical spark ignition reaches its physical borders due to different reasons like the demand for very lean mixtures to realise higher efficiencies and the increasing effective ignition pressure within stationary gas engines. A reduction of pollutant emissions and of energy consumption play the most important role in the advancement of internal combustion engines.

Improvements of combustion processes are as necessary as new ignition mechanisms to find satisfying solutions for the future. The shortcomings of both, the ignition and the entire burn process through quenching and cooling effects and, last but not at least, the high electrode wear, especially at high compression ratios, are turning the classical spark plug into a critical status during the technical improvement of combustion engines [6].

It is necessary to find a way out of these problems and one of most promising possibilities is offered by the innovative concept of laser-induced spark ignition.

The main advantages of laser ignition are [5, 9].

- The position of the focus and consequently the kernel of combustion can be chosen freely.
- There are no erosion effects on the laser spark plug electrodes and so the maintenance efforts are reduced when applying solid-state lasers which are preferentially diode-pumped.
- It is possible to ignite even more efficiently at high load and high ignition pressures as opposed to the requirement of even higher ignition voltages in the conventional case.
- The probability to ignite leaner mixtures is higher. As a consequence the flame temperature is lowered and also the NO_x emissions can be reduced, whereas the efficiency of the engine can be increased.

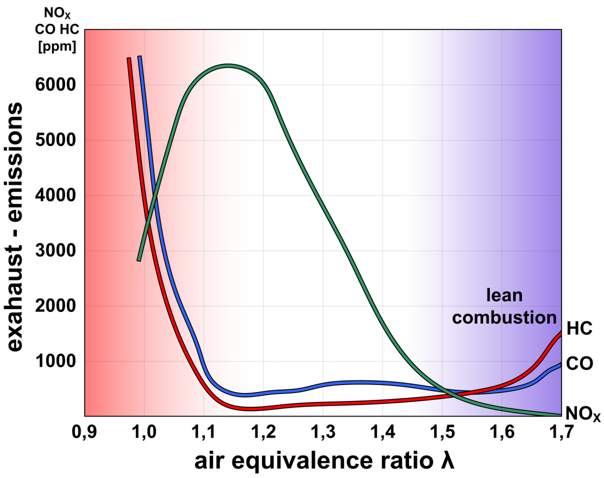

Figure 2.1: *Exhaust emissions from CO, NO_x and hydrocarbons depending on a change of the air-equivalence ratio λ. Figure taken from [11].*

One of the most dominant advantages of laser ignition, the reduction of the NO_x emissions is shown in Figure 2.1. For engines in stationary combined heat and power plants an increase of the thermal efficiency

$$\eta = 1 - \frac{1}{\epsilon^{\kappa-1}} \tag{2.1}$$

where ϵ is the compression ratio and $\kappa = c_p/c_v$ the adiabatic coefficient is preferable. The efficiency can be optimised by high compression ratios and high adiabatic coefficients. The compression ratio ϵ is limited by engine knock and the fuel/air ratio is limited by the flammability limit [10].

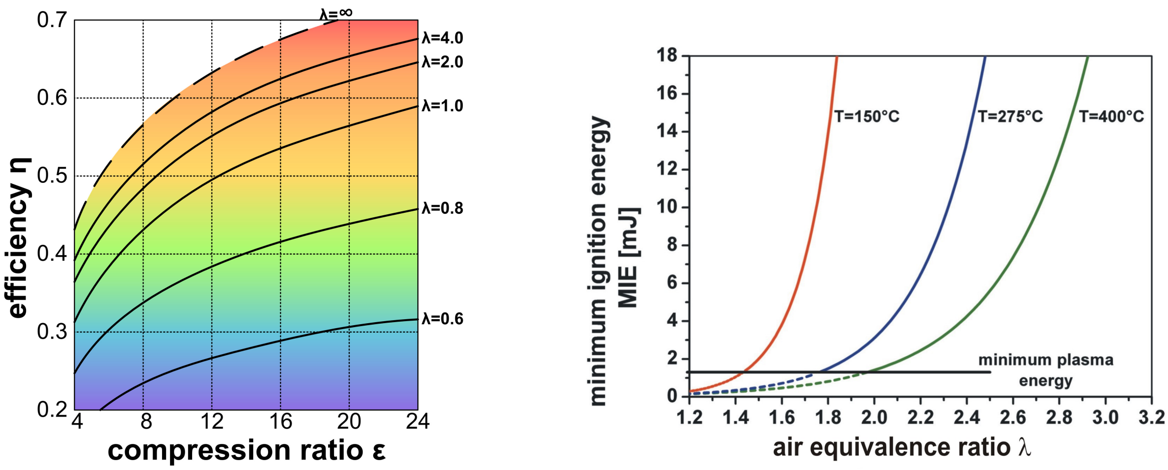

(a) (b)

Figure 2.2: *(a) Interdependence of compression ratio ϵ and efficiency η. Figure taken from [10]. (b) Minimum ignition energies as a function of the fuel/air equivalence ratio λ for different ignition temperatures. Pulse duration τ = 6 ns, beam quality $M^2 \leq 1.4$.*

Figure 2.2 shows the compression ratio ϵ and efficiency η. It is possible to see how it is possible to increase the efficiency. The minimum ignition energies versus fuel/air equivalence ratio λ for several temperatures are also illustrated. The pulse duration τ is $\leq$ 10 ns.

In the concept of laser ignition, the compression ratio ϵ can be enhanced up to the limit (referred to limit of self-ignition) and the fuel mixture can be much leaner due to the absence of electrodes and quenching effects. The combustion temperature is lower and, as a desirable consequence, lowest NO_x emissions are obtained. For gas engine operation with $\lambda = 2$, an effective ignition pressure of 30 bar and a temperature of 275 °C, the minimum pulse energy is about 5.5 mJ [12]. Using laser ignition, the laser beam can be focused in the center of the combustion chamber. This enables the initiation of combustion in the center of the chamber in contrast to conventional ignition where the origin of combustion is near the cooling chamber surface. The flammability limits and the comparison of the ignition probabilities of conventional spark plugs and laser spark plugs are shown in Figure 2.3.

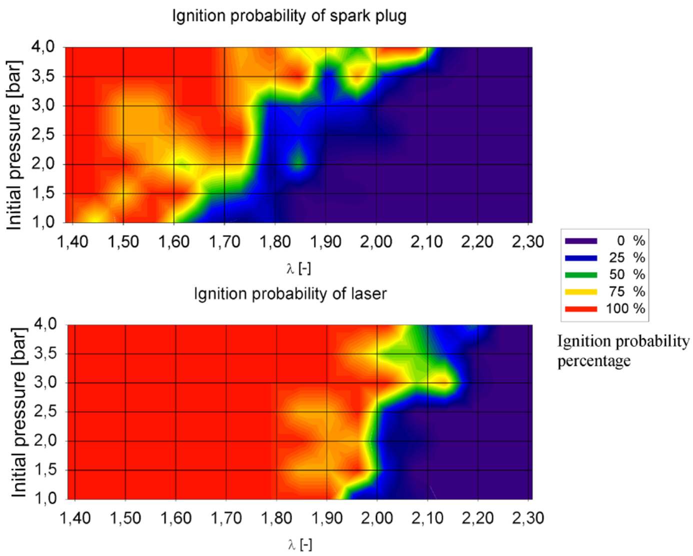

Figure 2.3: *Ignition probabilities of conventional spark plugs and laser spark plugs. Laser ignition provides higher probability for very lean mixtures. Figure taken from [5].*

Large, stationary gas engines for electrical and thermal power generation and automotive engines in cars are the field for the future to benefit from the advantages of the laser ignition concept.

2.2 Requirements on the laser system for ignition

The main requirements and parameters of laser ignition were studied very well in recent investigations [3, 4]. The prototype ignition laser consists of a Q-switched solid-state laser of good beam quality, sufficient energy and short enough pulse duration for reliable plasma generation [5].

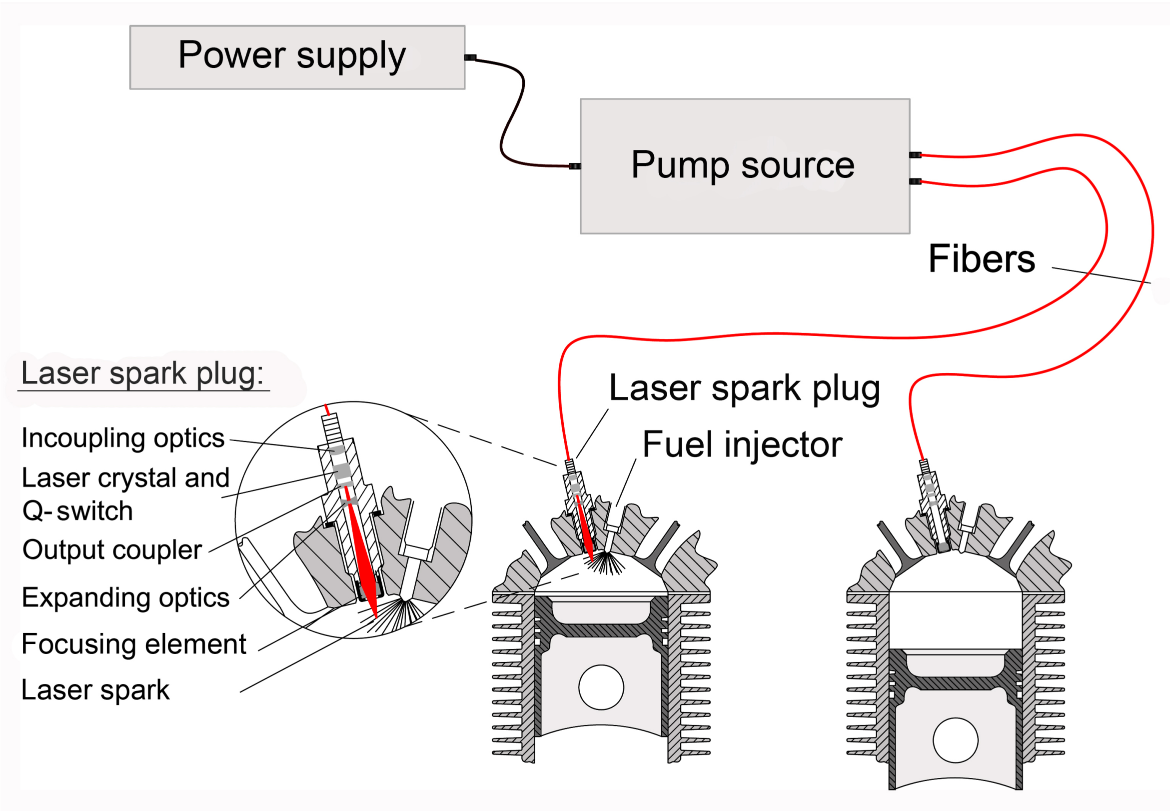

Figure 2.4: *Schematical setup of a laser ignition system. The pump source is not affected by thermal and vibrational distortions of the engine.*

Figure 2.4 shows a schematical setup of a laser ignition system with an external pump source. The main problems of this laser spark plug concept are the lifetime of the pump source, costs and the improvement of the combustion process. The introduction on the market needs to be low-priced to be competitive compared to conventional spark plugs. The search of companies providing compact laser systems which meet demands all the requirements was unsuccessful. Therefore, it was necessary to start a new development of the laser system which was able to fulfill all requirements. This development contains the analysis of all included parameters as well as the development of an ignition laser.

The requirements on a laser system for ignition are enlisted in the following [5, 6]:

- The pulse duration for ignition should be in the ns range.
- The laser system must deliver the required pulse energy of about 8-12 mJ.
- The repetition frequency of the laser system should be variable to ignite the mixture in the combustion chamber over the whole range of operation.
- Reliable ignition performance and a long lifetime for all components in order to extend the maintenance intervals of the laser system and hence the engine.
- The laser pulses have to be triggered with a timing precision in the range of a few μs, according to the speed of the engine.
- Last, but not least, a very important factor are the costs of the laser system. The costs for an ignition system for a large GE Jenbacher gas engine with 20 cylinders are about 10.000 EUR.

3 Fundamentals of Lasers

3.1 Laser as a light source

The word laser is an acronym for Light Amplification by Stimulated Emission of Radiation. The first laser was demonstrated in 1960 by Maiman based on the theoretical work of Basov, Prokhorov and Townes. According to modern physics, light reveals a dual nature, i.e. light has wave and particle properties. 1917 Einstein described for the first time how to treat light as a particle [14]. The energy of a light particle (PHOTON) is

$$E_{\text{photon}} = \hbar\omega \tag{3.1}$$

where $\hbar = h/2\pi$ and h represents the Planck's constant and ω is the angular frequency of the light [5]. The wavelength λ is

$$\lambda = \frac{2\pi c}{\omega} \tag{3.2}$$

where c is the velocity of light in vacuum ($3 \cdot 10^8\ m/s$). The difference in energy between levels which an excited electron transits determines the wavelength of the emitted light [15].

The laser as a light source has some specific properties. This light source is monochromatic (Monochromatic light is light of a single wavelength, of though in practice one can refer to light of very narrow bandwidth) and coherent (Coherence is a property of waves, that enables stationary (i.e. temporally and spatially constant) interference. More generally, coherence describes all correlation properties between physical quantities of a wave) [13].

Light sources can be very different like incandescent light of the sun or from stars or fluorescence light from electronic transitions. If the light is modified by matter on its way, some characteristic parts may be missing being called an absorption spectrum. It is necessary to consider the inner structure of an atom to understand the following processes like absorbtion, spontaneous and stimulated emission as it will be explained later in Figure 3.6. Several electrons circle around the nucleus according to its positive charge. The electrons can reside in electron clouds around the nucleon, so called orbitals. Electrons can only hop between such orbitals thereby gaining or loosing energy which often is exchanged radiatively by photons, the quanta of light [14].

The laser represents a very special light source, because it is rather directed, rather narrow band, rather polarized (polarization of light is described by specifying the direction of the wave's electric field) and rather coherent. The most important property is, that it can be made very intensive which is described best by the quantity brightness. The output power of a laser can reach 100-1000 W in the CW regime (Continuous Wave operation of a laser means that the laser is continuously pumped and continuously emits light) and Megawatt to Terrawatt in the pulse regime(pulsed lasers emit light not in a continuous mode, but rather in the form of optical pulses) [16]. Various physical effects play a role in laser physics, the following subsections give an introduction into the principles of solid-state lasers and the appropriate physics. The books of Köchner [19], Svelto [18] and Reider [17] give a very good overview about this very broad field.

3.2 Key elements of lasers

The operation of a laser requires that electronic excitation energy can be stored in the laser active medium. A laser consists of three main components [6]:

- The active medium which amplifies the oscillating electromagnetic wave.
- The energy source which introduces energy into the active medium to populate selected excited levels and to create population inversion.
- The optical cavity, composed of at least two mirrors in a mostly linear arrangement, which stores part of the induced (= stimulated) emission of laser radiation, concentrated within a few resonator modes.

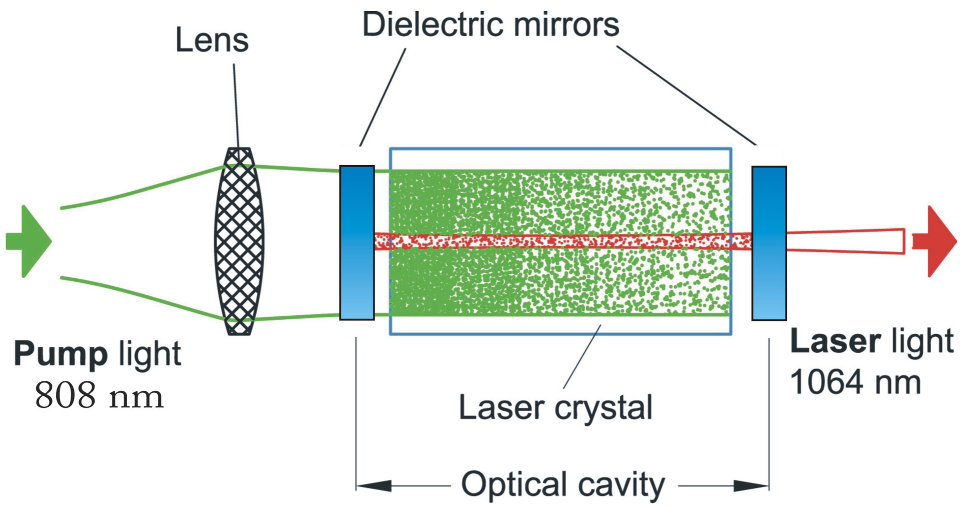

Figure 3.1: *Key elements of a cw laser illustrated for the case of a longitudinally pumped solid-state laser with Nd^{3+}:YAG as laser active medium. The dielectric output mirror possesses a reflectivity smaller than 100 % in contrast to the incoupling mirror which is completely reflective. The photons are amplified due to stimulated emission at each single roundtrip [5].*

Figure 3.1 shows a schematical setup of all important elements that are included in the laser system.

3.2.1 Optical resonators

An optical resonator (optical cavity, laser resonator) is an arrangement of mirrors that forms a standing wave open cavity resonator for light waves. The optical cavity is, besides the gain medium a key element of the laser providing feedback of the laser light. The stationary wave patterns produced are called modes: longitudinal modes and transversal modes. While longitudinal modes of the resonator and the gain medium determine the wavelength of the laser, transversal modes describe the spatial intensity distribution [13].

Different resonator types are distinguished by the focal lengths of the two mirrors and the distance between them. The geometry (resonator type) must be chosen so that the beam remains stable (that the size of the beam does not continually grow with multiple reflections. Resonator types are also designed to meet other criteria such as minimum beam waist or having no focal point (and therefore intense light at that point) inside the cavity.

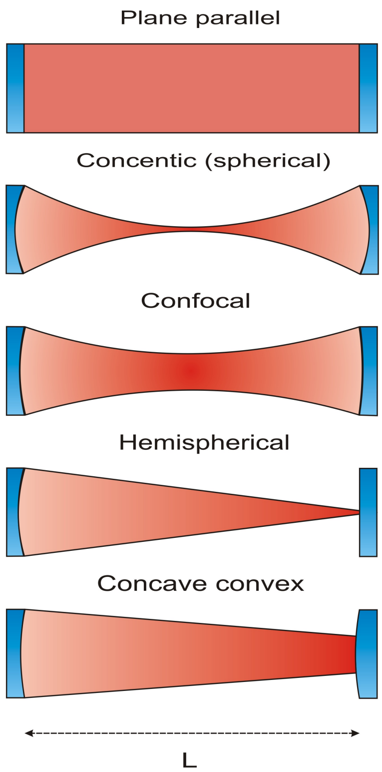

Figure 3.2: *Different types of optical cavities with two mirrors. The mirrors have different curvatures and distances, and hence different radiation patterns inside each typ of resonator.*

The mostly used types of optical resonators are shown in Figure 3.2.

The plane-parallel type is the simplest resonator, but this arrangement is rarely used in large-scale lasers due to the difficulty of alignment; the mirrors must be aligned parallel within a few seconds of arc, or instability of the cavity will be the result. This type is applicable in pulses laser regime due to the finitely many roundtrips a stable resonator is not required.

The concentric (spherical) and the semispherical type produce a diffraction-limited beam waist in the centre of the cavity, with large beam diameters at the mirrors, filling the whole mirror aperture.

The confocal resonator is a common and important design which produces the smallest possible beam diameter at the cavity mirrors for a given cavity length, and is often used in lasers where the purity of the transverse mode pattern is important.

The concave-convex typ consits of one convex mirror with a negative radius of curvature. This design produces no intracavity focus of the beam, and is very useful in very high-power lasers where the intensity of the intracavity light might damage the intracavity medium if brought to a focus [16].

The conditions for development of laser generation are obtained after the analysis of one single roundtrip trough the laser system. The intensity after one single roundtrip is:

$$I_{rt} = I_0 + \Delta I \tag{3.3}$$

I_{rt} is the intensity of light after one roundtrip through the laser system.

$$I(l) = I_0 + e^{gl} \tag{3.4}$$

where $g = \sigma_{21} \cdot \Delta N$ is the amplification of the active medium in the cavity as explained in equation 3.29 and l is the length of the active medium.

$$I(l) = I_0 + e^{-(\alpha+\beta)l} \tag{3.5}$$

where α and β are the coefficients of losses due to absorption and scattering.

$$\underbrace{I_{rt}}_{\substack{Intensity\\ after\\ roundtrip}} = \underbrace{I_0}_{\substack{Initial\\ Intensity}} \underbrace{\left[e^{gl}e^{-\beta l}\right]r_1}_{\substack{First\\ reflection}} \underbrace{\left[e^{gl}e^{-\beta l}\right]r_2}_{\substack{Second\\ reflection}} \tag{3.6}$$

I_0 is the initial intensity and I_{rt} is the intensity after one roundtrip.

$$\Delta I = I_{rt} - I_0 \tag{3.7}$$

ΔI is the intensity increment. The factor $r_1 r_2$ is an additional loss due to non-complete reflection < 1.

$$\Delta I = \left[e^{2l-(g-\beta)} r_1 r_2 - 1\right] I_0 \tag{3.8}$$

$$r_1 r_2 = \exp\left[-ln\left(\frac{1}{r_1 r_2}\right)\right] \tag{3.9}$$

$$\Delta I = \exp\left[2l - (g - \beta) - ln\left(\frac{1}{r_1 r_2}\right)\right] - 1 \tag{3.10}$$

$$\Delta I \geq 0 \tag{3.11}$$

Laser generation is observed when the energy, that is transferred from the active medium to the field in the cavity, exceeds or compensates the losses.

$$\Delta I = 0 \tag{3.12}$$

Equation 3.12 describes the state of threshold of the laser system. In this case,

$$\exp\left[2l - (g - \beta) - ln\left(\frac{1}{r_1 r_2}\right)\right] = 1 \tag{3.13}$$

and the minimal gain coefficient g_{th} is obtained as:

$$g_{th} = \beta + \frac{1}{2l} ln\left(\frac{1}{r_1 r_2}\right) \tag{3.14}$$

In every optical resonator, one of the mirrors is partially transparent and part of the circulating light is emitted to the outside through this mirror as a laser beam. The stability of the optical resonator is also very important in a laser system. In a stable resonator, the wave travels along the cavity axis during the numerous roundtrips in contrast to a non-stable resonator, where the wave experiences increasing declination from the cavity axis at every roundtrip.

In a stable cavity, the electromagnetic field is kept close to the axis for a long time ($10^{-6} - 10^{-7}$ s). Consequently, there are small losses and it is easy to obtain a laser operation, wheras in the other case, at every round trip the rays move away from the axis and after a certain number of round trips they leave the resonator. There are great losses and its only possible to work with high-gain media [16]. The typical feature of every stable cavity is the ability to keep an electromagnetic field with a specific intensity distribution in any cross-section and on the surfaces of the dielectric mirrors at discrete equidistant oscillation frequencies.

It is possible to calculate values for stability of a resonator because only certain ranges of values for r_1, r_2, and L (length of the resonator) produce stable resonators. The two important parameters are g_1 and g_2.

$$g_1 = 1 - \frac{L}{r_1} \tag{3.15}$$

$$g_2 = 1 - \frac{L}{r_2} \tag{3.16}$$

$$0 < g_1 g_2 < 1 \tag{3.17}$$

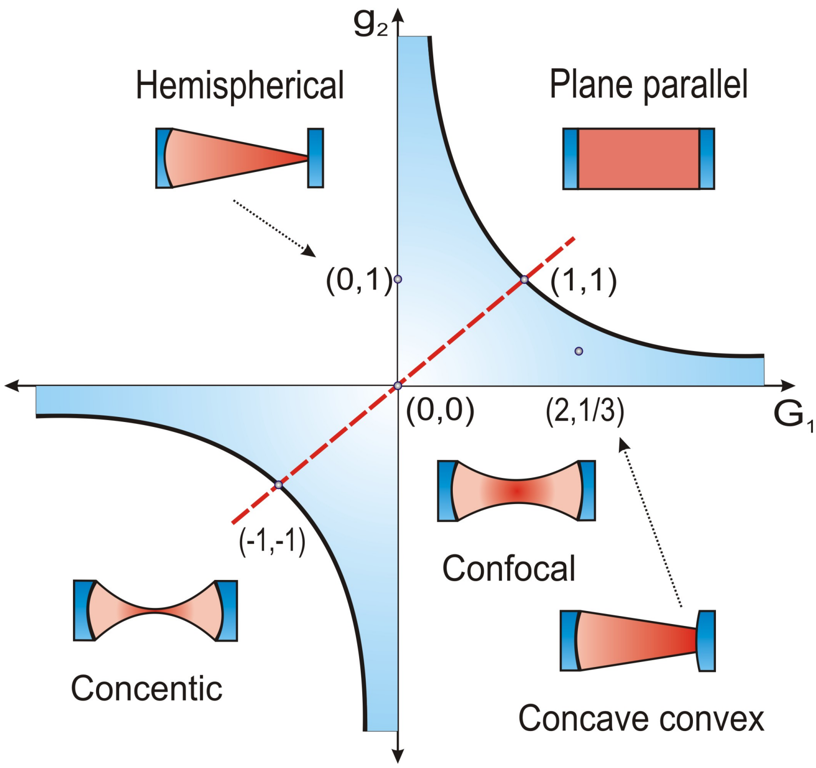

Figure 3.3: *Stability diagram for a two-mirror cavity. Blue-shaded areas correspond to stable configurations.*

Areas bounded by the line $g_1 g_2 = 1$ and the axes are stable as shown in Figure 3.3. Cavities at points exactly on the line are marginally stable; small variations in cavity length can cause the resonator to become unstable, and so lasers using these cavities are in practice often operated just inside the stability line. The Q-factor is also a general cavity parameter.

The Q-factor is a dimensionless parameter that describes the quality of an oscillator. Higher values for the Q-factor indicate a lower rate of energy loss relative to the stored energy of the oscillator.

$$Q = 2\pi \frac{Energy\ stored}{Energy\ dissipated\ per\ cycle} \tag{3.18}$$

Light confined in a resonator is reflected many times from the included mirrors and due to the effects of interference, only specific patterns and frequencies of radiation are able to stay in the cavity constantly. The others are suppressed by destructive interference [29]. Radiation patterns which are reproduced on every single roundtrip through the system are eigenmodes, known as modes of the resonator.

Modes can be divided into two types: longitudinal modes, which differ in frequency from each other and transverse modes, which may differ in both frequency and the intensity pattern of the light.

A longitudinal mode of a cavity is a particular standing wave pattern formed by waves confined in the resonator. They correspond to the wavelengths of the wave which show constructive interference. All other wavelengths are suppressed due to destructive interference. Longitudinal modes have their pattern nodes located axially along the length of the cavity. A common example of longitudinal modes is the light emission produced by a laser. In the simplest case, the laser's optical cavity is formed by two opposed plane (flat) mirrors surrounding the gain medium (a plane-parallel or Fabry-Perot cavity). L is equal to an exact multiple of half wavelength [13].

$$L = q\frac{\lambda}{2} \tag{3.19}$$

where q is an integer known as mode order.

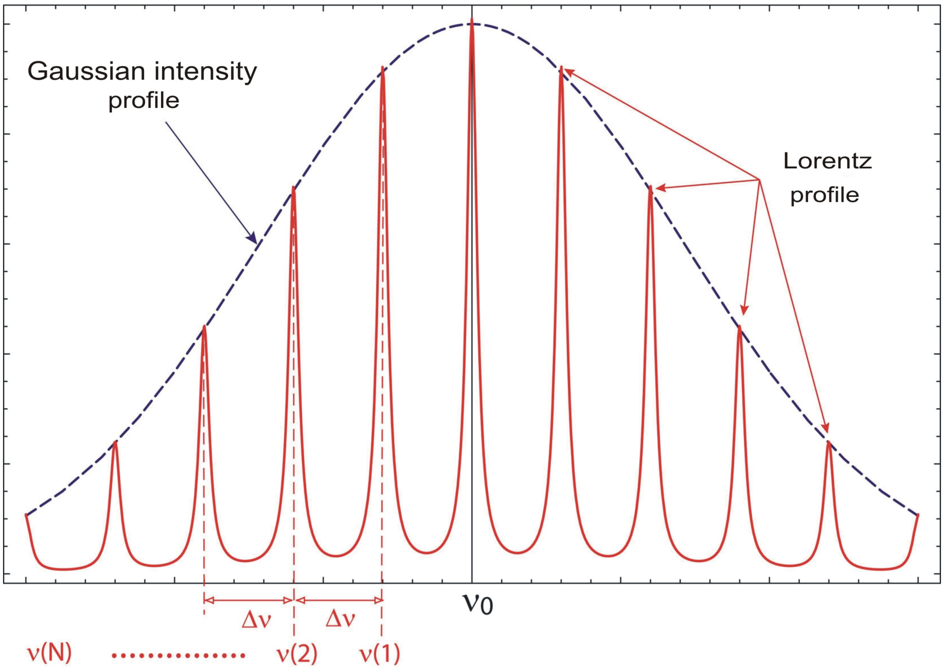

Figure 3.4: *Longitudinal modes in an optical resonator with Gaussian beam.*

Longitudinal modes of a laser system with Gaussian beam are shown in Figure 3.4. The frequency separation between two modes is:

$$\Delta v = \frac{c}{2L} \tag{3.20}$$

A transverse mode of a beam of electromagnetic radiation is a particular elecromagnetic field pattern measured in a plane perpendicular to the propagation direction of the beam. The nodes are located perpendicular to the axis of the cavity. The basic, or fundamental transverse mode of a resonator is a Gaussian beam (Gaussian beam is a beam of electromagnetic radiation whose transverse electric field and intensity distributions are described by Gaussian functions).

Many lasers emit beams with a Gaussian profile, in which case the laser is said to be operating on the fundamental transverse mode, or TEM_{00} mode of the laser's optical resonator.)

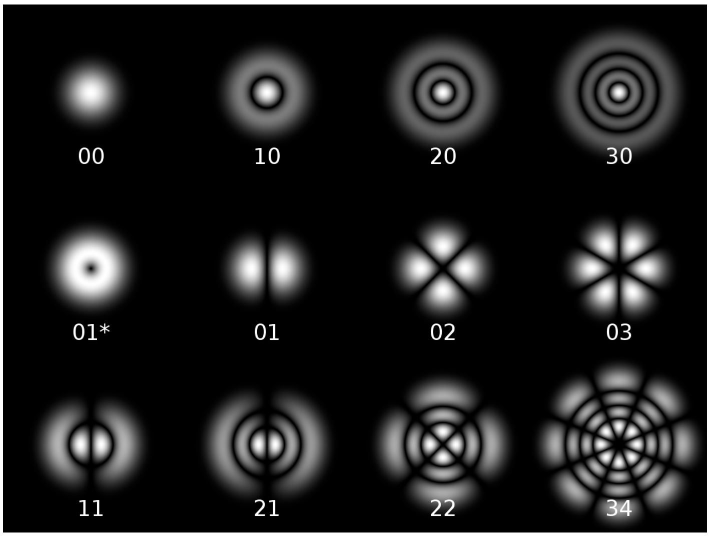

Figure 3.5: *Laguerre-Gaussian transverse mode patterns.*

In a laser with cylindrical symmetry, the transverse mode patterns are described by a combination of a Gaussian beam profile with a Laguerre polynomial. The patterns are illustrated in Figure 3.5.

3.2.2 Laser medium

The active medium or gain medium is the source of optical gain within a laser. In order to lase, the active gain medium must be in a non-thermal energy distribution known as a population inversion. The preparation of this state requires an external energy source and is known as laser pumping. It is necessary to analyse the threefold interaction between light and matter to establish understanding for laser operation:

- Absorption
- Spontaneous emission
- Stimulated emission

These processes are illustrated in Figure 3.6, they are necessary to allow laser operation. In many cases, energy is deployed within the laser medium by the absorption of an optical pump source which might be a flash or arc lamp or, following a much more modern concept, a highly efficient diode laser [14].

Absorption is indicated by the transfer of an electron from the energy level $|1\rangle \rightarrow |2\rangle$. When an electromagnetic wave passes through an atomic system, absorption takes place. The population density of the lower level N_1 will be diminished due to Beer's law [19].

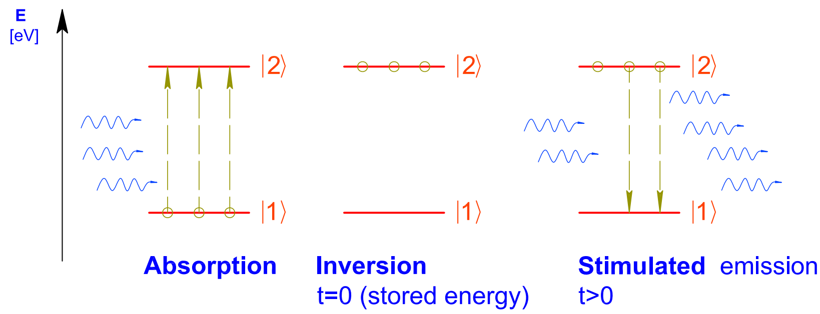

Figure 3.6: *The system absorbs the photons and the electrons are excited to the upper energy level $|2\rangle$. Incident photons activate stimulated emission and therefore, additional photons are emitted [5].*

$$\frac{\partial N_1}{\partial t} = -B_{12}\rho(\omega)N_1 \tag{3.21}$$

where B_{12} is the Einstein coefficient for absorption and $\rho(\omega)$ is the radiation density. There exist three Einstein coefficients: B_{12} is the coefficient of absorption, A_{21} is the coefficient of spontaneous emission and B_{21} is the coefficient of stimulated emission. These coefficients describe the probabilities in a two-level system for atomic interactions.

Spontaneous emission is the result of the typical radiative decay of excited electronic states of atoms. It describes electronic transition from the upper to the lower energy level.

$$\frac{\partial N_2}{\partial t} = -A_{21}N_2 \tag{3.22}$$

The lifetime of the upper laser level can be calculated by solving the equation 3.22. It leads to

$$N_2(t) = N_2(0) \cdot \exp\left[-\frac{t}{\tau_{21}}\right] \tag{3.23}$$

$$\tau_{21} = \frac{1}{A_{21}} \tag{3.24}$$

wheras τ_{21} is the lifetime of the upper level.

Stimulated emission describes the complementary decay mechanism. It is the result if a photon intracts with an atom being in excited state causing the emission of a second identical photon (with respect to direction, frequency, phase and polarisation) [14]. The appropriate rate equation is

$$\frac{\partial N_2}{\partial t} = N_1P_{12} - N_2P_{21} - \frac{N_2}{\tau_{21}} \tag{3.25}$$

whereas P_{12} and P_{21} are the probabilities for absorption and emission. This probabilities are proportional to the Einstein coefficients.

In the state of thermal equilibrium, the number of transitions per unit time from E_2 to E_1 must be equal to the number of transitions from E_1 to E_2. Applying Boltzmann's occupation law and

$$\underbrace{N_2 A_{21}}_{\substack{Spontaneous\\emission}} + \underbrace{N_2 B_{21}\rho(\omega)}_{\substack{Stimulated\\emission}} = \underbrace{N_1 B_{12}\rho(\omega)}_{Absorption} \tag{3.26}$$

lead to the relations [17, 19, 27]

$$\frac{A_{21}}{B_{21}} = \frac{\hbar\omega^3}{\pi^2 c^3} \tag{3.27}$$

$$g_2 B_{21} = g_1 B_{12} \tag{3.28}$$

whereas g_1 and g_2 denotes the degeneracy of the levels E_1 and E_2, respectively. Assuming z as the laser axis, the intensity $I(z)$ of the radiation field in the laser medium is given by

$$\frac{I(z)}{I(0)} = \exp\left[(N_2 - N_1)\sigma z\right] \tag{3.29}$$

In equation 3.29 σ is the cross section. In laser physics, transition cross sections are used to quantify the likelihood of optically induced transition events, for example of absorption or stimulated emission [21]. Since the gain of the medium $(N_2 - N_1) \geq 0$ the signal is amplified [5].

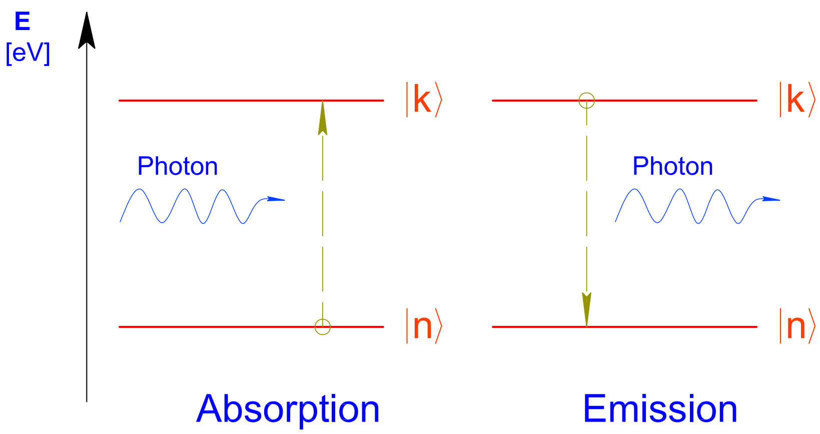

Figure 3.7: *Difference between absorption and emission.*

The schemes of absorption and emission are explained in Figure 3.7. For any two energy levels, only one of the three Einstein coefficients is independent. Once its value is known, the values of all three coefficients are determined as shown in equation 3.28.

A laser gain medium is a medium which can amplify the power of light (typically in the form of a light beam). Such a gain medium is required in a laser to compensate for the resonator losses, and is also called an active medium.

As the gain medium adds energy to the amplified light, it must itself receive some energy through a process called pumping, which may typically involve electrical currents (electrical pumping) or some light inputs (optical pumping), typically at a wavelength which is shorter than the signal wavelength.

There exists a variety of very different gain media, the most common of them are enlisted [21]:

- Certain direct bandgap semiconductors such as GaAs, AlGaAs or InGaAs, they are typically pumped with electrical currents (→ semiconductor lasers).
- Certain laser crystals and glasses such as Nd:YAG (Neodymium-doped Yttrium Aluminium Garnet), Yb:YAG (Ytterbium-doped YAG) or Ti:sapphire, they are used in the form of solid pieces (→ bulk lasers) or optical glass fibers (→ fiber lasers, fiber amplifiers).
- There are ceramic gain media, which are also normally doped with rare earth ions.
- Laser dyes are used in dye lasers, typically in the form of liquid solutions.
- Gas lasers are based on certain gases or gas mixtures, mostly pumped with electrical discharges.
- More exotic gain media are chemical gain media (converting chemical energy to optical energy), nuclear pumped media, and undulators in free electron lasers.

Compared with most crystalline materials, ion-doped glasses usually exhibit much broader amplification bandwiths, allowing for large wavelength tuning ranges and the generation of ultra-short pulses.

3.2.3 Pulse generation

Short or ultra-short optical pulses in principle can be generated by starting with a continuous light source and using a fast external modulator, which lets the light pass only for a short period of time. However, such a method is not efficient, since most of the light will be lost at the modulator, and also the pulse duration is limited by the speed (bandwidth) of the modulator. Pulses with much higher energies and much shorter durations can be generated in pulsed lasers. The most frequently used methods are [21]:

- Q-switching: With this method it is possible to generate energetic pulses with energies of millijoules or more, the pulse duration is typically in the nanosecond range. It is also possible to create even more shorter pulses [22]. A type of variable attenator is put inside the laser's optical resonator. This corresponds to a decrease in the Q-factor of the cavity. A high Q-factor corresponds to low losses per roundtrip and contrawise. The amount of energy stored in the gain medium increases as the medium is pumped. After the stored energy reaches its mamixum level the Q-modulator is switched off to allow feedback and the process

of optical amplification by stimulated emission can start [30].
Q-switching can be subdivided into active and passive Q-switching. In the active case, the Q-switch is an externally controlled variable attenator. The most common modulators are acousto-optical devices or electro-optical devices like Pockels cell or Kerr cell. In the passive case, the Q-switch is a saturable absorber (property of materials where the absorption of light decreases with increasing light intensity). This case is very useful in laser cavities [23, 24]. The possibility to generate such high peak power single pulses with a duration range of several nanoseconds enables the laser systems for applications like the ignition of engines [25, 28].

- Mode locking: In active or passive form it is used for generating ultra-short pulses (with typical durations between 30 fs and 30 ps), having megahertz or gigahertz pulse repetition rates and moderate pulse energies (typically picojoules to nanojoules). Mode locking is a method (or actually a group of methods) to obtain ultra-short pulses from lasers, which are then called mode-locked lasers. Here, the laser resonator contains either an active element (an optical modulator) or a non-linear passive element (a saturable absorber), which causes the formation of an ultra-short pulse circulating in the laser resonator. The pulse duration is much lower: typically between pico- and femtoseconds. For that reason, the peak power of a mode-locked laser can be orders of magnitude higher than the average power.

- Cavity dumping: This can be used for nanosecond pulses, sometimes in combination with Q-switching, but also for ultra-short pulses with mode-locked lasers. Cavity dumping is a technique for pulse generation which can be combined either with Q-switching or with mode-locking, or sometimes even with both techniques at the same time. In any case, the basic idea is to keep the optical losses of the laser resonator as low as possible for some time, so that an intense pulse builds up in the resonator, and then to extract this pulse within about one cavity roundtrip time using a kind of optical switch ('cavity dumper'), such as an acousto optic modulator or a Pockels cell.

- Gain switching: It is a method for pulse generation by quickly modulating the laser gain via the pump power. If a high pump power is suddenly applied to a laser, laser emission sets in only with a certain delay, as it starts with weak fluorescence light, which first needs to be amplified in a number of resonator roundtrips. Therefore, some amount of energy can be stored in the gain medium, which is subsequently extracted in the form of a short pulse. The pulse obtained can be shorter than the pump pulse and also shorter than the upper level lifetime, the dynamics are essentially as in the phenomenon of spiking, where the pump power is applied for a short enough time to generate only a first spike [26].

Q-switching is the most important method for laser ignition and for that reason, this method will be explained in more detail in chapter 4 of this diploma thesis. The calculations and simulations that are presented in this thesis are based on a actively Q-switched solid-state laser system.

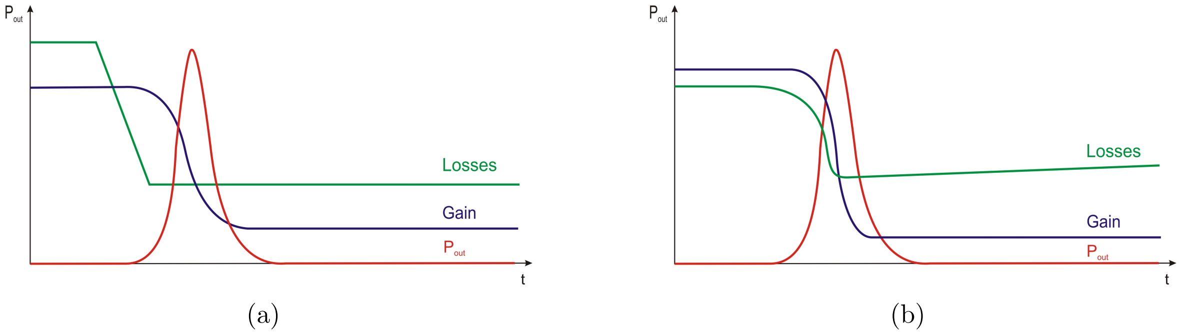

Figure 3.8: *(a) Temporal evolution of gain and losses in an actively Q-switched laser. The Q-switch is activated at $t = 0$. (b) Temporal evolution of gain and losses in a passively Q-switched laser.*

Figure 3.8 explains the temporal evolution of Q-switched laser systems. In the case of active Q switching, the losses are modulated with an active control element. The pulse is formed shortly after the Q-switch is switched off. In the passive case, the losses are automatically modulated with a saturable absorber.

3.2.4 Pump source

Optical pumping some medium essentially means to inject light in order to electronically excite the medium or some of its constituents into other (usually higher-lying) energy levels. In the context of lasers or laser amplifiers, the goal is to achieve a population inversion in the gain medium and thus to obtain optical amplification via stimulated emission for some range of optical frequencies.

The most common optically pumped lasers are doped-insulator solid-state lasers. As the host medium (a laser crystal, glass or piece of ceramic) is electrically insulating, optical pumping is the only way to supply the laser-active ions (e.g. rare earth ions) with energy [21]. A frequently used alternative to optical pumping is electrical pumping, applied particularly to laser diodes and gas lasers. All optically pumped lasers can be divided into two categories:

- Lamp-pumped lasers which have some kind of discharge lamp as the pump source.
- Diode-pumped lasers which are pumped with some kind of laser diodes.

In the case of lamp-pumped lasers, the discharge lamps that are used for laser pumping are grouped in two categories: arc lamps and flash lamps. Arc lamps are optimized for continuous wave operation (cw operation) wheras flash lamps generate pump pulses for free running or Q-switched lasers.

Both types consist of a glass tube, filled with some gas and having a metallic electrode at each end. The laser crystal of a lamp-pumped laser is usually a relatively long side-pumped rod, adapted to the length of the lamp. In many cases, laser rod and lamp are placed within an elliptical pump chamber with reflective walls, so that a large percentage of the generated pump light can be absorbed in the laser rod. Excess heat is removed by cooling water, and an additional filter glass may be used to protect the laser rod from ultraviolet light emitted by the lamp. Concerning the gain medium, the most common type of lamp-pumped laser is the Nd:YAG laser.

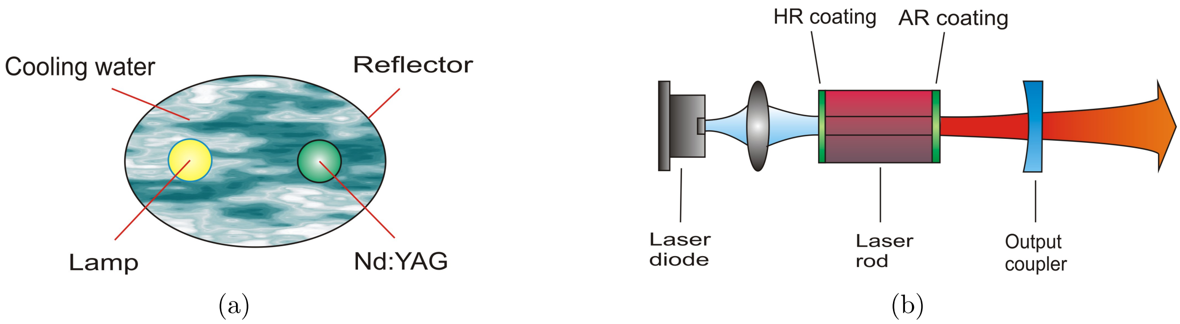

Figure 3.9: *(a) Setup of a lamp-pumped laser rod in a water-cooled elliptical pump chamber with reflective walls. The laser crystal and the lamp are placed in the two focal points of the ellipse. (b) Setup of a typical end-pumped solid-state laser.*

A typical setup of a lamp-pumped laser is shown in Figure 3.9. The elliptical pump chamber with reflective walls is used because in this arrangement a larger percentage of the generated pump light can be absorbed in the laser rod.

The main advantages of lamp-pumping are:

- It is possible to generate very high pump powers (particularly peak powers).
- The costs per watt of the generated pump power are much lower for lamps compared with laser diodes.
- Lamps are fairly robust, nearly immune to voltage or current spikes.

Most diode-pumped lasers are solid-state lasers. There exist different types of laser diodes which can be used for diode pumping. For example broad area laser diodes which are used in solid-state lasers with output powers up to a few watts, high power diode bars which are able to emit tens of watts or up to more than 100 watts or diode stacks which are use for highest powers (multiple kilowatts).

In most cases, the pump diodes are operated continuously. This applies to all continuous wave and mode-locked lasers, and also to many Q-switched lasers. However, quasi-continuous wave operation with higher peak power for limited time intervals ($\approx 100\ \mu s$) is sometimes used for Q-switched lasers with a high pulse energy and low pulse repetition rate [21].

The main advantages of diode-pumping are:

- Very good electrical to optical efficiency of the pump source leads to a high overall power efficiency of the laser. For that reason small power supplies are needed, and both the electricity consumption and the cooling demands are drastically reduced, compared with lamp-pumped lasers.
- Diode-pumped low power lasers can be pumped with diffraction-limited laser diodes. Therefore, it is possible to construct very low power lasers with reasonable power efficiency. In this case only a very small amount of electrical pump power is needed which is very important for battery powered devices.
- Compared to discharge lamps, the lifetime of laser diodes is longer (typically many thousands up to 10.000 hours) but the exchange of laser diodes is much more costly than that of discharge lamps.
- The compactness of the pump source, the power supply and the cooling arrangement makes the whole laser much smaller and easier to use. Diode pumping makes it possible to use a very wide range of solid-state gain media for different wavelength regions. Furthermore, for many solid-state gain media, the lower brightness of discharge lamps would not be sufficient.

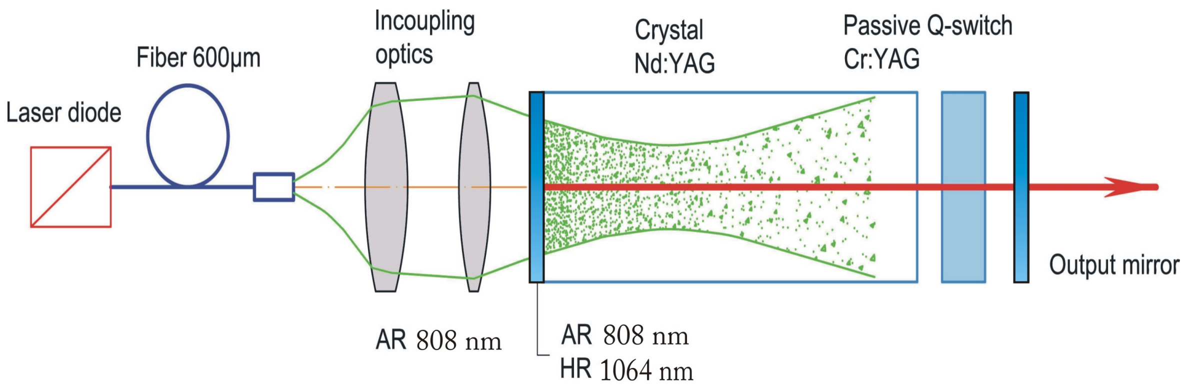

Figure 3.10: *Schematic setup of a diode end-pumped passively Q-switched Nd^{3+}:YAG laser. The incoupling lenses are coated with an anti reflection (AR) coating for 808 nm while the back side of the laser rod is coated by a high reflection (HR) coating for 1064 nm and a AR coating for 808 nm [5].*

The setup of a diode-pumped Q-switched laser is illustrated in Figure 3.10.

3.3 Three- and four-level laser systems

Optical amplification in the gain medium of a laser or laser amplifier arises from stimulated emission. The input light induces transitions of laser active ions from some excited state to a lower level.

In a three-level system, the laser transition terminates at the ground state. A population inversion and consequently net laser gain result only when more than half of the ions (or atoms) are pumped into the upper laser level, the threshold pump power is rather high in this case. Population inversion can be achieved only by pumping into a higher energy level, followed by a rapid radiative or non radiative transfer into the upper laser level, because in this way one avoids stimulated emission caused by the pump wave. The laser transition takes place between the excited laser level and the final ground state which represents the lowest energy level of the system. This leads to low efficiency. An example of a three-level laser medium is ruby (Cr^{3+}:Al_2O_3), as used by Maiman for the first laser. Figure 3.11 shows the different energy level systems.

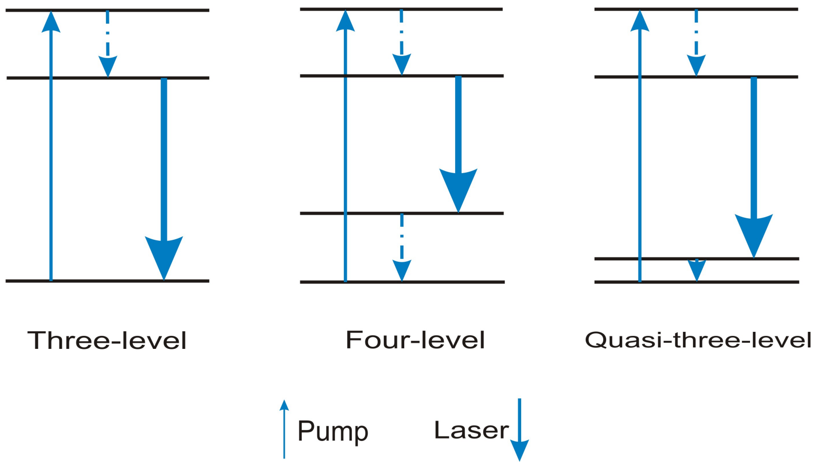

Figure 3.11: *The left figure shows a three-level system, where the laser transition ends on the ground state, the middle figure shows a four-level system, where the laser transition ends on a level above the ground state level and the right picture illustrates a quasi-three-level system, where the lower laser level has some population in the state of thermal equilibrium.*

In the four-level system, the lower laser level is well above the ground state and is quickly depopulated by non-radiative transitios (so called phonons). The pump transition extends again from the ground state to a wide absorption band. The laser transition proceeds in this case to the ground level. This level will be empty. Ideally, no appreciable population density in the lower laser level can occur even during laser operation. The most popular four-level solid-state gain medium is Nd:YAG. All lasers based on Neodymium-doped gain media, except those operated on transitions around $0.9 - 0.95$ μm are four-level lasers. In a four-level system, the threshold pump power is lower.

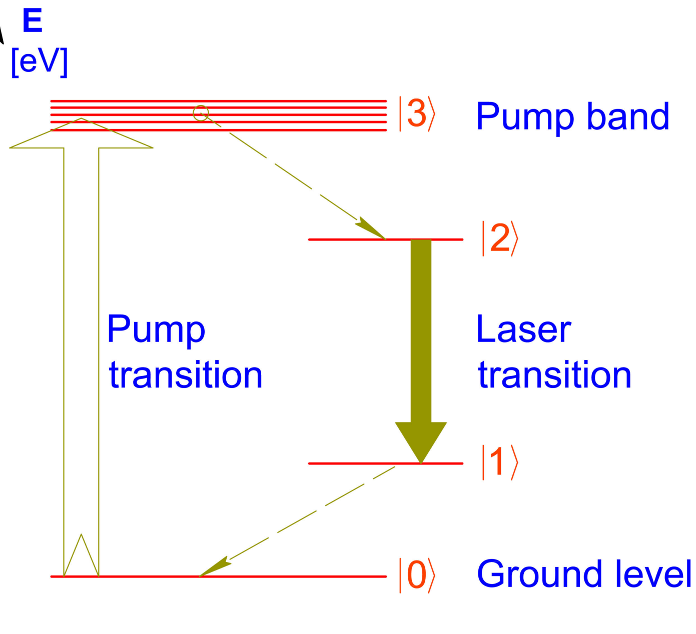

Figure 3.12: *A four-level system which represents the relevant selected energy levels of Nd^{3+}:YAG.*

Figure 3.12 illustrates a four-level laser system more detailed.

In a quasi-three-level system, the lower laser level is so close to the ground state that an appreciable population in that level occurs in thermal equilibrium at the operating temperature. Consequentely, the unpumped gain medium causes some reabsorption loss at the laser wavelength, the transparency is reached only for some finite pump intensity. For higher pump intensities, there is gain, as required for laser operation. Examples of quasi-three-level media are all Ytterbium-doped gain media, Neodymium-doped media operated on the ground state transition (for Nd:YAG 946 nm) and Thulium-doped crystals and glasses [5, 6, 21, 18].

3.4 Main parameters of an ignition laser system

There are several important parameters and requirements on the laser system that are necessary to be fulfilled for ignition concepts. The laser system should deliver pulses with a certain energy and duration and specific repetition rate. A certain configuration of important parameters in the laser system is necessary to fullfil all requirements for ignition.

3.4.1 Selection criteria for laser material and the components of the laser system

A very important compontent of the laser system is the laser medium. After different experimental series, the conclusion was made, that Nd:YAG (Neodymium-doped Yttrium Aluminium Garnet, more precisely Nd^{3+}:YAG) is the best solid-state media for laser ignition. Nd:YAG possesses a combination of advantageous properties for laser operation. YAG is the acronym for Yttrium Aluminium Garnet ($Y_3Al_5O_{12}$), a synthetic crystal material which became popular in the form of laser crystals in the 1960s. Yttrium ions in YAG can be replaced with laser active rare earth ions without strongly affecting the lattice structure, because these ions have a similar size. YAG is a host medium with favorable properties, particularly for high power lasers and Q-switched lasers emitting at 1064 nm. The YAG host is mechanically hard, can be produced with good optical quality, has a high thermal conductivity and is therefore, besides glass, the most used host for Nd-ions.

Nd:YAG is a four-level gain medium, offering substantial laser gain even for moderate excitation levels and pump intensities. The gain bandwidth is relatively small, but this allows for a high gain efficiency and thus low threshold pump power. Nd:YAG lasers can be diode-pumped or lamp-pumped. Lamp-pumping is possible due to the broadband pump absorption mainly in the 800 nm region and the four-level characteristics. The most common Nd:YAG emission wavelength is 1064 nm. When used at the 946 nm transition, Nd:YAG is a quasi-three-level gain medium, requiring significantly higher pump intensities [21, 31]. The pump absorption and the emission lines of Nd:YAG are shown in Figure 3.13.

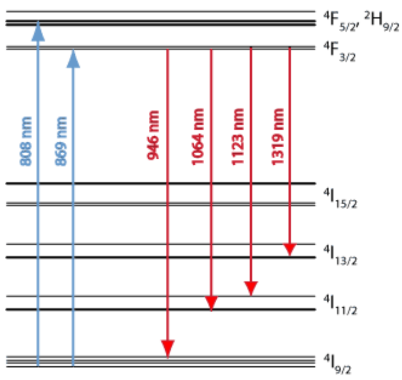

Figure 3.13: *Energy level structure and common pump and laser transitions of the trivalent Neodymium ion in Nd^{3+}:YAG.*

An other important part is the incoupling optics. It consists of either one or two lenses and transfers the pump light into the crystal. Normal lenses with a spherical surface exibit too many lens errors. One way out of this problem is the aspheric lens which eliminats spherical aberrations and reduces other optical aberrations. A complex multi lens system can be substituted by one single aspheric lens which results in a simpler, lighter and cheaper design. The lenses are AR coated (anti-reflection) in order to keep the reflection losses low.

The cavity mirrors are the third essential part of the laser system. A dielectric mirror consists of multiple thin layers of, in general two different transparent optical materials. They are always of dielectric nature in order to reach very high reflectivity. Their limited reflection bandwidth can be employed to allow the transmission of the pump light at a wavelength of 808 nm in the case of Nd^{3+}:YAG through one oscillator mirror designed for 1064 nm [5].

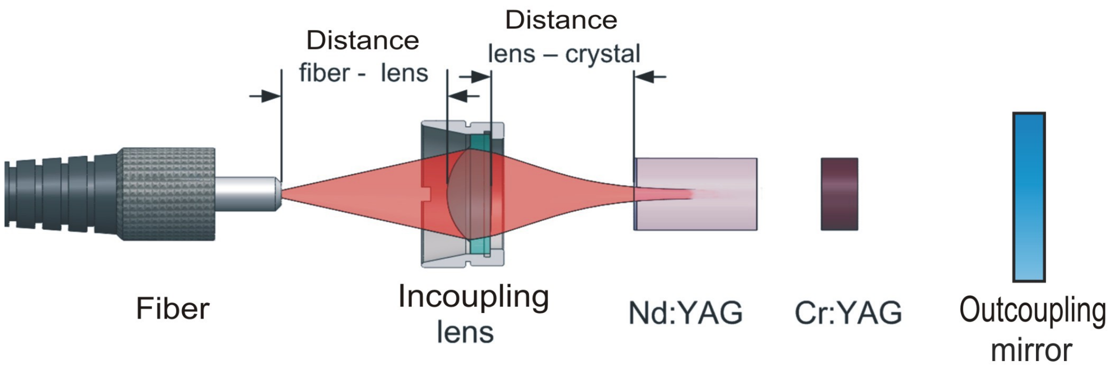

Figure 3.14: *Schematical setup of the laser system including all the main components.*

The main constituents of a laser system including the incoupling optics and the cavity mirrors are depicted in Figure 3.14.

3.4.2 Requirements on the laser system, laser design parameters

The laser system for this ignition concept should deliver single pulses with an energy between 8-12 mJ, a peak power in the range of megawatts and a pulse duration of ≈ 1 ns at a repetition rate of 12.5 Hz (for gas engines running at 1500 rpm). Furthermore, the laser system has to be robust, simple with a small design and low priced. In the laser arrangement there are some variable parameters that can be varied to fulfill all the requirements.

These variables are enlisted:

- Reflectivity R_1 of the output coupler.
- Transmissions of the Q-switch (initial transmission $T_{Qmodclosed}$ and end transmission $T_{Qmodopened}$ in the case of active Q-switching and the initial transmission T_0 in the case of passive Q-switching).
- Pumping energy E_{pump}.
- Starting time for opening the Q-modulator $time_Q$ in the case of active Q-switching.
- Length L of the optical resonator.
- Length l of the active medium.
- Distance U and V between the fiber, incoupling optics and the laser crystal.
- Time for opening the Q-modulator t_{open} in the case of active Q-switching.

One of the most important features of the compact laser system is the price which increases directly proportional to the power of the laser diode. For that reason it is indispensable to keep the input power as low as possible. The reflectivity R_1 and the transmissions of the Q-modulator are mainly accountable for the laser behaviour.

The corresponding output parameters of the compact laser system are:

- Output power P_{out}
- Output energy E_{out}
- Pulse duration $\Delta\tau$

The analysis and the understanding of the temporal combination of the laser pulse, the development of the flame kernel, the pressure pattern, the ignition delay and the plasma emission is the important background to understand all the involved processes. A well established understanding about all these factors is necessary for the development of such a laser system for ignition.

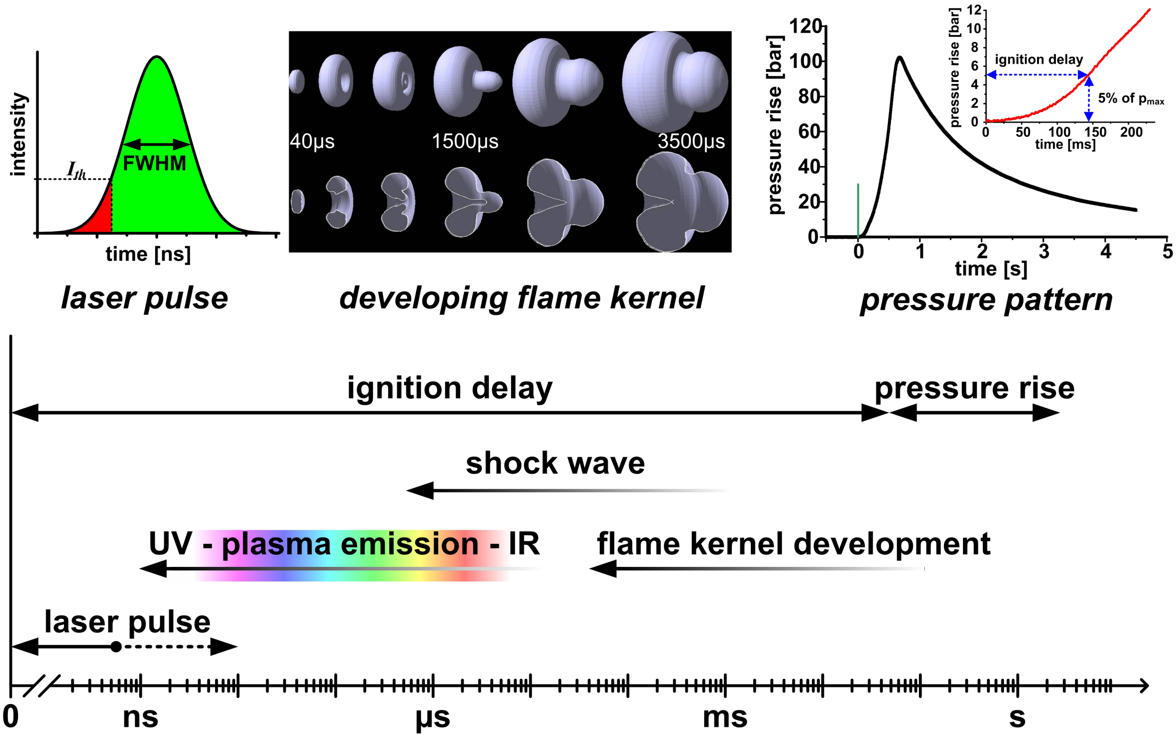

Figure 3.15: *Temporal evolution of different processes initiated by the laser pulse.*

In Figure 3.15 the temporal sequences of the different physical-chemical processes involved after the deployment of the laser pulse are illustrated. The formation of the laser pulse is the first process with a duration in the range of several ns and the following processes with their associated time scales are depicted graphically to establish better understanding which is necessary for the optimisation of the combustion process.

4 Theoretical description of Q-switched Lasers

The scope of the following chapter is to present a detailed theoretical description of Q-switched lasers which includes all necessary calculations like the analysis of one single roundtrip through the laser system, the analysis of the applied rate equations or the calculus of the treshold conditions and the output power. The obtained results are the substructure for the simulation approach which will also be explained in the next section.

4.1 General description of Q-switching

In the case of normal lamp-pumped lasers it is only possible to obtain one powerful pulse in the range of kilowatts and after that first pulse there are many weaker pulses (relaxation oscillations). Later on, the amplification will stay around the threshold level. It is possible to collect all the pulses to one single giant pulse by installing a Q-switch into the laser system. The Q-modulator is an additional device between the two mirrors of the optical resonator which is placed between the active medium and the total reflective mirror. During pumping, the Q-switch adds additional losses besides the normal losses in the resonator. After the population inversion reaches its maximum value, the Q-switch is turned on and consequentely the losses in the cavity fall immediately to the normal level.

In this case, the gain coefficient is very high because there is no feedback before opening of the Q-switch. Installing a Q-modulator corresponds to a decrease in the Q-factor of the cavity. A high Q-factor corresponds to low losses per roundtrip and contrawise. The amount of energy stored in the gain medium increases as the medium is pumped. After the stored energy reaches its mamixum level the Q-modulator is opened to allow feedback and the process of optical amplification by stimulated emission can start [30].

The pulse duration achieved by Q-switching is typically in the nanosecond range (corresponding to several cavity round trips), and usually well above the cavity round-trip time. The energy of the generated pulse is typically higher than the saturation energy of the gain medium and can be in the millijoule range even for small lasers. The peak power can be orders of magnitude higher than the power which is achievable in continuous-wave (cw) operation.

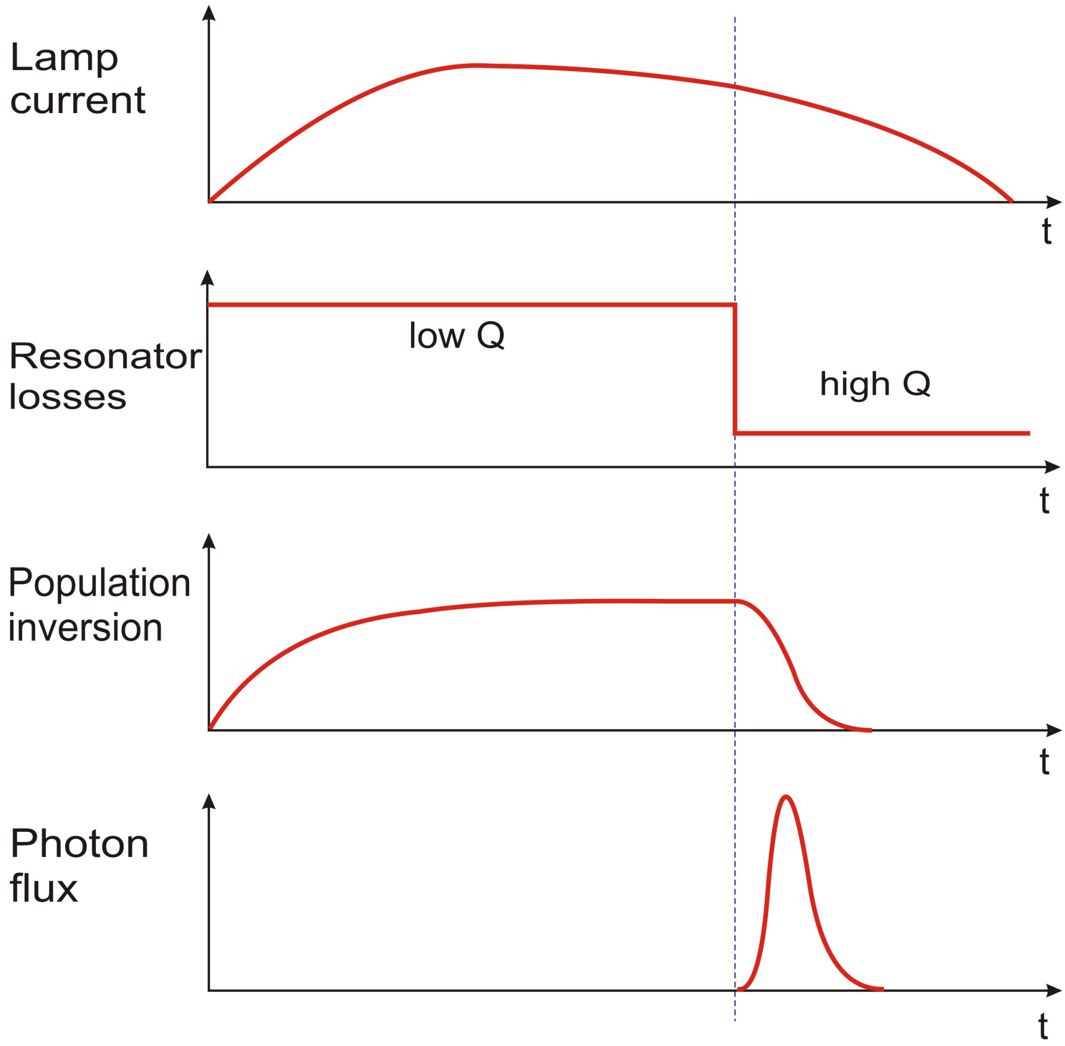

Figure 4.1: *Temporal characteristics of the lamp current, the losses in the resonator, the inversion and the photon flux* Φ *in the case of an actively Q-switched laser.*

Figure 4.1 illustrates the temporal behaviour of a Q-switched laser system. Q-switching can be subdivided into active and passive Q-switching.

In the active case, the Q-switch is an externally controlled variable attenator. The most common modulators are acousto-optical devices or electro-optical devices like Pockels cells or Kerr cells. In this case, it is possible to choose freely the time for opening of the Q-modulator. Practically it is measured, that the best moment for opening is after the population inversion reaches its maximum value. The possible devices in this case can be mechanical devices such as a shutter, a chopper wheel or a spinning mirror. More common are acousto-optical devices or electro-optical devices like a Pockels cells or a Kerr cells because it is possible to open the Q-switch very fast. Mechanical devices allow to form pulse in the range of μs. In order to generate pulses in the range of ns acousto-optical or electro-optical devices are needed. The reduction of the losses is triggered by an external, typically electrical signal. The pulse repetition rate can be controlled externally [16]. The transmission of the Q-modulator is a function of time in this case.

In the passive case, the Q-switch is a saturable absorber (property of materials where the absorption of light decreases with increasing light intensity). This case is very useful in laser cavities because of compactness and the low price of such devices [23, 24]. The key parameters are the wavelength range, its dynamic response and its saturation intensity. The transmission increases when the intensity of the light exceeds some threshold level. The used material may be ion doped crystals like Cr:YAG (Cr^{4+}:YAG) which is a high power, solid-state and compact passive Q-switch, or passive semiconductor devices. Initially, the loss of the absorber is high, but low enough to permit some lasing once a large amount of energy is stored in the gain medium. As the laser power increases, it saturates the absorber and after that, the resonator losses decrease rapidly. Ideally, this brings the absorber into a state with low losses to allow efficient extraction of the stored energy by a laser pulse. After this pulse, the absorber recovers, so that the next pulse is delayed until the energy in the gain medium is fully replenished.

The pulse repetition rate can only be controlled indirectely by varying the pump power in the cavity. The transmission of the Q-modulator is a function of the intensity in this case of passive Q-switching.

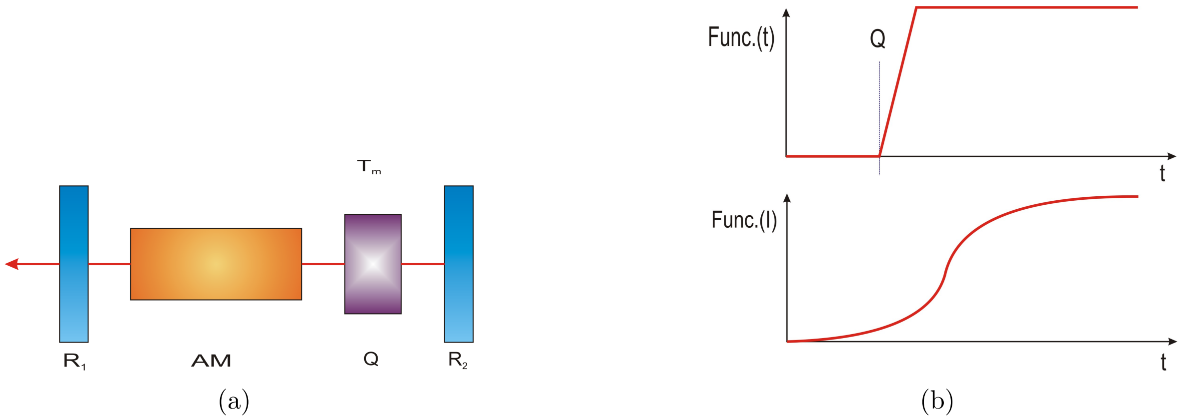

Figure 4.2: *(a) Scheme of a laser system with a Q-modulator in the optical resonator. (b) Transmissions of the Q-modulator in both active and passive Q-switching.*

Figure 4.2 explaines the setup of a Q-switched laser system and the difference of the transmission functions for the case of active and passive switching. The typical Q-switched laser (Nd:YAG laser) with a resonator length of ≈ 10 cm can produce light pulses with a duration in the range of several tens of nanoseconds. Even if the average power is well below 1 W, the peak power can be in the range of many kilowatts. Large scale laser systems are able to generate Q-switched pulses with energies of many joules and a peak power in the area of gigawatts.

Passively Q-switched microchip lasers with very short resonators have generated pulses with durations far below one nanosecond and pulse repetition rates from hundreds of Hertz to several MHz. The possibility to generate such high peak power single pulses with a duration range of several nanoseconds enables the laser systems for the applications of ignition of engines [25, 28, 16].

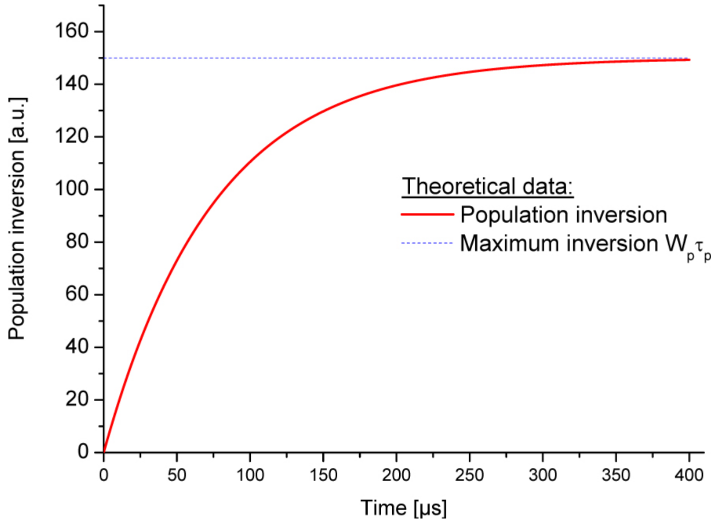

Figure 4.3: *Temporal characteristics of the population inversion after pumping.*

In Figure 4.3 the temporal behaviour of the population inversion is displayed. The best moment for opening of the Q-modulator is after the population inversion has reached its maximum value.

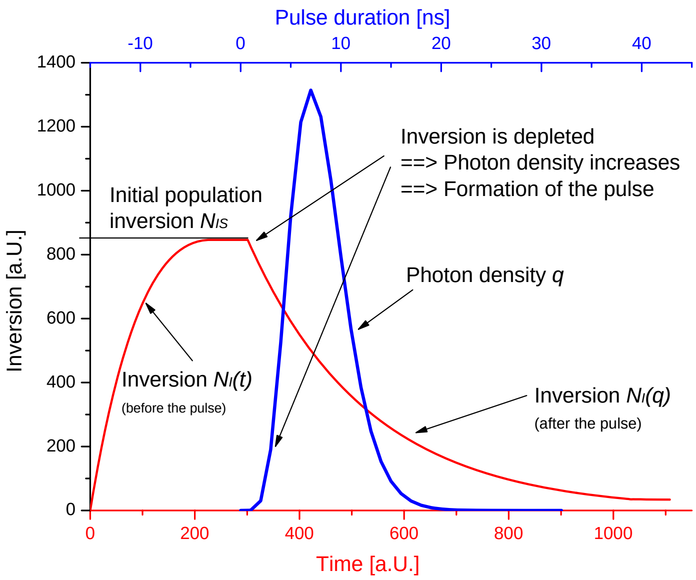

Figure 4.4: *Population inversion coupled with the developed laser pulse.*

In Figure 4.4 the temporal evolution of the population inversion and the generated pulse is described. The generated pulse changes the function of the population inversion rapidly which is explained in this figure. This is very important for a better understanding of the principle of Q-switching.

4.1.1 Rate equations

The first important factor to generate laser operation is to create a population inversion. It is necessary to study the population of the energetic levels in the normal situation to establish better understanding.

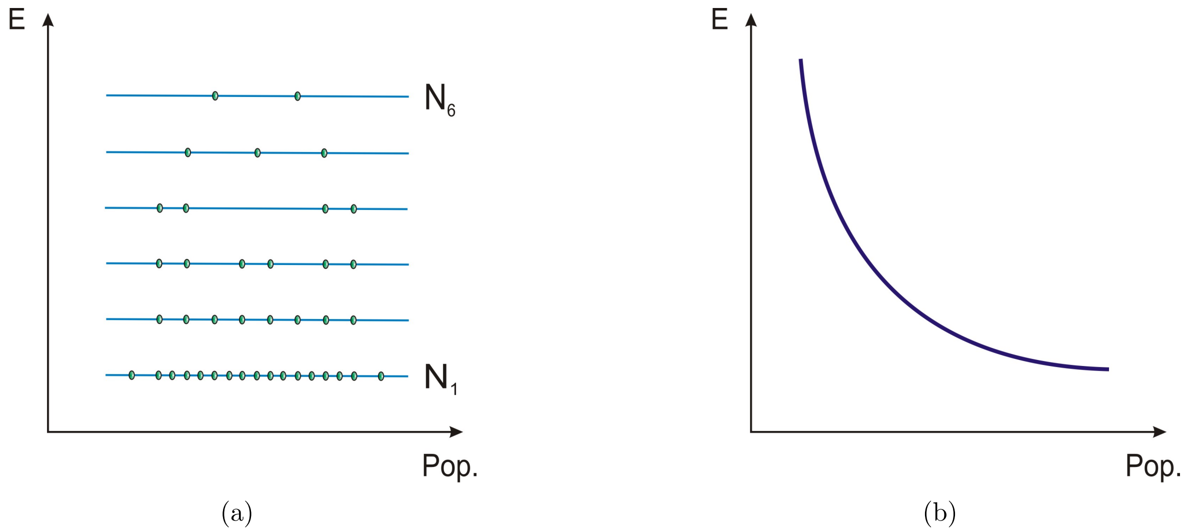

Figure 4.5: *(a) Normal population of the different energetic levels. (b) Distribution function of the particles in the energetic levels.*

The normal situation of the population of the energetic levels is displayed in Figure 4.5. Most of the particles are in the ground level. Boltzman's law predicts the distribution function for the fractional number of particles N_i/N occupying a set of states i with energy E_i. The population in the ground state level is higher than in the 2^{nd} energetic level, the population is exponential diminishing (Boltzmann's law).

$$N_3 < N_2, N_1 \tag{4.1}$$

In this case, N represents the number of particles.

$$\frac{N_i}{N} = \frac{g_i \cdot \exp\left[-\frac{E_i}{(k_B T)}\right]}{z(T)} \tag{4.2}$$

wheras k_B is Boltzmann's constant, T is the temperature and g_i represents the degeneracy, i.e. number of states with energy E_i.

$$z(T) = \sum g_i \cdot \exp\left[-\frac{E_i}{(k_B T)}\right] \tag{4.3}$$

$$\exp\left[\frac{-\Delta E}{(k_B T)}\right] > 0 \tag{4.4}$$

$$\frac{1}{\exp\left[\frac{-\Delta E}{(k_B T)}\right]} < 1 \tag{4.5}$$

$$N_2 = N_1 \frac{1}{\exp\left[\frac{-\Delta E}{(k_B T)}\right]} \tag{4.6}$$

Equations 4.5 and 4.6 lead to

$$N_2 < N_1 \tag{4.7}$$

For amplification it is necessary to change the normal situation as shown in equation 4.7. The photon density in the different energetic levels can be described as follows:

$$-\frac{dN_2}{dt} = \sigma \Phi N_2 \tag{4.8}$$

$$-\frac{dN_1}{dt} = \sigma \Phi N_1 \tag{4.9}$$

wheras Φ is the photon flux inside the resonator, N_i is the occupation of level i and σ is the laser stimulated cross section. It is necessary to create a situation, where $N_2 > N_1$ is fulfilled to start laser amplification.

$$\left[cm^{-1}\right] = \left[cm^2\right] \cdot \left[cm^{-3}\right] \tag{4.10}$$

$$\alpha = \sigma(N_1 - N_2) \tag{4.11}$$

where α is the coefficient of absorption.

$$I = I_0 \cdot \exp\left[-\alpha \cdot x\right] \tag{4.12}$$

$$I < I_0 \tag{4.13}$$

$$g = -\alpha = -\sigma(N_1 - N_2) = \sigma(N_2 - N_1) \tag{4.14}$$

and in this case,

$$N_2 > N_1 \tag{4.15}$$

which describes the situation of population inversion. It is necessary that there is one metastable level with a lifetime in the range of μs in contrast to the short living levels which have a lifetime around ns.

4.1.2 Roundtrip through the laser system

It is possible to describe all the processes in the laser system by a certain system of rate equations. The background for this calculation is a four-level laser system.

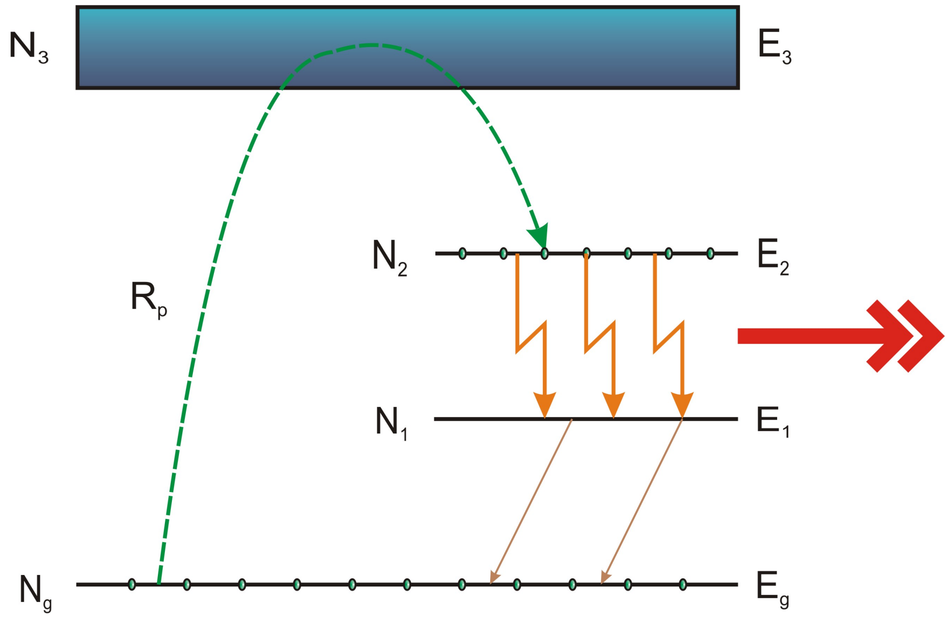

Figure 4.6: *Four-level laser system with the different energetic levels, the different populations and the pump function.*

In Figure 4.6 the needed four-level laser system is illustrated. In such a system,

$$N_1 \approx 0, N_3 \approx 0 \tag{4.16}$$

$$N_t = N_g + N_2 \tag{4.17}$$

where N_t is the total number of particles and N_g is the ground state level of the system. Ordinary differential equations relate numbers of density of photons.

The system of used rate equations is presented as

$$\frac{dN_2}{dt} = \underbrace{R_p(t)}_{\substack{Pump\\Function}} - \underbrace{BqN_2}_{\substack{Stimulated\\emission}} - \underbrace{\frac{N_2}{\tau}}_{\substack{Spontaneous\\emission}} \tag{4.18}$$

$$\frac{dq}{dt} = \underbrace{BqN_2}_{\substack{Stimulated\\emission}} - \underbrace{V_a}_{\substack{Active\\volume}} - \frac{q}{\tau_c} \tag{4.19}$$

where $R_p(t)$ represents the pump function, q is the number of photons, N_2 represents the population number of the upper laser level, τ is the lifetime of the upper laser level, V_a is the active volume and B represents a coefficient of proportionality.

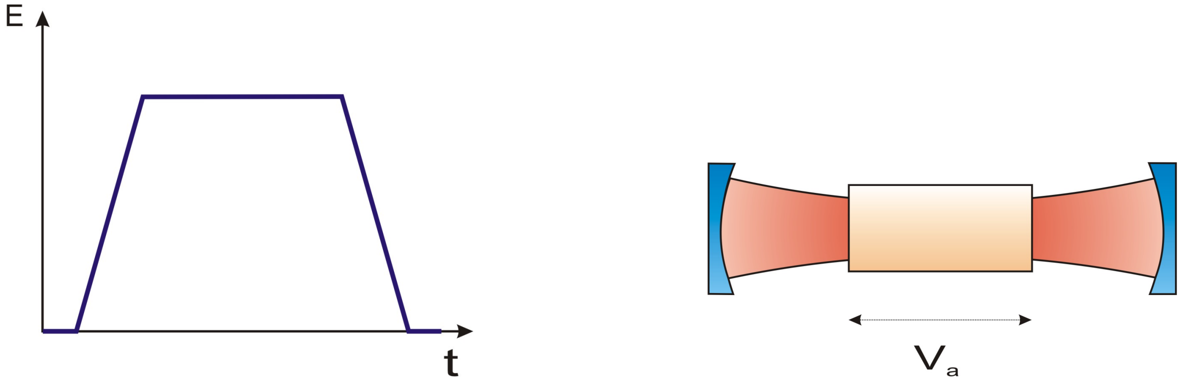

(a) (b)

Figure 4.7: *(a) The approximation of the pump function $R_p(t)$. (b) The active volume V_a of the laser system.*

The pump function which is approximated as a trapezoid function and the active volume are displayed in Figure 4.7.

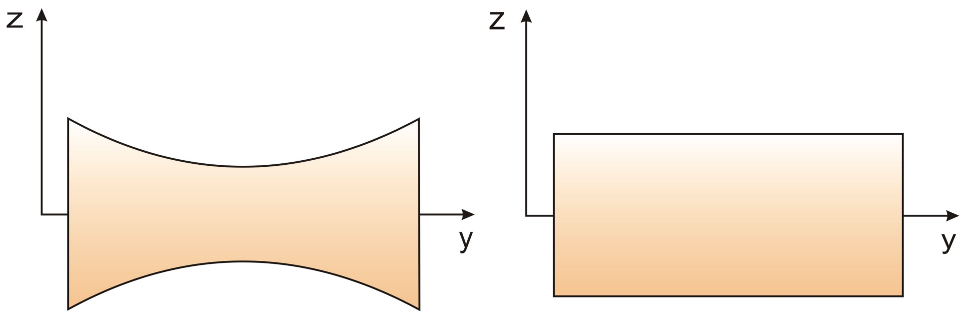

Figure 4.8: *Single hyperboloid converted to a cylinder.*

The active volume is a single hyperboloid but in the calculations it is converted to a cylider with the same capacity which is shown in Figure 4.8.

$$R_p(t) \approx P(t) \tag{4.20}$$

The area under the pump function represents the energy in the system. τ and V_a are known but it is inevitable to find values for the unknown coefficients B and τ_c. To obtain the values for B and τ_c it is essential to analyse one single roundtrip through the laser system.

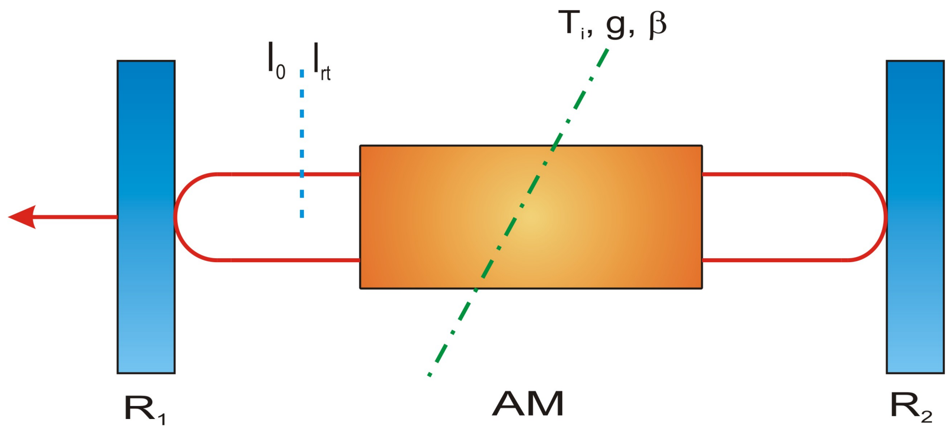

Figure 4.9: *Scheme of one single roundtrip through the laser system.*

In Figure 4.9 the roundtrip is displayed schematically. g is the gain and β represents the losses due to absorption and scattering.

$$v = \frac{c}{n} \tag{4.21}$$

describes the speed of the light in the active medium (for Nd:YAG, n=1.83).

$$T_{absorption} = e^{-\beta l} \tag{4.22}$$

L is the physical length of the resonator. L' is the optical length of the resonator,

$$L' = L + (n-1)l \tag{4.23}$$

wheras l is the length of the active volume. The duration of one single roundtrip through the laser system can be written as

$$t = \frac{l}{v} = \frac{l}{\frac{c}{n}} = \frac{nl}{c} \tag{4.24}$$

Calculation for one single roundtrip:

$$\underbrace{I_{rt}}_{\substack{Intensity\\after\\roundtrip}} = \underbrace{I_0}_{\substack{Initial\\Intensity}} \cdot \underbrace{r_1}_{\text{Reflection}} \cdot \underbrace{r_2}_{\text{Reflection}} \cdot 2\Big[\underbrace{e^{gl}}_{\text{Gain}} \cdot \underbrace{e^{-\beta l}}_{\substack{Loss\\(1-T_i)}}\Big] \tag{4.25}$$

T_i is the coefficient of equivalent reflection of active medium $\approx \beta$. $(1-T_i)$ is the transmission of the light trough the active medium.

$$I_{rt} = I_0 \cdot r_1 \cdot r_2 \cdot (1-T_i)^2 \cdot e^{2gl} \tag{4.26}$$

Logaritmic losses are introduced:

$$\gamma_1 = -ln \cdot r_1 \tag{4.27}$$
$$\gamma_2 = -ln \cdot r_2 \tag{4.28}$$
$$\gamma_i = -ln \cdot (1-T_i) \tag{4.29}$$

$$r_1 = e^{-\gamma_1} = e^{-(-ln \cdot r_1)} = e^{ln \cdot r_1} = r_1 \tag{4.30}$$
$$r_2 = e^{-\gamma_2} \tag{4.31}$$
$$(1-T_i) = e^{-\gamma_i} \tag{4.32}$$

These logaritmic losses are deployed in equation 4.26.

$$I_{rt} = I_0 \cdot e^{2gl} \cdot e^{-\gamma_1} \cdot e^{-\gamma_2} \cdot e^{-2\gamma_i} \tag{4.33}$$

$$I_0 = \exp\left[2gl\right] \cdot \exp\left[-2\left(\frac{\gamma_1+\gamma_2}{2} + \gamma_i\right)\right] \tag{4.34}$$

$$\gamma = \left(\frac{\gamma_1+\gamma_2}{2} + \gamma_i\right) \tag{4.35}$$

$$I_0 = \exp\left[2gl - 2\gamma\right] \tag{4.36}$$

ΔI is the change of the light intensity in one single roundtrip through the optical resonator.

$$\Delta I = I_{rt} - I_0 \tag{4.37}$$

$$\Delta I = I_0 \cdot \exp\left[2gl - 2\gamma\right] - I_0 \tag{4.38}$$

$$\Delta I = I_0 \cdot \Big(\exp\left[2gl - 2\gamma\right] - 1\Big) \tag{4.39}$$

$$2(gl - \gamma) \ll 1 \tag{4.40}$$

$$e^x \approx x + 1 + (\dots) \tag{4.41}$$

$$\exp\left[2gl - \gamma\right] \approx (2gl - \gamma) + 1 + (\dots) \tag{4.42}$$

$$\Rightarrow \Delta I = I_0\left[(2gl - \gamma) + 1 - 1\right] = I_0(2gl - \gamma) \tag{4.43}$$

Equations 4.40, 4.41, 4.42 lead to the final value for ΔI.

$$\Delta I = I_0 \cdot 2(2gl - \gamma) \tag{4.44}$$

The duration of one single roundtrip is also very important to obtain the values for B and τ_c for the system of rate equations 4.18, 4.19.

$$\Delta t = \frac{2L'}{c} \tag{4.45}$$

$$g = \sigma_{21} \cdot \Delta N \tag{4.46}$$

$$\frac{\Delta I}{\Delta t} = \frac{Ic}{2L'} \cdot 2 \cdot l \cdot \sigma_{21} \cdot N - \frac{2 \cdot I \cdot c}{2 \cdot L'} \cdot \gamma \tag{4.47}$$

$$\frac{\Delta I}{\Delta t} \approx \frac{dI}{dt} \tag{4.48}$$

$$\frac{dI}{dt} = I \cdot \frac{c \cdot l \cdot \sigma_{21}}{L'} \cdot N - I \cdot \frac{c \cdot \gamma}{L'} \tag{4.49}$$

Equation 4.49 is now compared with equation 4.19 in order to obtain B and τ_c. Comparing the two equations lead to the following coherence [16, 18, 27, 28].

$$I = \Phi \cdot \hbar\omega \tag{4.50}$$

$$\frac{dq}{dt} = B \cdot q \cdot N \cdot V_a - \frac{q}{\tau_c} \tag{4.51}$$

$$\frac{dI}{dt} = I \cdot \frac{c \cdot l \cdot \sigma_{21}}{L'} \cdot N - I \cdot \frac{c \cdot \gamma}{L'} \tag{4.52}$$

$$B \cdot V_a = \frac{c \cdot l \cdot \sigma_{21}}{L'} \tag{4.53}$$

$$\frac{1}{\tau_c} = \frac{c \cdot \gamma}{L'} \tag{4.54}$$

Finally, equations 4.53 and 4.54 lead to results for B and τ_c.

$$B = \frac{c \cdot l \cdot \sigma_{21}}{L'} \tag{4.55}$$

$$\tau_c = \frac{L'}{c \cdot \gamma} \tag{4.56}$$

4.1.3 Threshold conditions

The threshold of a laser is the state where the small-signal gain just equals the resonator losses. This is the case for a certain pump power (the threshold pump power), or (for electrically pumped lasers) a certain threshold current. Significant power output, good power efficiency and stable, low-noise performance requires operation well above the threshold. A low threshold power requires low resonator losses and consequentely a high gain efficiency. This can be achieved by using a small laser mode area in an efficient gain medium. The overall optimization of laser performance may have to take into account additional aspects such as the pulse duration in a Q-switched laser and avoiding Q-switching instabilities [21]. The threshold conditions can be calculated by the help of the system of rate equations 4.18, 4.19.

No laser generation $\Rightarrow$

$$\frac{dq}{dt} < 0 \tag{4.57}$$

Threshold $\Rightarrow$

$$\frac{dq}{dt} = 0 \tag{4.58}$$

Laser generation $\Rightarrow$

$$\frac{dq}{dt} > 0 \tag{4.59}$$

Equation 4.19 is set to zero to obtain the threshold conditions.

$$\frac{dq}{dt} = B \cdot q \cdot N \cdot V_a - \frac{q}{\tau_c} \tag{4.60}$$

after dividing by $q, (q \neq 0)$,

$$B \cdot N \cdot V_a - \frac{1}{\tau_c} = 0 \tag{4.61}$$

is obtained.

$$N_{th} = (B \cdot V_a \cdot \tau_c)^{-1} \tag{4.62}$$

$$\Rightarrow \left(\frac{c \cdot l \cdot \sigma_{21}}{L' \cdot V_a} \cdot V_a \cdot \frac{L'}{c \cdot \gamma} \right)^{-1} \tag{4.63}$$

The obtained values for B and τ_c are assembled in equation 4.63 to find the proper value for N_{th}.

$$N_{th} = \frac{\gamma}{l \cdot \sigma_{21}} \tag{4.64}$$

This is the minimum population inversion to start laser generation. The minimum energy required to start population inversion at the upper laser level can be written as

$$E_{th}^{opt} = N_{th} \cdot \Phi \cdot V_a \tag{4.65}$$

The threshold coefficient of amplification is

$$g_{th} = \sigma_{21} \cdot N_{th}. \tag{4.66}$$

4.2 Simulation approach

For the used code, written in Borland PASCAL, it is also necessary to define the additional losses in the laser system due to the presence of a Q-switch.

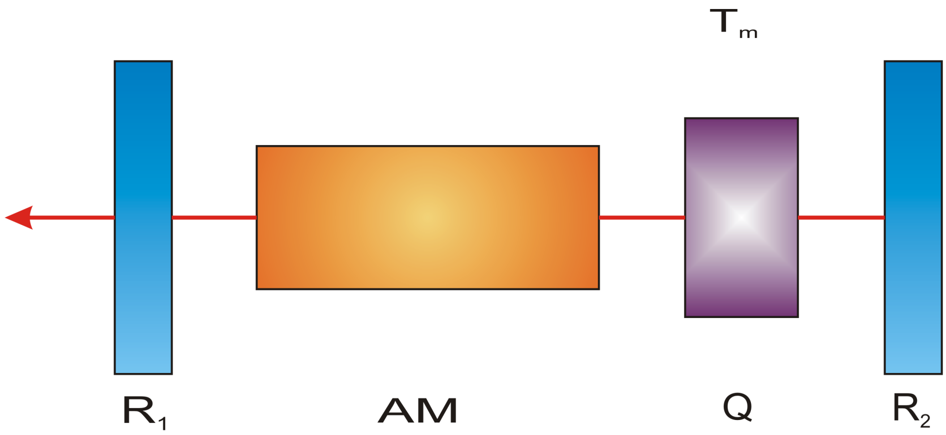

Figure 4.10: *Laser system with added Q-switch. AM is the active medium, Q the Q-switch, R_1 and R_2 are the reflectivities of the two mirrors of the optical resonator and T_m represents the transmission of the Q-switch.*

In Figure 4.10 a scheme of an optical resonator with an additional Q-modulator is presented. The additional losses can be written as

$$T_m(t), T_m(I) \tag{4.67}$$

In the case of active Q-switching, the function of transmission is dependent on the time in contrast to the passive case in which the intensity influences the function as shown in 4.2. The calculation for one single roundtrip changes a bit due to the Q-modulator.

$$\underbrace{I_{rt}}_{\substack{Intensity\\after\\roundtrip}} = \underbrace{I_0}_{\substack{Initial\\Intensity}} \cdot \underbrace{r_1}_{\text{Reflection}} \cdot \underbrace{r_2}_{\text{Reflection}} \cdot 2\left[\underbrace{e^{gl}}_{\text{Gain}} \cdot \underbrace{e^{-\beta l}}_{\substack{Loss\\(1-T_i)}}\right] \cdot \underbrace{(T_m)^2}_{\substack{Passing\\the\\Q-modulator}} \tag{4.68}$$

After introducing logaritmic losses, the additional factor can be written as

$$\gamma_m = -ln \cdot T_m \tag{4.69}$$

$$T_m = e^{-\gamma_m} \tag{4.70}$$

The intensity after one roundtrip is finally

$$I_{rt} = I_0 \cdot \exp\left[2 \cdot gl - 2\left(\frac{\gamma_1 + \gamma_2}{2} + \gamma_i + \gamma_m\right)\right] \tag{4.71}$$

$$\gamma = \frac{\gamma_1 + \gamma_2}{2} + \gamma_i + \gamma_m \tag{4.72}$$

$$I_{rt} = I_0 \cdot \exp\left[2 \cdot gl - 2(\gamma)\right] \tag{4.73}$$

The value for N_{th} is also changing after introducing a Q-modulator.

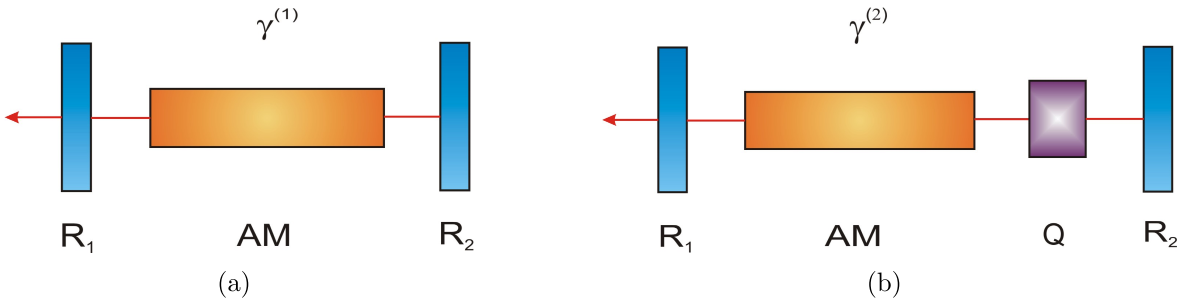

Figure 4.11: *(a) $\gamma^{(1)}$ describes the value for the losses without Q-switch. (b) $\gamma^{(2)}$ describes the value for the losses with Q-switch.*

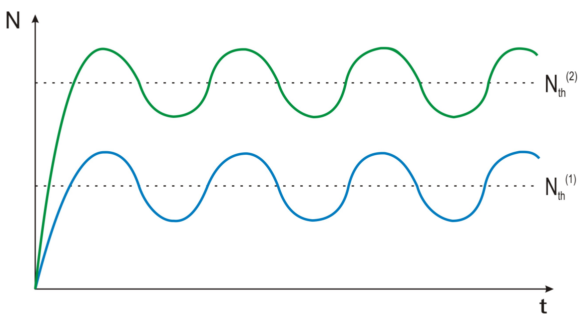

Figure 4.12: *Different threshold levels due to introduced Q-switch in the cavity.*

In Figure 4.11 the difference of the the losses $\gamma^{(i)}$ are explained and the discrepancy of the threshold level is displayed in Figure 4.12.

$$N_{th}^{(1)} = \frac{\gamma^{(1)}}{\sigma_{21} \cdot l} \tag{4.74}$$

$$N_{th}^{(2)} = \frac{\gamma^{(2)}}{\sigma_{21} \cdot l} \tag{4.75}$$

$$\gamma^{(1)} \ll \gamma^{(2)} \tag{4.76}$$

$$\Rightarrow N_{th}^{(1)} \ll N_{th}^{(2)} \tag{4.77}$$

It is also fundamental to calculate the output power of the laser system for the simulation.

$$\frac{dq}{dt} = B \cdot q \cdot N \cdot V_a - \frac{1}{\tau_c} \tag{4.78}$$

wheras τ_c is the lifetime of the photon in the resonator.

$$\tau_c = \frac{L'}{c \cdot \gamma} \tag{4.79}$$

$$\frac{q}{\tau_c} = \frac{q}{L'} \cdot c \cdot \gamma \tag{4.80}$$

with

$$\gamma = \frac{\gamma_1 + \gamma_2}{2} + \gamma_i \tag{4.81}$$

$$\Rightarrow \frac{q}{\tau_c} = \underbrace{\frac{q \cdot c \cdot \gamma_1}{2 \cdot L'}}_{\substack{Useful\\losses}} + \underbrace{\frac{q \cdot c \cdot \gamma_2}{2 \cdot L'}}_{\substack{Losses\\of\\r_2}} + \underbrace{\frac{q \cdot c \cdot \gamma_i}{L'}}_{\substack{Losses\\in\\active\\medium}} \tag{4.82}$$

where γ represents the total losses with introduced Q-switch in the cavity. The output power can be descibed as the useful losses of the laser system [32, 33, 34, 35].

$$P_{out} \approx q \tag{4.83}$$

$$P_{out} = q \cdot \frac{c \cdot \gamma 1}{2 \cdot L'} \cdot \hbar\omega \tag{4.84}$$

where $\hbar\omega$ is the energy of one photon.

$$[W] = \frac{[J]}{[s]} \tag{4.85}$$

The final value for the output power of the laser is [16]

$$P_{out} = q \cdot \hbar\omega \cdot \frac{c \cdot \gamma_1}{2L'} \tag{4.86}$$

To obtain laser action, $N_2 > N_1$ is needed, and $T_1 < T_{21}$ with T_{21} is the lifetime of $2 \rightarrow 1$ transition. If this equality is not satisfied, laser action is only possible on a pulsed basis provided, that the pumping pulse is shorter than the lifetime of the upper laser level. The laser action continues till the number of atoms accumulate in the lower laser level, as a result of stimulated emission.

In the other case, if the equality is satisfied and $R_p(t)$ is sufficiently strong, the steady state oscillator condition is reached finally. Laser transmission in initiated when population inversion N exceeds the critical value N_{th}.

In order to define the laser slope efficiency

$$\eta_s = \frac{dP_{out}}{dP_p} \tag{4.87}$$

where P_p is the pumping power, the output power P_{out} can be also written as

$$\phi_0 = \frac{A_b \cdot \gamma}{\sigma} \cdot \frac{\tau_c}{\tau} \cdot \left(\frac{P_p}{P_{th} - 1} \right) \tag{4.88}$$

where $A_b = V_a/l$ which describes the sectional area of the mode (beam area) which is smaller or equal to the cross sectional $A = V/l$.
Output power is

$$P_{out} = (A_b \cdot I_s) \cdot \frac{\gamma_1}{2} \cdot \left(\frac{P_p}{P_{th}} - 1 \right) \tag{4.89}$$

where $I_s = \hbar\omega/\sigma\tau$ the saturation density for a four-level system. η_s is constant for a given system

$$\eta_s = \frac{A_b \cdot \hbar\omega}{\sigma \cdot \tau} \cdot \frac{\gamma_1}{2} \cdot \frac{1}{P_{th}} \tag{4.90}$$

with

$$P_{th} = \frac{\gamma}{\eta_p} \cdot \frac{\hbar\omega_{mp}}{\tau} \cdot \frac{A}{\sigma} \tag{4.91}$$

ω_{mp} is the frequency difference between the upper laser level and the ground state level, A is the area of the active medium.

$$\eta_s = \eta_p \cdot \frac{\gamma_1}{2\gamma} \cdot \frac{\hbar\omega}{\hbar\omega_{mp}} \cdot \frac{A_b}{A} \tag{4.92}$$

$$\Rightarrow \eta_s = \eta_p \cdot \eta_c \cdot \eta_q \cdot \eta_t \tag{4.93}$$

with η_p is the pump efficiency,

$$\eta_c = \frac{\gamma_1}{2\gamma} \tag{4.94}$$

is the fraction of the generated photons that are coupled out of the cavity, this value is always smaller than 1, reaches 1 in the case that $\gamma_1 = \gamma_i = 0$.

$$\eta_q = \frac{\hbar\omega}{\hbar\omega_{mp}} \tag{4.95}$$

is the fraction of the minimum pump energy transformed into laser energy (laser quantum efficiency).

$$\eta_t = \frac{A_b}{A} \tag{4.96}$$

is the fraction of the active medium cross section used by beam cross section (transverse efficiency) [16, 18, 19].

4.3 Details and parameters of simulation

In this section, some other important parameters for the simulation of a Q-switched laser system are presented and explained in more detail.

4.3.1 Approximation of the pump pulse

The pump pulse is represented by a curve, but the pulse can be approximated by a trapezoid function very well.

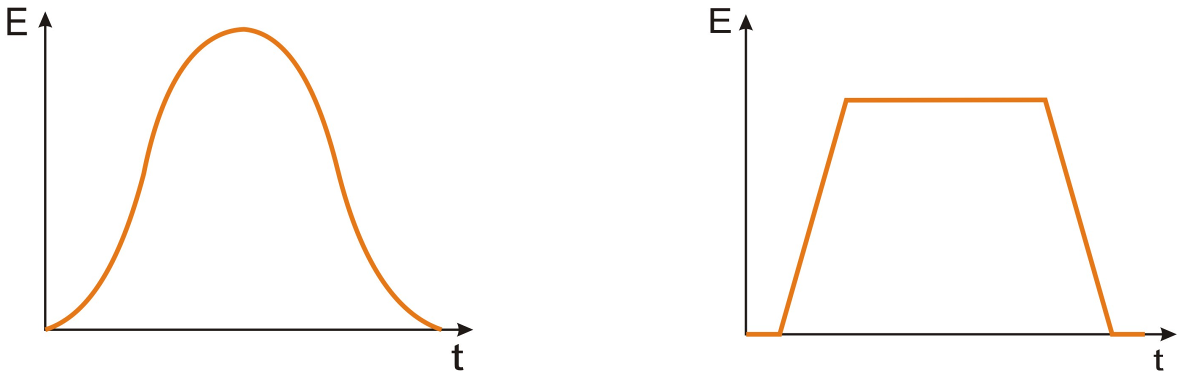

(a) (b)

Figure 4.13: *(a) Original shape of the pump pulse. (b) Approximation of the used pump pulse as a trapezoid.*

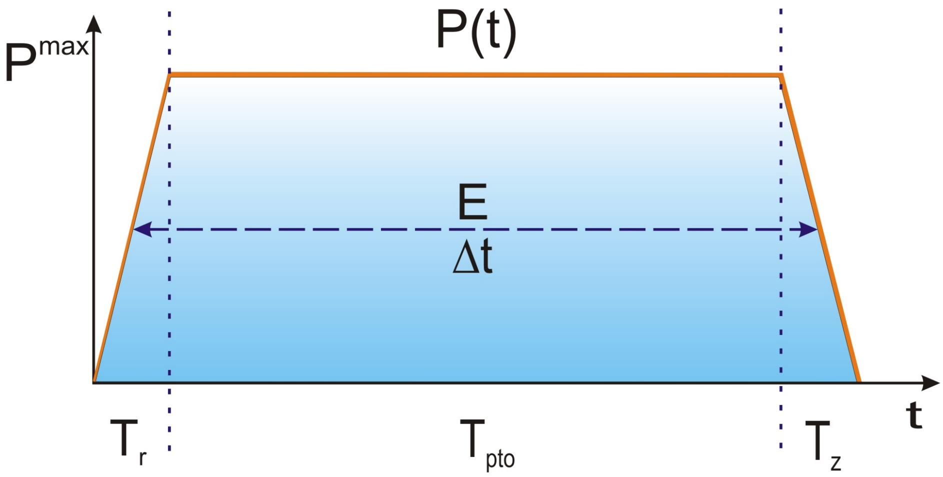

Figure 4.14: *More detailed scheme of the approximated curve.*

Figure 4.13 shows the original shape and the approximated shape of the pump pulse. This pump function can be subdivided into a rising edge, a plateau and a falling edge as illustrated in Figure 4.14.

The area beneath the pump pulse represents the energy of the pulse.

$$P(t) = P_p^{max} \cdot f(t) \tag{4.97}$$

with $f(t)$ is a trapezoid function.

$$R_p(t) = \frac{P(t)}{\hbar\omega \cdot V_a} \tag{4.98}$$

describes the whole pump function. The calculation of the length of the pump pulse Δt is also inevitable for the simulation.

$$\Delta t = \frac{E_{th}}{P^{max}}, P^{max} = \frac{E}{\Delta t} \tag{4.99}$$

$$E > E_{th} \tag{4.100}$$

The approximation as the trapezoid is very useful for the analysis of the pump pulse. This pulse can be calculated as

$$\begin{aligned} T_r &= \text{rising edge} \\ T_{pto} &= \text{plateau} \\ T_f &= \text{falling edge} \end{aligned}$$

$$\begin{aligned} T_r &= a \cdot t + b \\ T_{pto} &= P^{max} \\ T_f &= c \cdot t + d \end{aligned}$$

$$P(t) = \begin{cases} a \cdot t + b = 0, & \text{if } t = 0 \\ a \cdot T_r + b = P^{max}, & \text{if } t = T_r \end{cases} \tag{4.101}$$

$$\Rightarrow a = \frac{P^{max}}{T_r} \tag{4.102}$$

$$P(t) = \begin{cases} P^{max}, & \text{if } t = T_r \\ P^{max}, & \text{if } t = T_r + T_{pto} \end{cases} \tag{4.103}$$

$$P(t) = \begin{cases} c \cdot (T_r + T_{pto}) + d = P^{max}, & \text{if } t = T_r + T_{pto} \\ c \cdot (T_r + T_{pto} + T_f) + d = 0 & \text{if } t = T_r + T_{pto} + T_f \end{cases} \tag{4.104}$$

$$\Rightarrow c = -\frac{P^{max}}{T_f} \tag{4.105}$$

$$\Rightarrow d = P^{max} \cdot \frac{(T_r + T_{pto} + T_f)}{T_f} \tag{4.106}$$

This leads to the final value for the pump pulse:

$$P(t) = \begin{cases} P^{max}/T_r, & 0 \ldots T_r \\ P^{max}, & T_r \ldots T_r + T_{pto} \\ P^{max}/T_f \cdot (T_r + T_{pto} + T_f - t) = 0, & T_r + T_{pto} \ldots T_f \end{cases} \tag{4.107}$$

4.3.2 Numerical solution of the system of rate equations

It is not possible to solve the used system of rate equations analytically. It is a system of coupled ordinary non-linear differential equations and it is only possible to find a solution by the help of numerical analysis. Ordinary differential equations (a relation that contains functions of only one independent variable, and one or more of its derivatives with respect to that variable) can be described as follows.

If y is an unknown function

$$y : \mathbb{R} \to \mathbb{R}$$

in x with $y^{(n)}$ is the $n^{(th)}$ derivative of y, an equation of the form

$$F(x, y, y', y'', \ldots, y^{(n)}) = 0 \tag{4.108}$$

is an ordinary differential equation of order n, for vector valued functions,

$$y : \mathbb{R} \to \mathbb{R}^m$$

it is called a system of ordinary differential equations of dimension m. A differential equation of order n in the form

$$F(x, y, y', y'', \ldots, y^{(n)}) = 0 \tag{4.109}$$

is called implicit wheras the form

$$F(x, y, y', y'', \ldots, y^{(n-1)}) = y^{(n)} \tag{4.110}$$

is called explicit differential equation.

A differential equation is said to be linear, if F can be written as a linear combination of the derivatives of y [13, 38, 36, 37].

$$y^{(n)} = \sum_{i=0}^{n-1} a_i(x) y^{(i)} + r(x) \tag{4.111}$$

with $a_i(x)$ and $r(x)$ continuous functions in x. The function $r(x)$ is called the source term, if $r(x) = 0$ the linear differential equation is called homogeneous, otherwise it is called inhomogeneous [41].

A function $u, I : \mathbb{R} \to \mathbb{R}$ is called a solution of integral curve for F, if u is n-times differentiable on I, and

$$F(x, u, u', u'', \ldots, u^{(n)}) = 0 \qquad x \in I. \tag{4.112}$$

The linear differential equations are a well understood class of differential equations and are also used in the simulation which is presented in this diploma thesis. Every explicit linear differential equation of any order can be reduced to a system of order 1.

$$y_i^{'}(x) = \sum_{j=1}^{n} a_{ij}(x) y_j + b_i(x), \quad i = 1, \ldots, n \tag{4.113}$$

which can be written in matrix and vector notation as

$$y'(x) = A(x)y(x) + b(x) \tag{4.114}$$

with

$$\begin{aligned} y(x) &= (y_1(x), \ldots, y_n(x)) \\ b(x) &= (b_1(x), \ldots, b_n(x)) \\ A(x) &= (a_{ij}(x)), \quad i, j = 1, \ldots, n \end{aligned}$$

Mostly, the differential equations cannot be solved analytically. The solutions of these equations can only be approximated by the help of numerical analysis. There are different algorithms that can be used to compute such an approximation. In the case of the used rate equations, it is a so called initial value problem. The initial conditions are given, but the development of the curve can only be approximated [43, 44].

One method to solve such a problem is the Euler method. From any point on a curve, it is possible to find an approximation of a nearby point on the curve by moving a short distance along the tangent to the curve.

Starting with the differential equation

$$y'(t) = f(t, y(t)), \qquad y(t_0) = y_0$$

the derivative y' is replaced by the finit difference approximation

$$y'(t) \approx \frac{y(t+h) - y(t)}{h}$$

which leads to

$$y(t+h) \approx y(t) + h \cdot y'(t)$$

and finally to

$$y(t+h) \approx y(t) + h \cdot f(t, y(t))$$

Afterwards, a step-size h is choosed to construct a certain sequence

$$t_0, t_1 = t_0 + h, t_2 = t_0 + 2h, \ldots$$

to estimate the exact solution $y(t_n)$ numerically. The recursive scheme can be written as

$$y_{n+1} = y_n + h \cdot f(t_n, y_n)$$

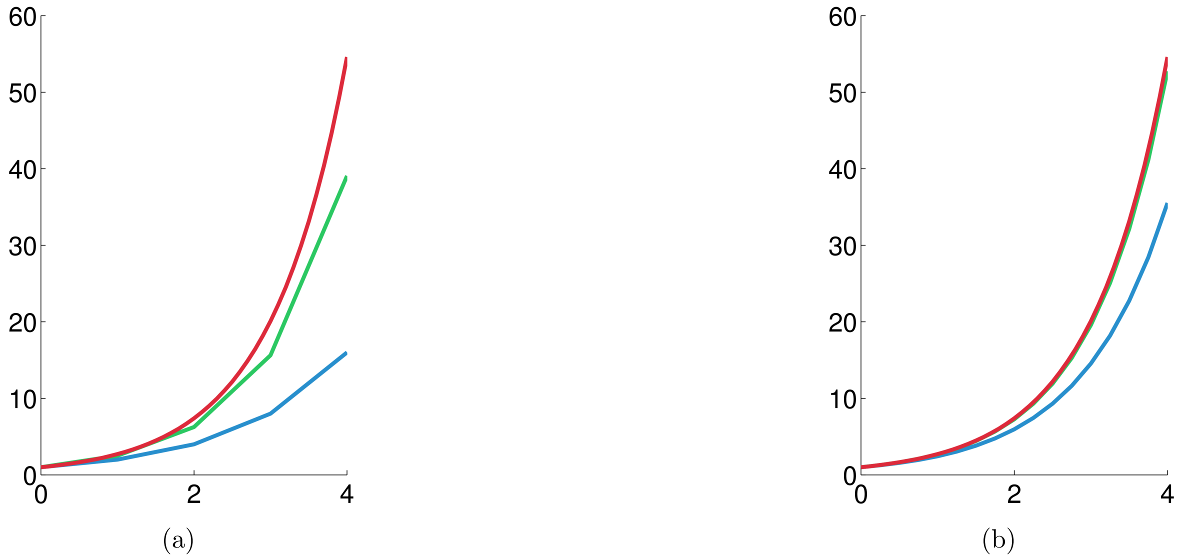

Figure 4.15: *(a) Numerical integration for the differential equation $y' = y, y(0) = 1$ The used step-size is $h = 1.0$. (b) The same integration for the step-size $h = 0.25$. Figure taken from [13].*

In Figure 4.15 a numerical integration for the differential equation $y' = y, y(0) = 1$ is displayed. The Euler method is marked blue, the midpoint method is marked green and the exakt solution $y = e^t$ is red. The step-size is a very important factor to obtain satisfying results.

These methods are not accurate enough which leads to higher order methods which are also used to solve the system of rate equations in this thesis. The most common method is the Runge-Kutta method.

In the numerical analysis, the Runge-Kutta methods are an important family of implicit and explicit iterative methods for the approximation of solutions of ordinary differential equations. In this thesis, the most common used Runge-Kutta method, the so called RK4 method is used.

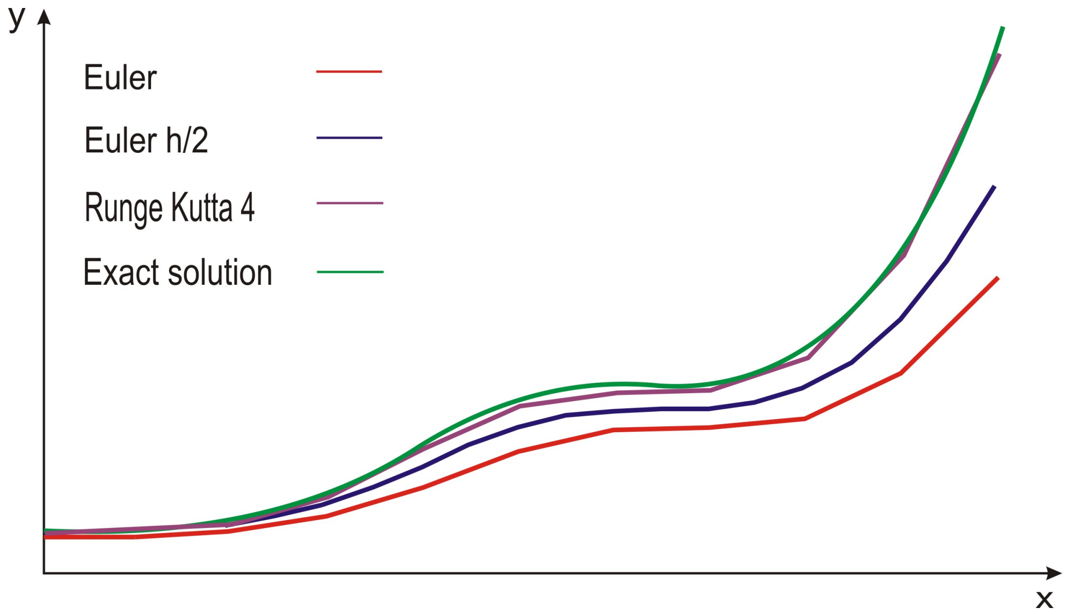

Figure 4.16: *Comparison of some common Runge-Kutta methods.*

The most common Runge-Kutta methods are shown in Figure 4.16. The specific initial value problem is

$$y^{'} = f(t, y), \qquad y(t_0) = y_0$$

The numerical solution is given by the following equations:

$$\begin{aligned} y_{n+1} &= y_n + \frac{1}{6} \cdot h \cdot (K_1 + 2 \cdot K_2 + 2 \cdot K_3 + K_4) \\ t_{n+1} &= t_n + h \end{aligned}$$

wheras y_{n+1} is the RK4 approximation of $y(t_{n+1})$ and

$$\begin{aligned} K_1 &= f(t_n, y_n) \\ K_2 &= f(t_n + \frac{1}{2} \cdot h, y_n + \frac{1}{2} \cdot h \cdot K_1) \\ K_3 &= f(t_n + \frac{1}{2} \cdot h, y_n + \frac{1}{2} \cdot h \cdot K_2) \\ K_4 &= f(t_n + h, y_n + h \cdot K_3) \end{aligned}$$

The next value y_{n+1} is determined by the present value y_n plus the product of the size of the step-size h and an estimated slope. This slope is a weighted average of slopes [41, 42, 39, 40, 13]:

- K_1 is the slope at the beginning of the interval.
- K_2 is the slope at the midpoint of the interval, using the slope K_1 to determine the value of y at the point $(t_n + h)/(2)$ using Euler's method.
- K_3 is the slope at the midpoint of the interval, using the slope K_2 to determine the y value.
- K_4 is the slope at the end of the interval, with its y value calculated by K_3.

In averaging the four slopes, greater weight is given to the two slopes at the midpoint. The RK4 method is a fourth order method, which means that the error per step is in the order of h^5 while the total accumulated error has the order h^4.

The explicit Runge-Kutta methods are a generalization of the used RK4 method and is given by

$$y_{n+1} = y_n + h \sum_{i=1}^{s} b_i k_i$$

where

$$\begin{aligned}
K_1 &= f(t_n, y_n) \\
K_2 &= f(t_n + c_2 \cdot h, y_n + a_{21} \cdot h \cdot K_1) \\
K_3 &= f(t_n + c_3 \cdot h, y_n + a_{31} \cdot h \cdot K_1 + a_{32} \cdot h \cdot K_2) \\
&\vdots \\
K_s &= f(t_n + c_s \cdot h, y_n + a_{s1} \cdot h \cdot K_1 + a_{s2} \cdot h \cdot K_2 + \cdots + a_{ss-1} \cdot h \cdot k_{s-1})
\end{aligned}$$

To specify a certain method, the integer s which is the number of stages, and the coefficients $a_{ij} (1 \leq j < i \leq s)$, $b_i (i = 1, 2, \ldots, s)$ and $c_i (i = 2, 3, \ldots, s)$ are provided. These coefficients are usually arranged in a Butcher tableau.

The Runge-Kutta method is consistent, if

$$\sum_{j=1}^{i-1} a_{ij} = c_i, \quad i = 2, 3, \ldots, s.$$

5 Results and Discussion

The results of the simulation of the laser system, with and without introduced Q-switch, are presented in this section of the thesis. The first simulations determined the case where no Q-switch was introduced into the optical resonator. The next step was the simulation of an active Q-switched laser system and its optimization. In order to find the best configuration of the laser, the most important parameters were iterated.

5.1 Simulation results of a system without Q-switch

The scope of the first simulations was to explore the behaviour of the laser system without a Q-switch. The calculation for different reflectivities of the output coupler and different pump energies were helpful to establish better understanding for the laser system and the relevant parameters. In all the presented results the length of the optical resonator was fixed at 5 cm, the length of the active medium was fixed at 1.5 cm and the other parameters like the reflectivity of the output mirror, the time for opening the Q-switch or the transmissions of the Q-switch were changed to obtain the different results.

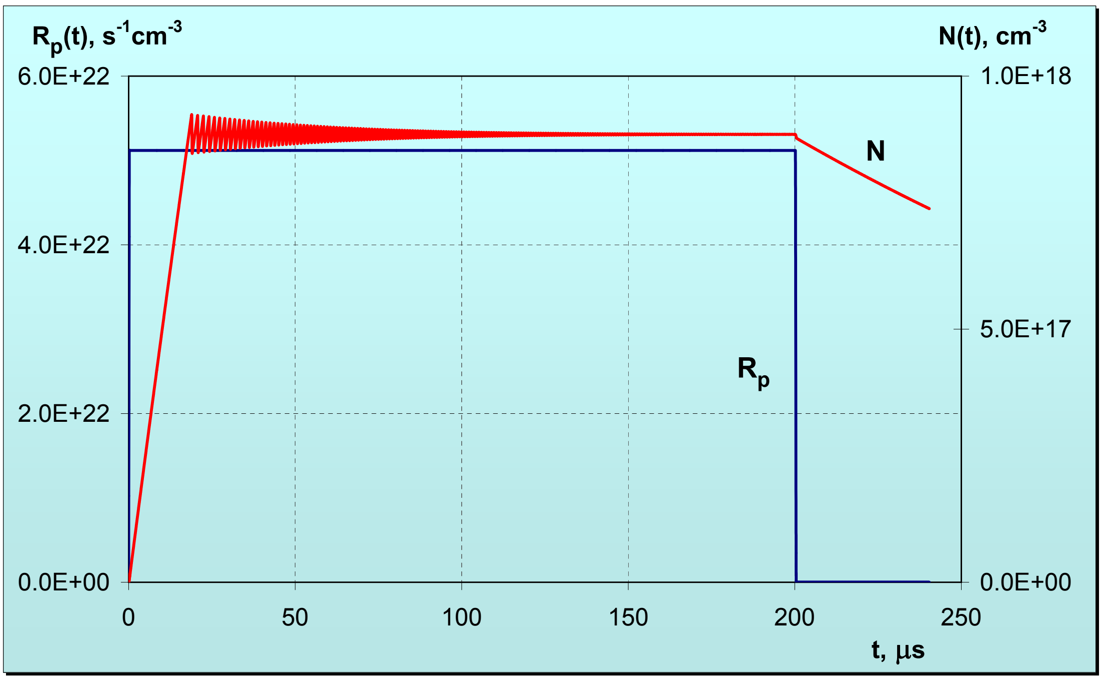

Figure 5.1: *The pump function $R_p(t)$ and the population inversion N for 20 mJ of introduced pump energy and a pulse duration of 200 μs.*

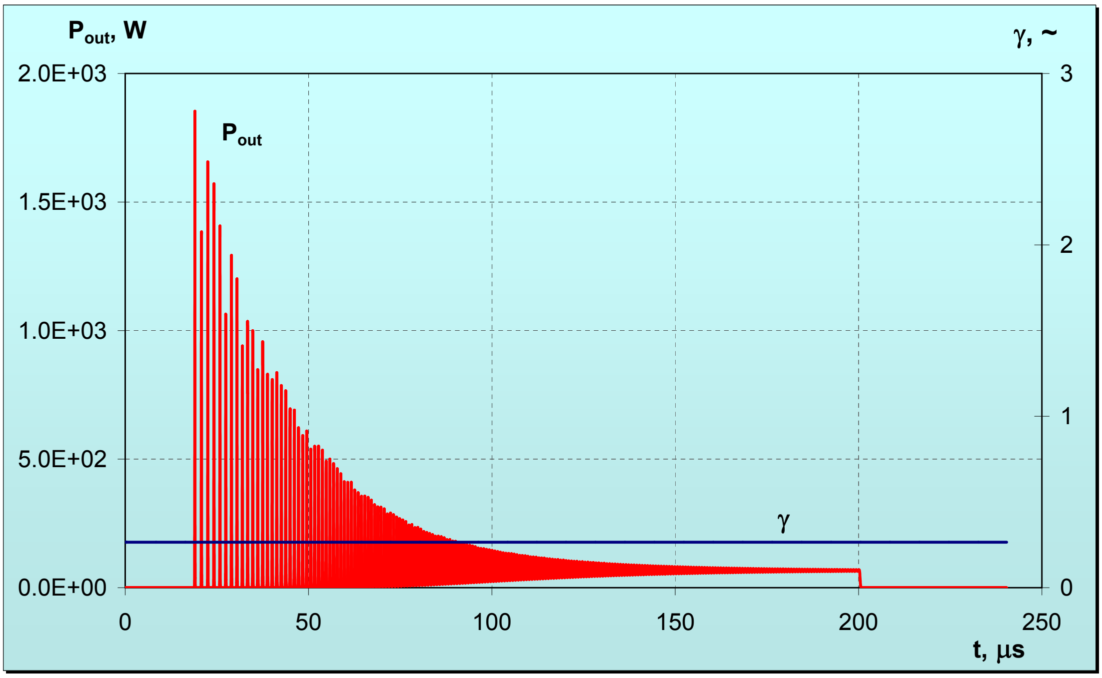

Figure 5.2: *The output power P_{out} and the losses γ of the resonator for 20 mJ of pump energy and a pulse duration of 200 μs.*

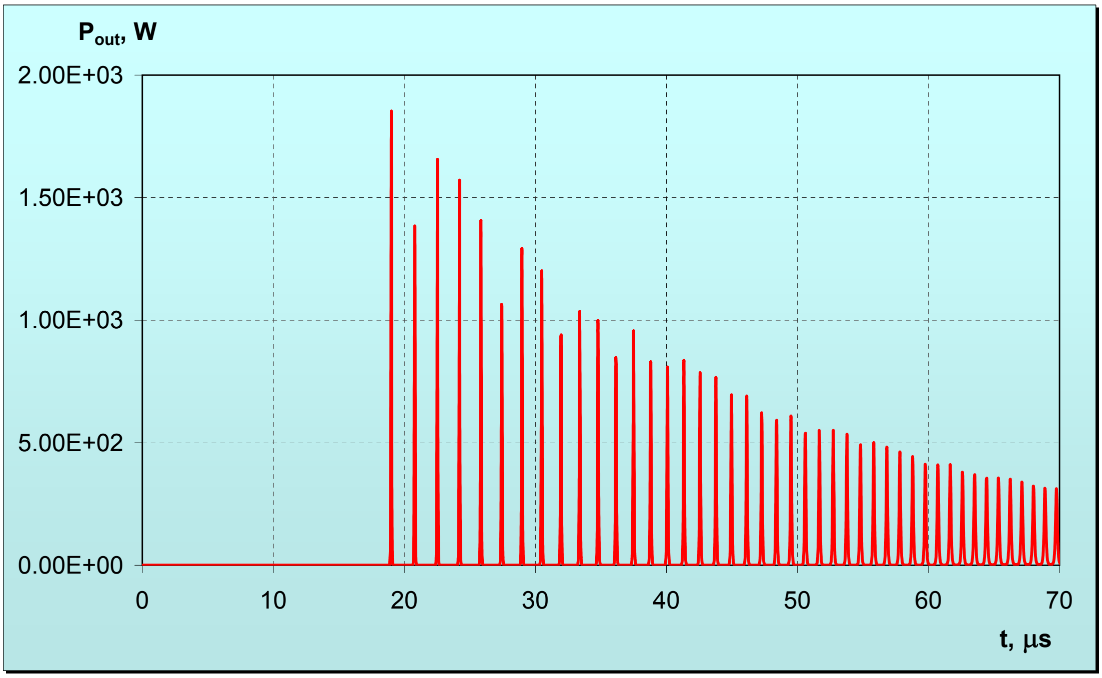

Figure 5.3: *Extension of Figure 5.2 for better overview of the single pulses.*

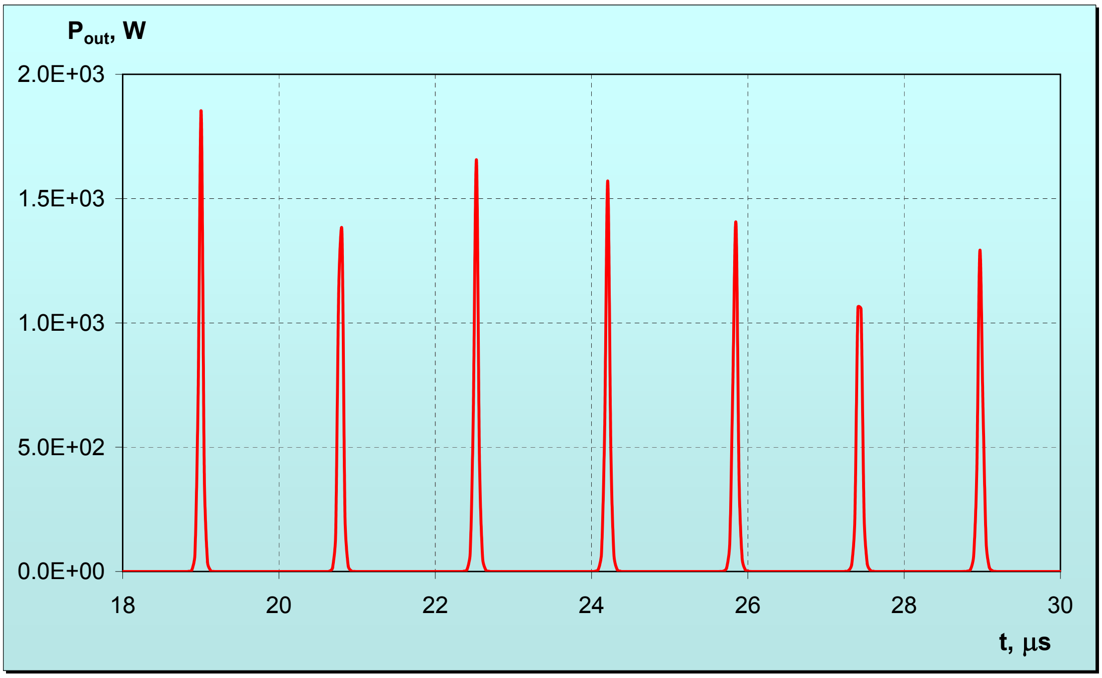

Figure 5.4: *Enlargement of Figure 5.3 to clearly depict the length of one single pulse and the distance between two pulses.*

The pump function $R_p(t)$, the losses γ and the output power P_{out} are shown in Figure 5.1, 5.2, 5.3, and 5.4.

After the population inversion N reaches a certain level over the threshold level, the first pulses are formed. After the first pulse the population inversion increases again until the second pulse is generated. The characteristics of the population inversion and the laser pulses are displayed in Figure 5.1, and 5.2. The losses γ in the optical resonator are constant over the whole duration of the pump pulse as shown in Figure 5.2.

The enlargements of the laser pulses are presented in the next two figures, Figure 5.3, and 5.4 to be able to quantitatively discern one single pulse and the distance between two pulses.

The first pulse reaches the maximum output power, the following pulses are a little weaker due to the lower level of inversion population. The next six figures show the same parameters and results for an other introduced pump energy. The simulation was made for 15, 20, 45, 60, and 90 mJ and two cases are presented detailed in this chapter.

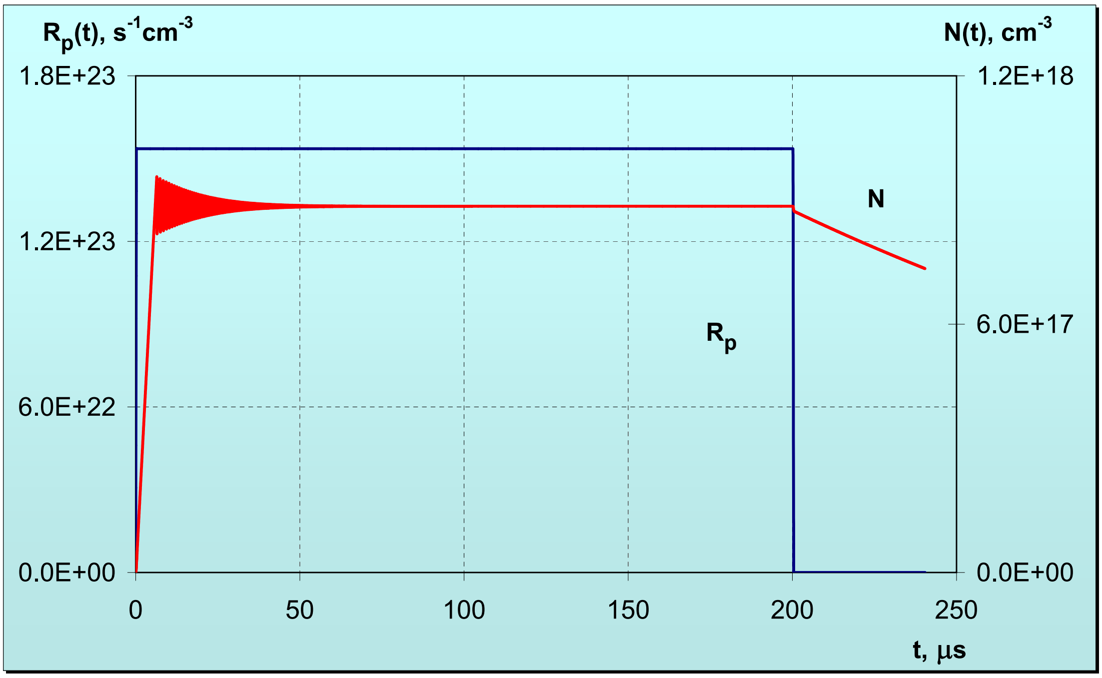

Figure 5.5: *The pump function $R_p(t)$ and the population inversion N for 60 mJ of puming energy and a pulse duration of 200 µs.*

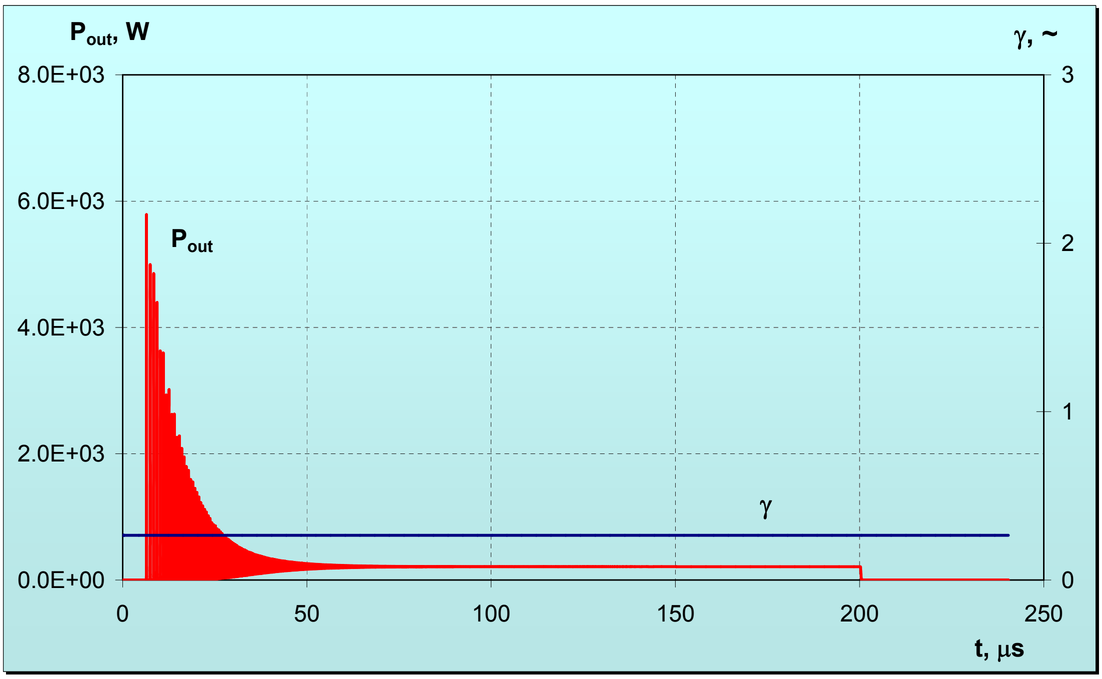

Figure 5.6: *The output power P_{out} and the losses γ of the resonator for 60 mJ of pump energy and a pulse duration of 200 µs.*

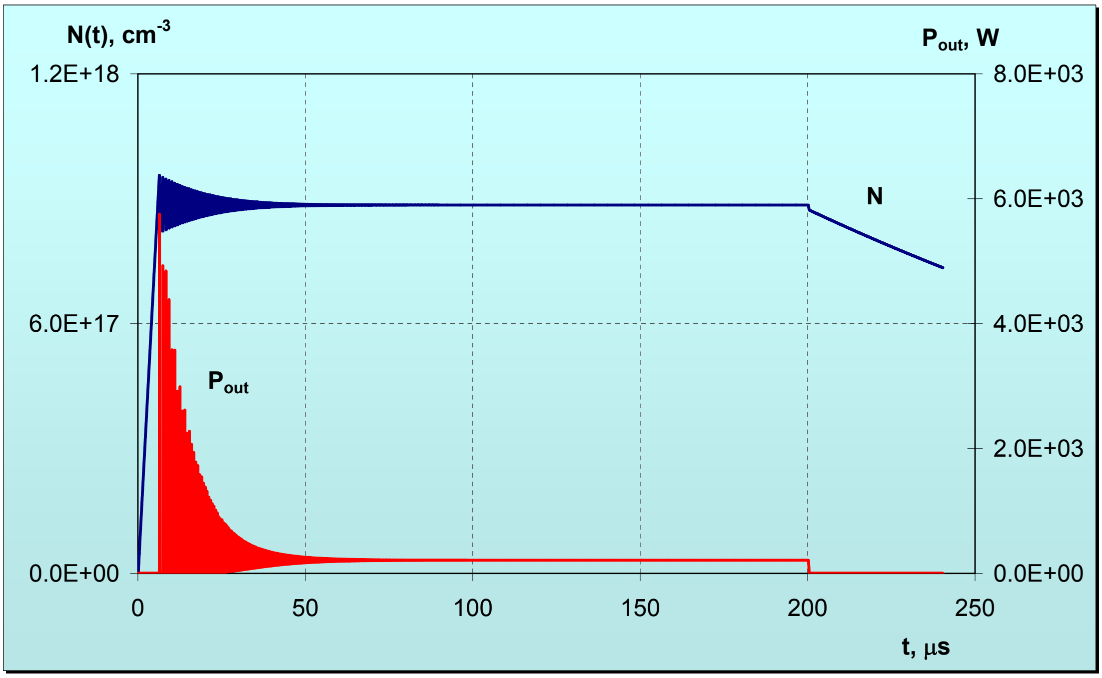

Figure 5.7: *The output power P_{out} and the population inversion N for 60 mJ of pump energy and a pulse duration of 200 µs.*

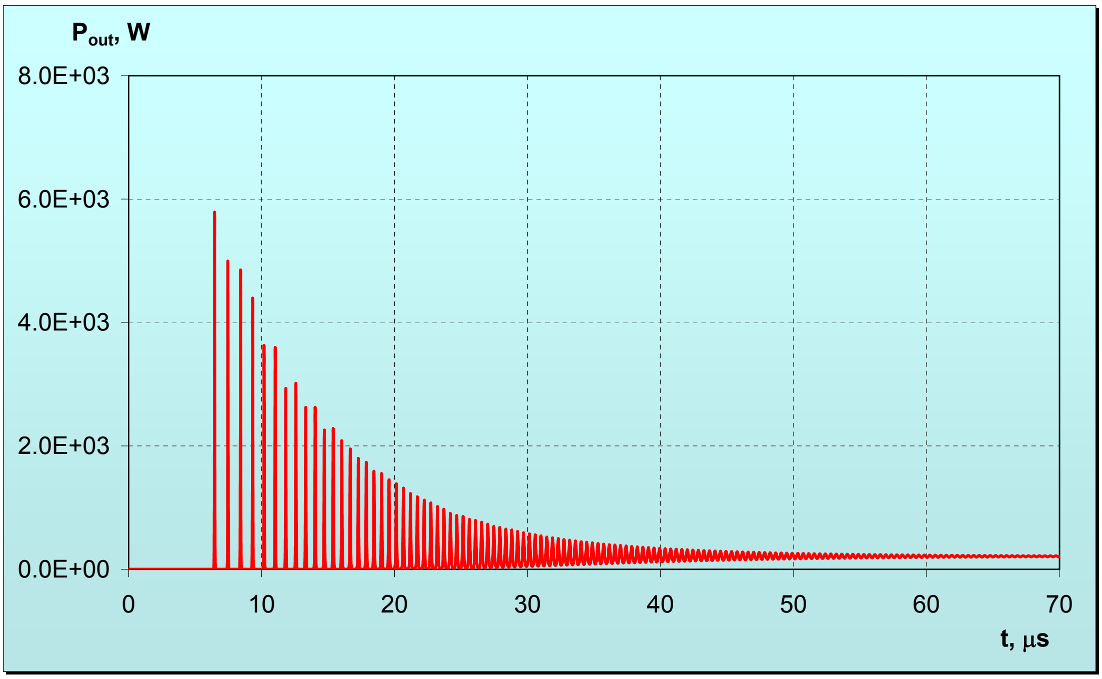

Figure 5.8: *Enlargement of Figure 5.6 for a better view of the single pulses.*

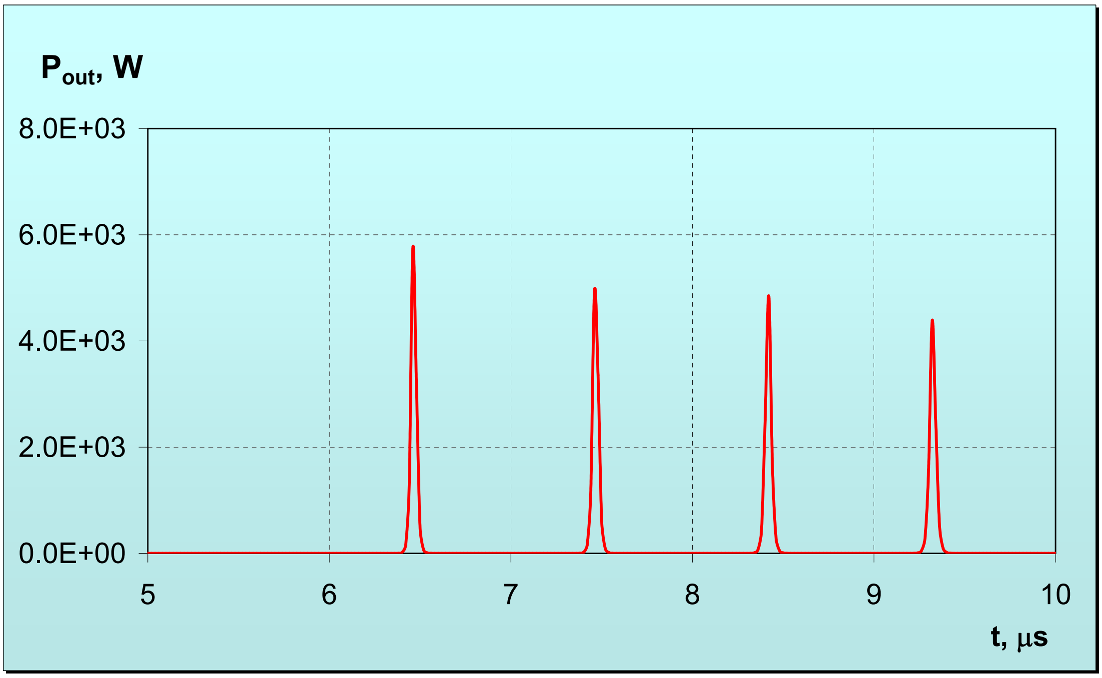

Figure 5.9: *Magnification of Figure 5.8 to estimate the length of one single pulse and the distance between two pulses.*

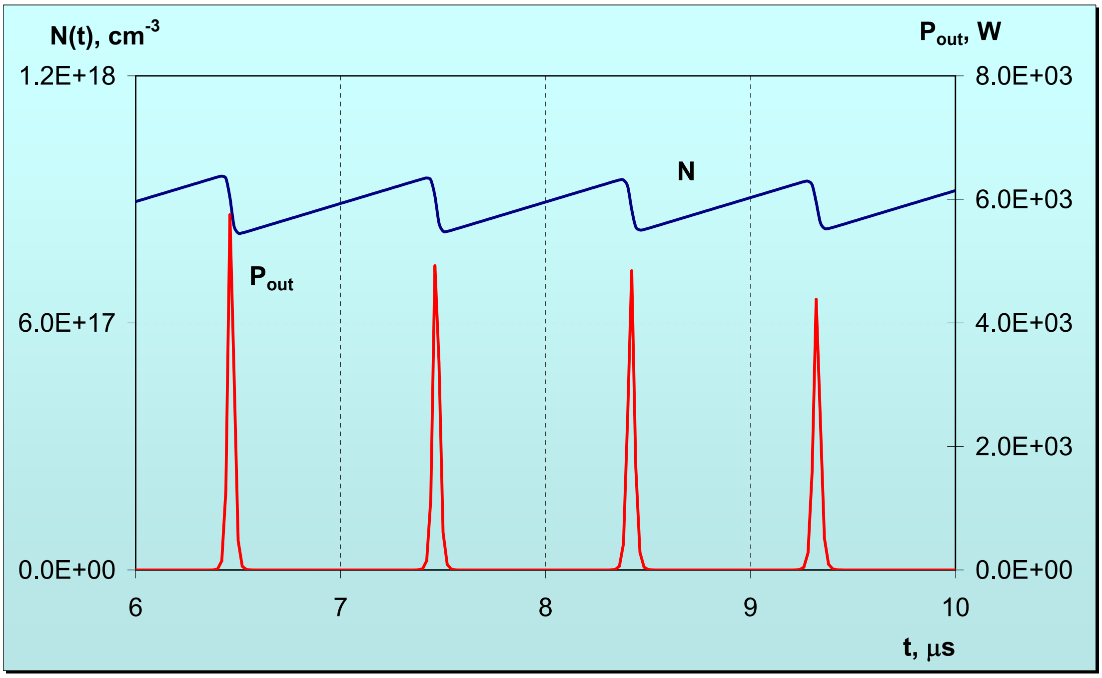

Figure 5.10: *Enlargement of Figure 5.7 to establish better understanding for the coherence between the population inversion N and the output power P_{out}.*

The second group of figures, Figure 5.5, 5.6, 5.7, 5.8, 5.9, and 5.10 presents the results for 60 mJ of pump energy and a pulse duration of 200 μs. Due to the same duration of the pump pulse it is possible to compare the other parameters like the length of the pulses or the distance between two pulses directly.

Due to the higher pump energy, the treshold level of population inversion is reached earlier and consequentely are the first pulses formed after $\approx 6\ \mu s$ compared to $\approx 19\ \mu s$ from the first presented case of 20 mJ of pump energy. The output power P_{out} reaches a higher level in the second case in the range of 6 kW in contrast to under 2 kW in the first case.

The length of the pulses is approximately the same in both cases but the distance between to pulses is shorter in the second case. The population inversion commutes in to the treshold level faster in the second case and this leads to a faster decline of the output power of the obtained laser pulses. Figure 5.10 shows the connection between the pulses and the inversion population N more detailed.

The results of the length of the pulses, the distance between two pulses, the output power and the starting times of the first pulses for different pump energies between 5 and 60 mJ and two different reflectivities of the output mirror are displayed on the next four figures.

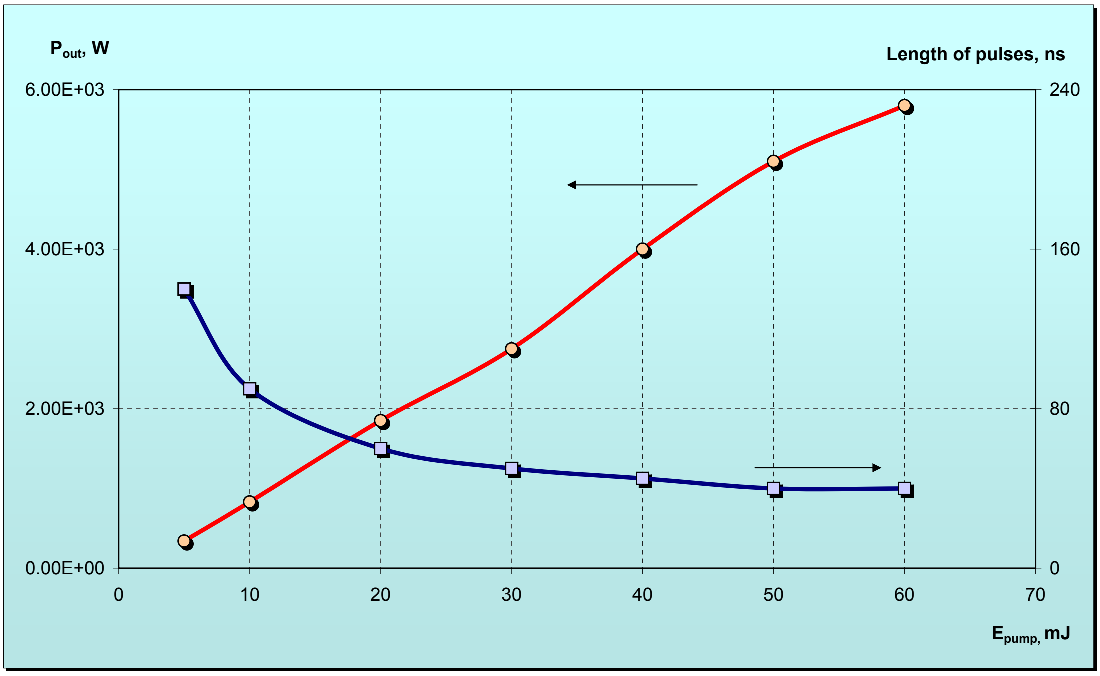

Figure 5.11: *Overview on the output powers P_{out} and the lengths of the pulses for 60 % reflectivity of the output coupler and pump energies varying from 5 to 60 mJ.*

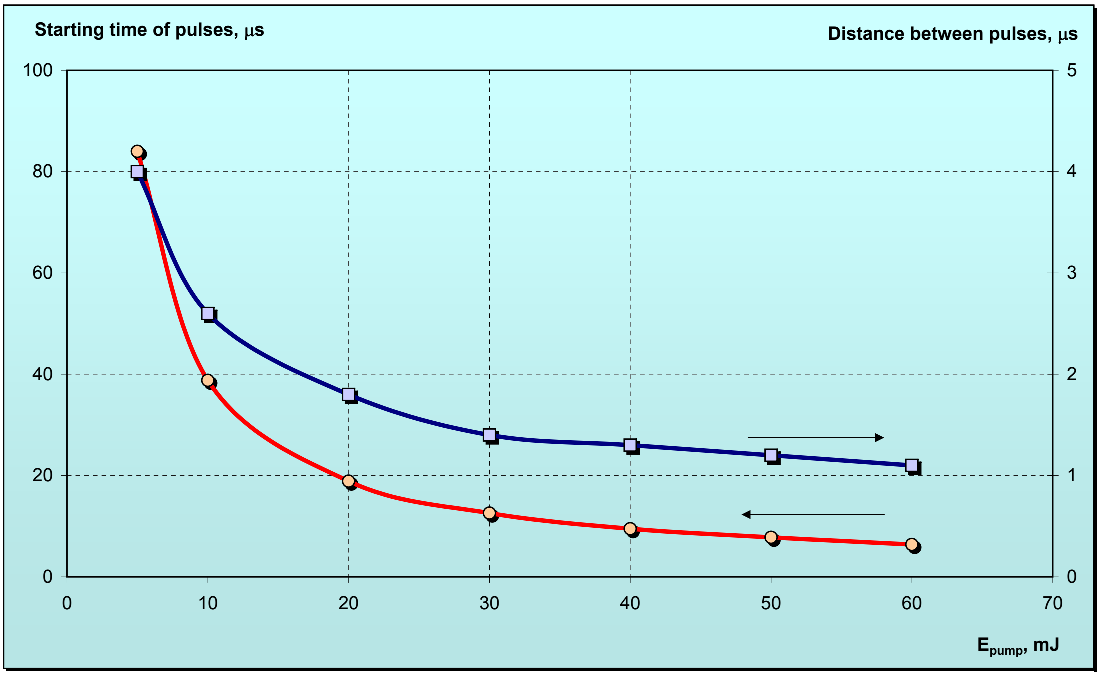

Figure 5.12: *Dependence of the starting time of the pulses and the distance between two pulses for 60 % reflectivity of the output coupler on pump energies varying from 5 to 60 mJ.*

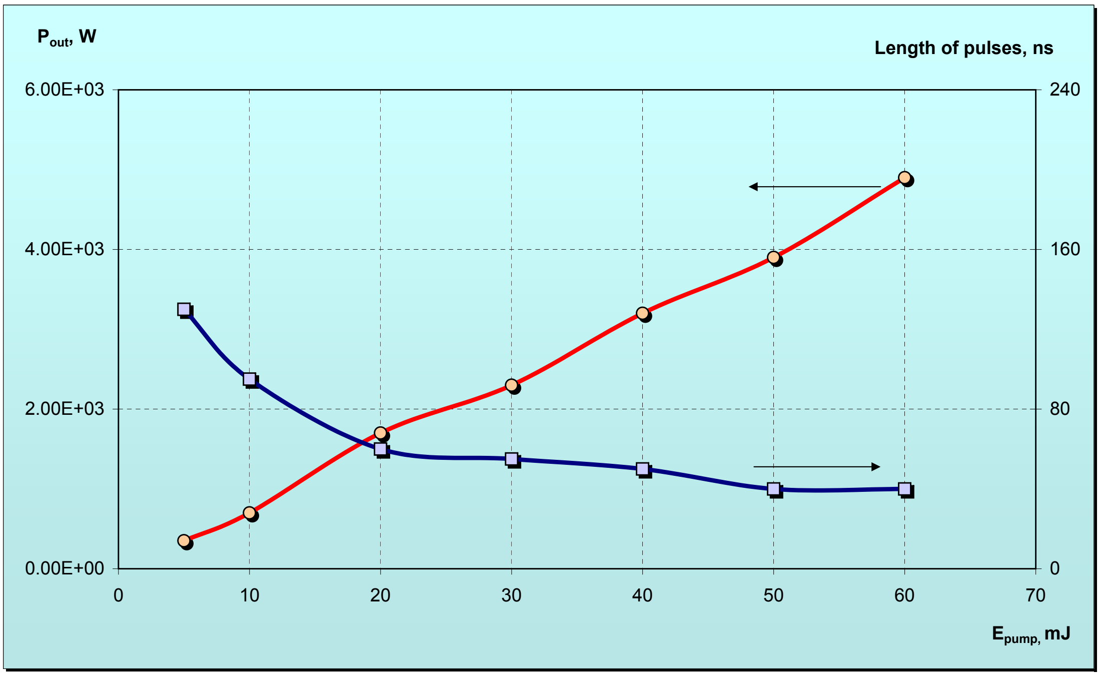

Figure 5.13: *Similar overview as in Figure 5.11 but for 90 % reflectivity of the output mirror.*

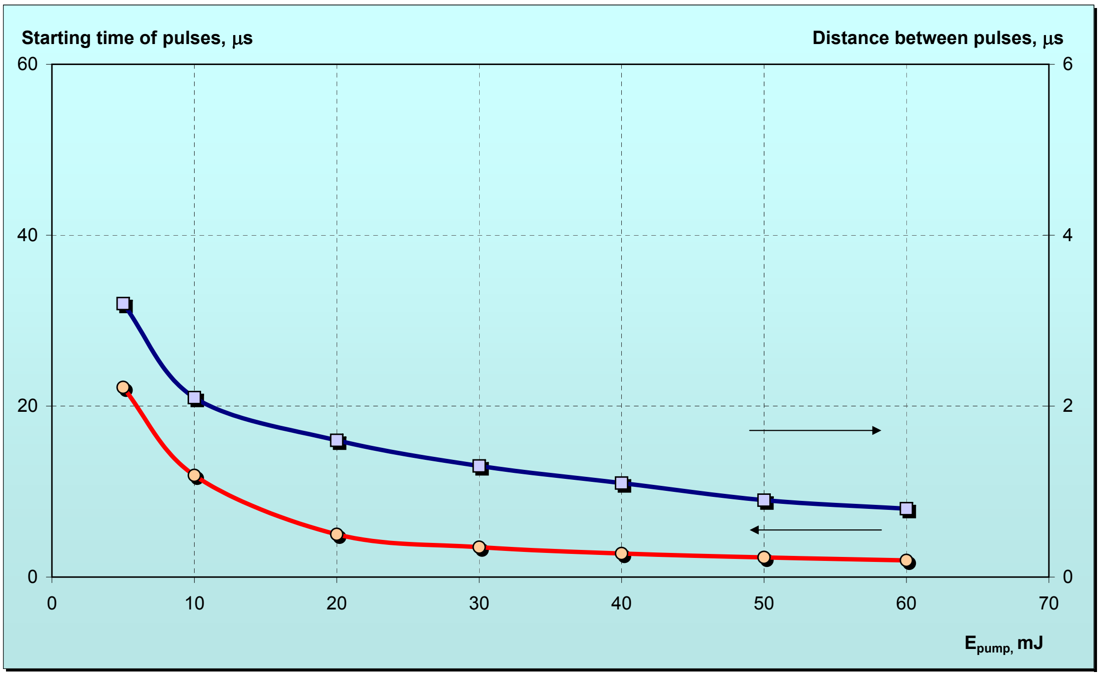

Figure 5.14: *Same conclusion as in Figure 5.12 but for 90 % reflectivity of the output mirror.*

This group of results, Figure 5.11, 5.12, 5.13, and 5.14 shows the overview for the output powers P_{out}, the lengths of the pulses, the starting times of the pulses and the distance between two pulses. P_{out} is higher in the case of 60 % reflectivity of the output mirror, the pulse development starts later in the case of 90 % reflectivity of the output coupler, in this case the pulses are also shorter and the distance between two pulses is shorter.

The temporal behaviour of the length of the pulses is the same in both cases for the different calculated pump energies with approximately the same values, the maximum output power is lower in the case of 90 % reflectivity of the output coupler. The biggest varieties are in the distance between two pulses and the starting times of the developed pulses. In the case of 5 mJ of introduced pump energy the pulses start later compared to the others and the same applies to the distance between the pulses too. The pulses start later at lower pump energies because the treshold level is reached later due to the slower increase of the population inversion N. These results were also calculated for 70 and 80 % reflectivity of the output mirror of the optical resonator and are presented in the following four graphics.

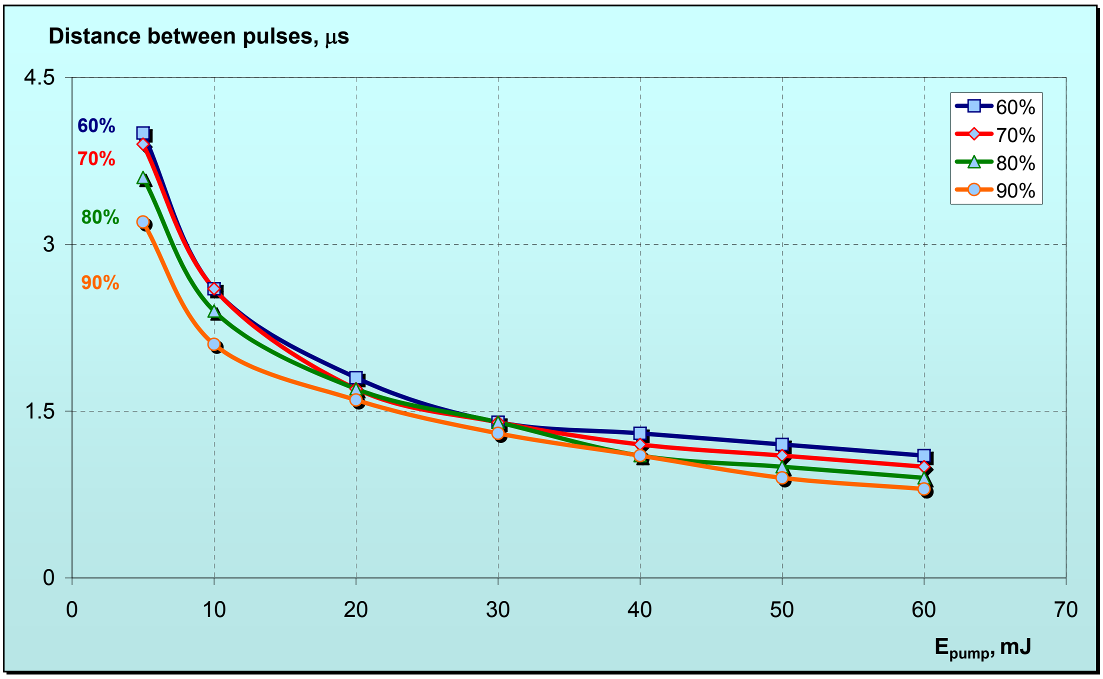

Figure 5.15: *Distance between two pulses for free lasing versus different reflectivities of the output mirror.*

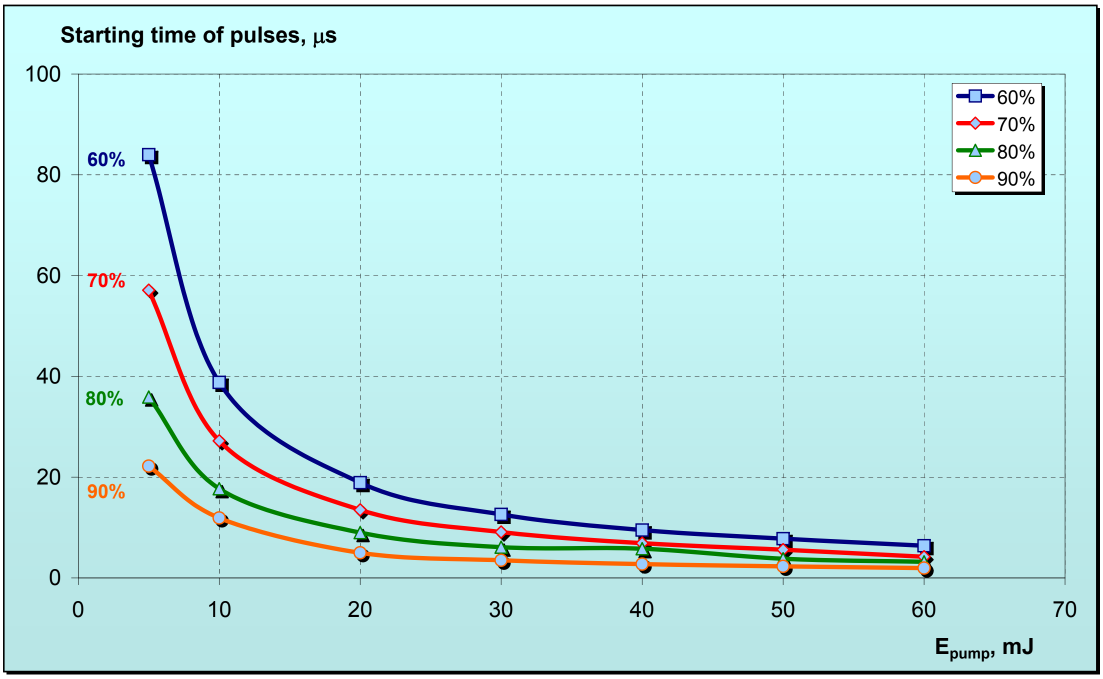

Figure 5.16: *Starting time of the pulses for free lasing versus different reflectivities of the output mirror.*

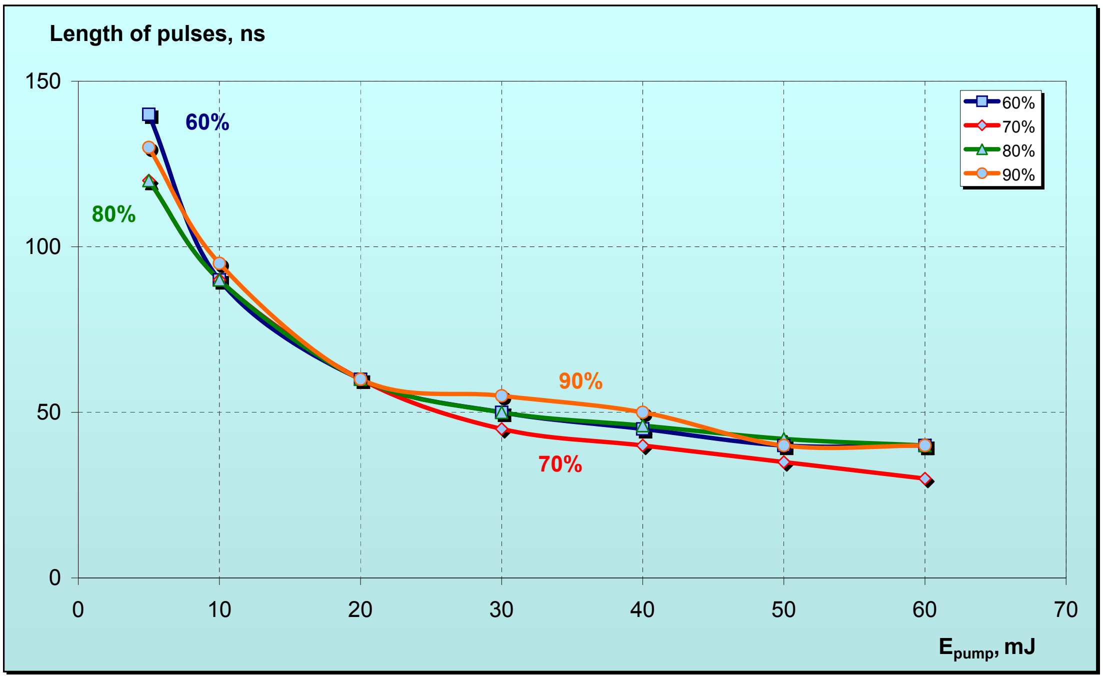

Figure 5.17: *Dependence of the length of the pulses for free lasing on different reflectivities of the output mirror.*

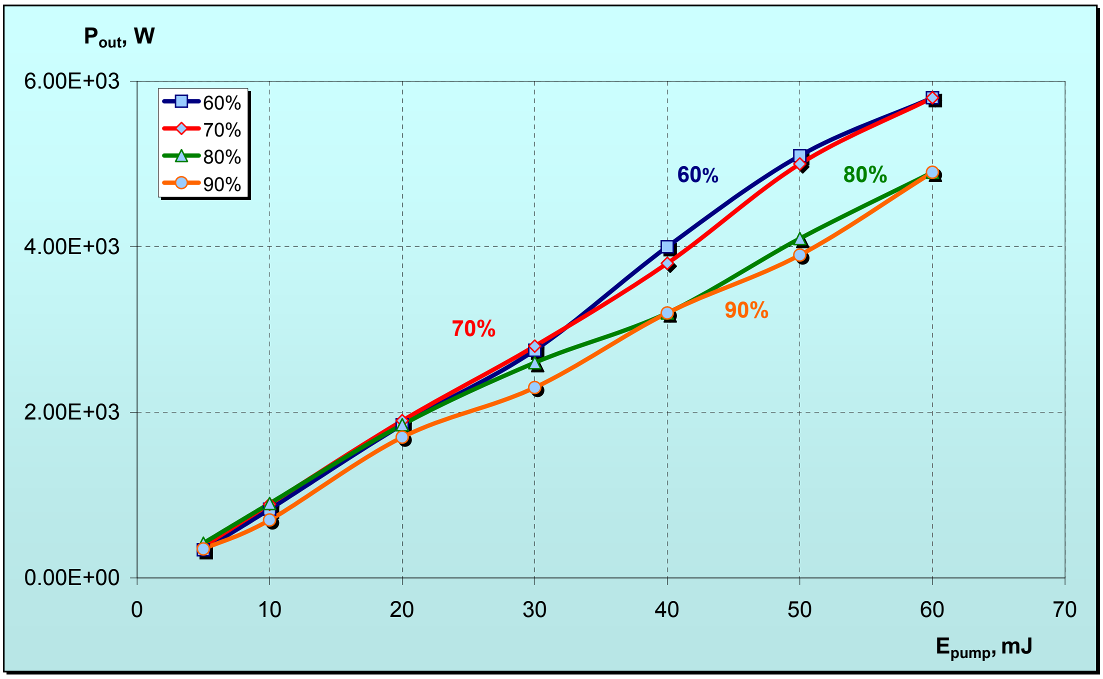

Figure 5.18: *Dependence of the output power P_{out} for free lasing on different reflectivities of the output mirror.*

In the group of figures, Figure 5.15, 5.16, 5.17, and 5.18 the results of the distance between two pulses, the length of the pulses, the starting time of the pulses and the output power P_{out} for 7 different pump energies and 4 different reflectivities of the output coupler are presented as the result for the case of free lasing. In these pictures the temporal behaviour of the compared parameters can be compared very easily to establish better understanding for the laser system in general.

The curve progressions for the different reflectivities are approximately the same, aside from the starting time of the pulses. In this case the difference between 60 % and 90 % reflectivity of the output mirror is significant higher than in the other compared parameters.

5.2 Simulation results of a system with active Q-switch

After a number of calculations for the case of free lasing a Q-switch was introduced into the laser system. The transmission of the closed Q-modulator was fixed at 10 % and the transmission of the opened Q-modulator was set to 90 % for the simulation and the optimisation of the system. Later on, these transmissions were also changed, the corresponding results are presented in the last section of this chapter.

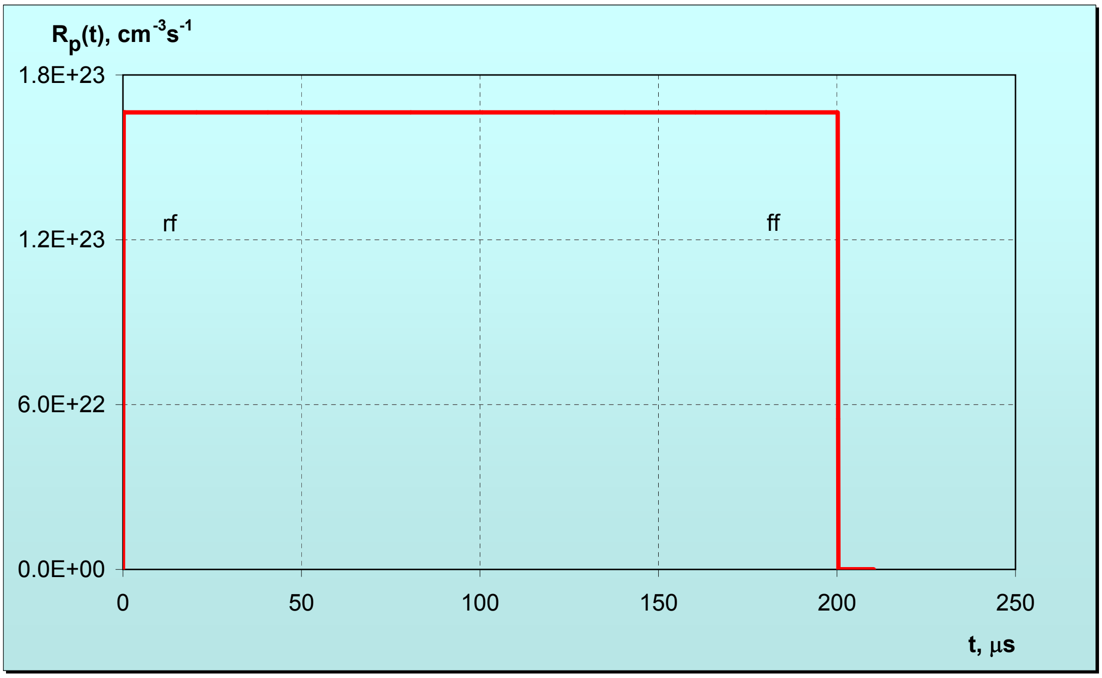

Figure 5.19: *The approximated pump pulse with a duration of 200 μs.*

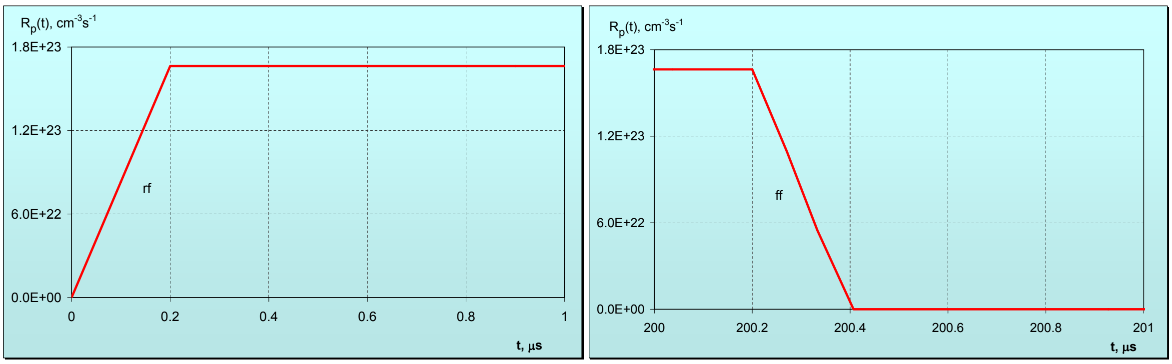

(a) (b)

Figure 5.20: *(a) Enlargement of the rising edge of the pump pulse from Figure 5.19. (b) Enlargement of the falling edge at the end of the pump pulse from Figure 5.19.*

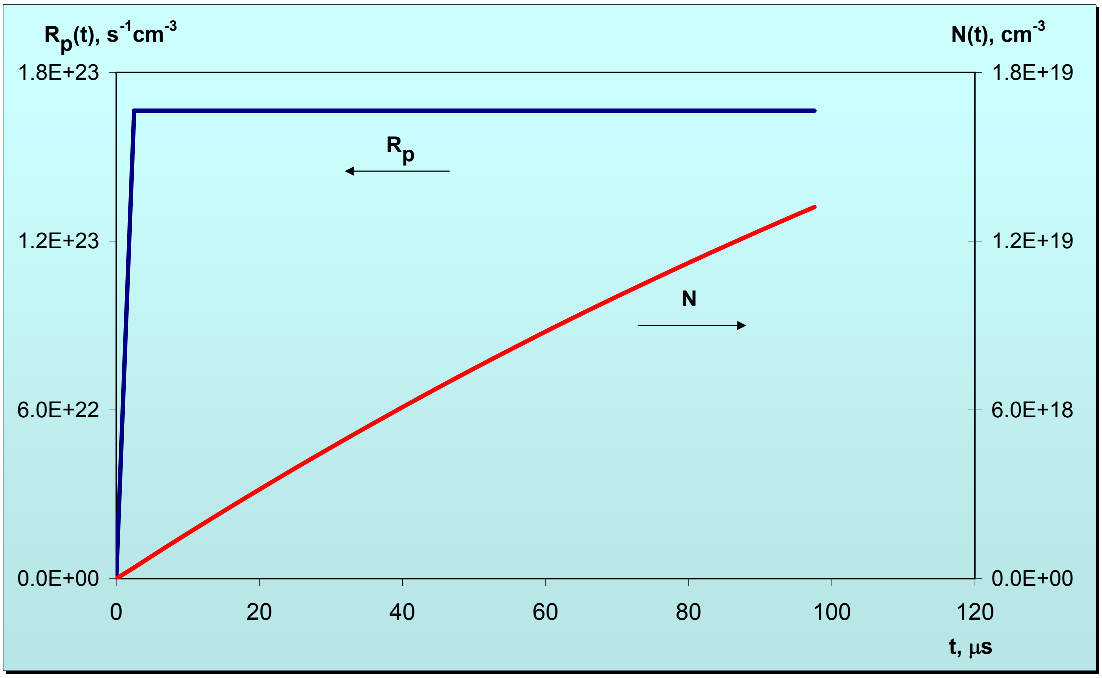

Figure 5.21: *The pump function $R_p(t)$ and the population inversion before opening the Q-switch which is introduced into the laser system.*

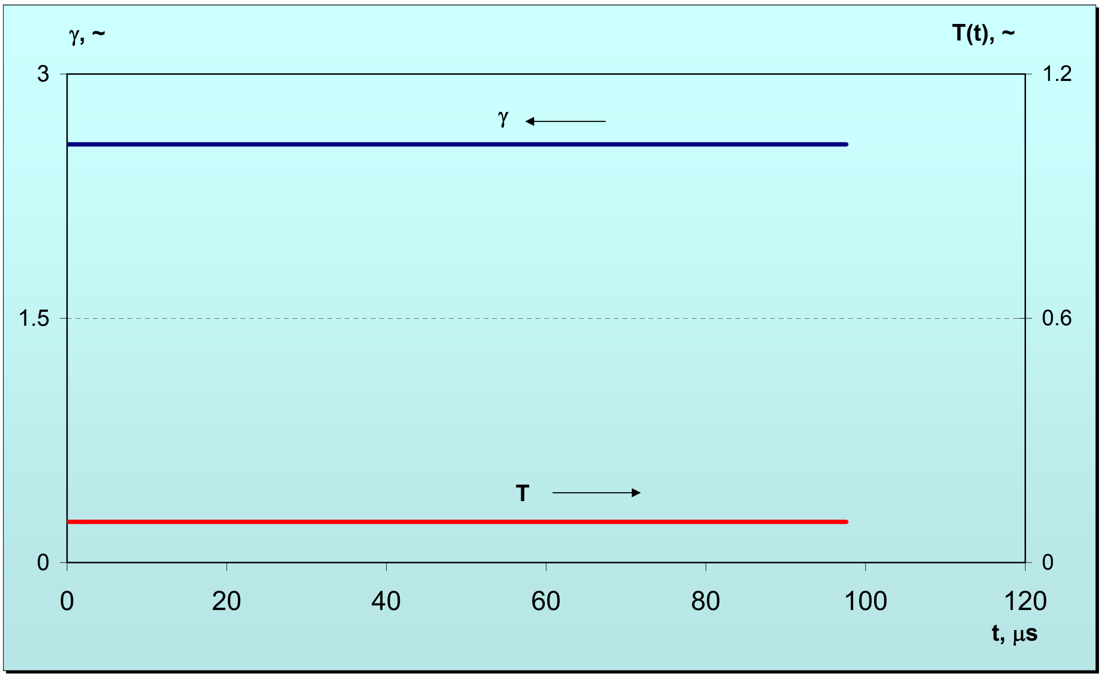

Figure 5.22: *The transmission T and the losses γ in the resonator before opening the Q-switch.*

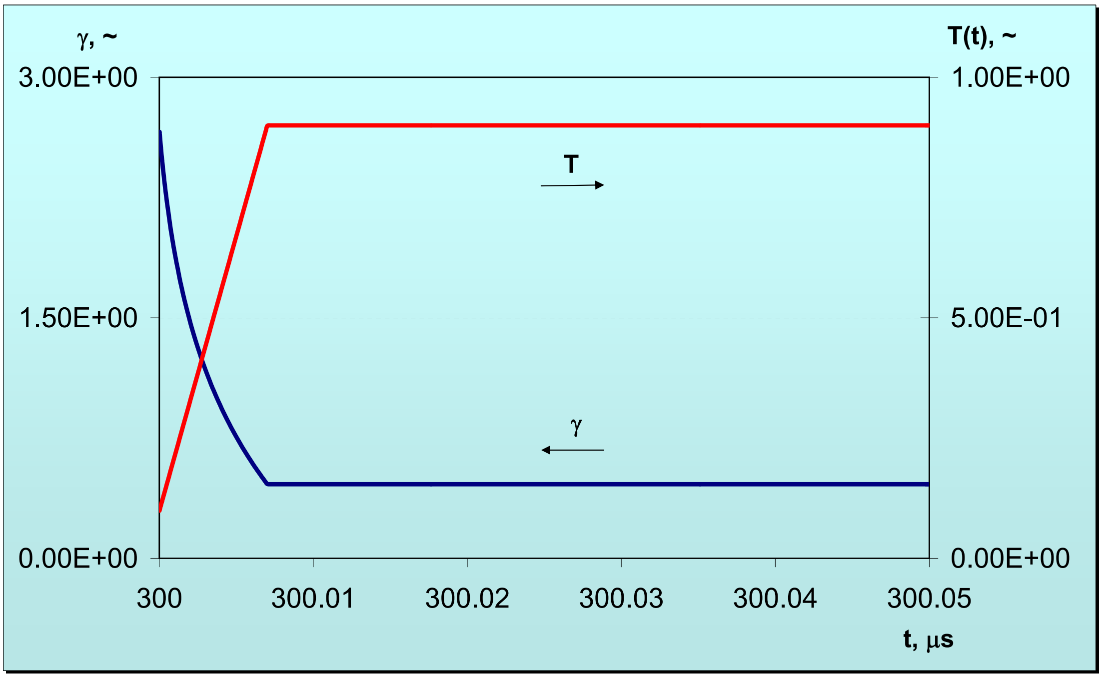

Figure 5.23: *The transmission T and the losses γ in the resonator after opening the Q-switch.*

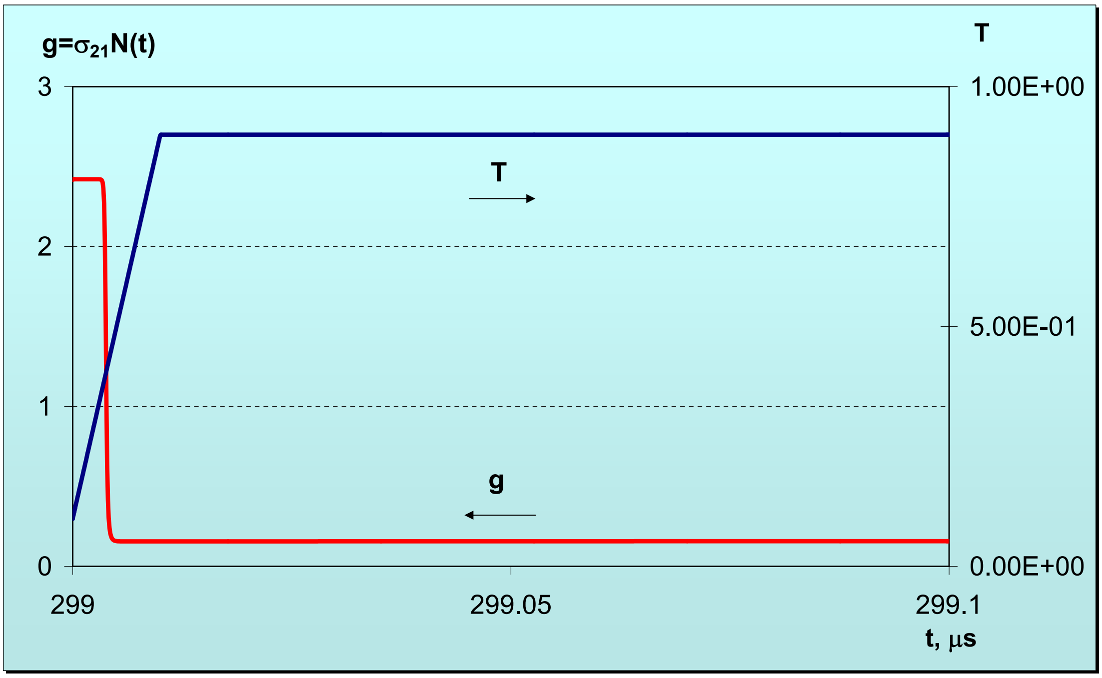

Figure 5.24: *The gain coefficient g after opening the Q-modulator.*

The first group of graphics in this section, Figure 5.19, 5.20, 5.21, 5.22, 5.23, and 5.24 present the approximated pump pulse $R_p(t)$, with an enlargement of the its rising and falling edges in Figure 5.20, the increasing population inversion N during the pump pulse, the combination of the losses γ of the resonator and the transmission T before opening the Q-switch in Figure 5.22 and after opening of the Q-switch in Figure 5.23. The losses γ are reduced due to the switching of the Q-modulator to a very low level and, as a consequence, immediately the transmission increases.

The gain coefficient g is displayed in combination with the transmission T in Figure 5.24. In the case of active Q-switching it is possible to choose the time for opening the modulator and this time for opening is one of the most important parameters. This influences the obtained results very keenly. A wrong time for opening leads to a situation like free lasing. It is not possible in this case to obtain the needed one single giant pulse for ignition.

The influences of the time for opening the Q-modulator are discussed more detailed in the following six graphics.

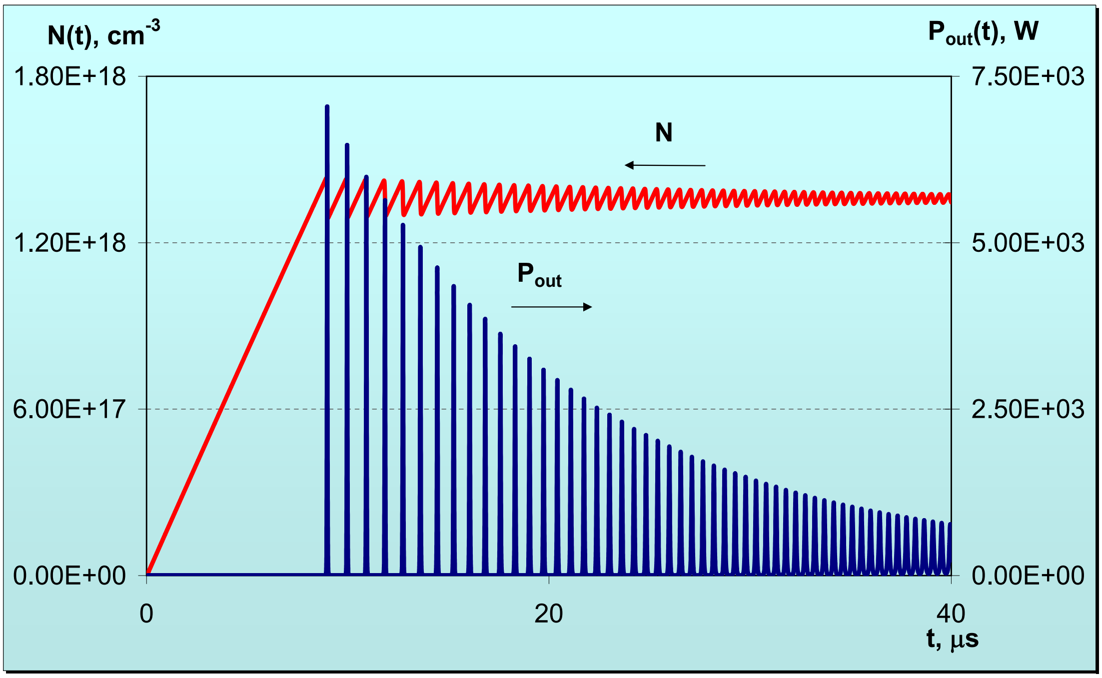

Figure 5.25: *The output power P_{out} and the population inversion N after very early opening of the Q-switch.*

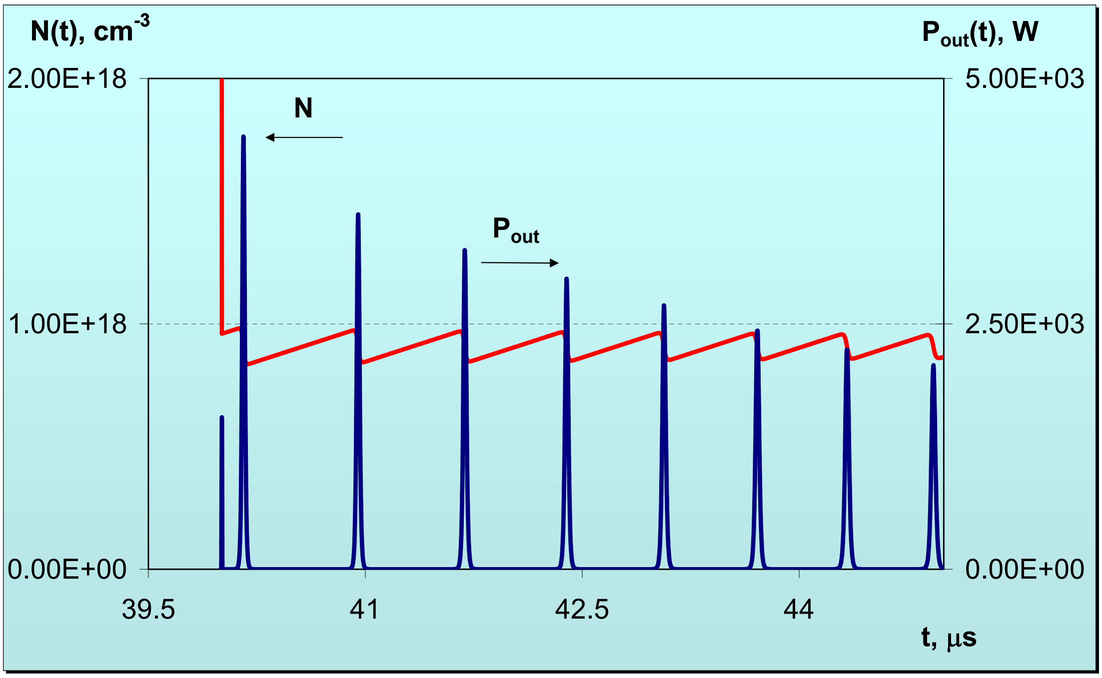

Figure 5.26: *Enlargement of Figure 5.25.*

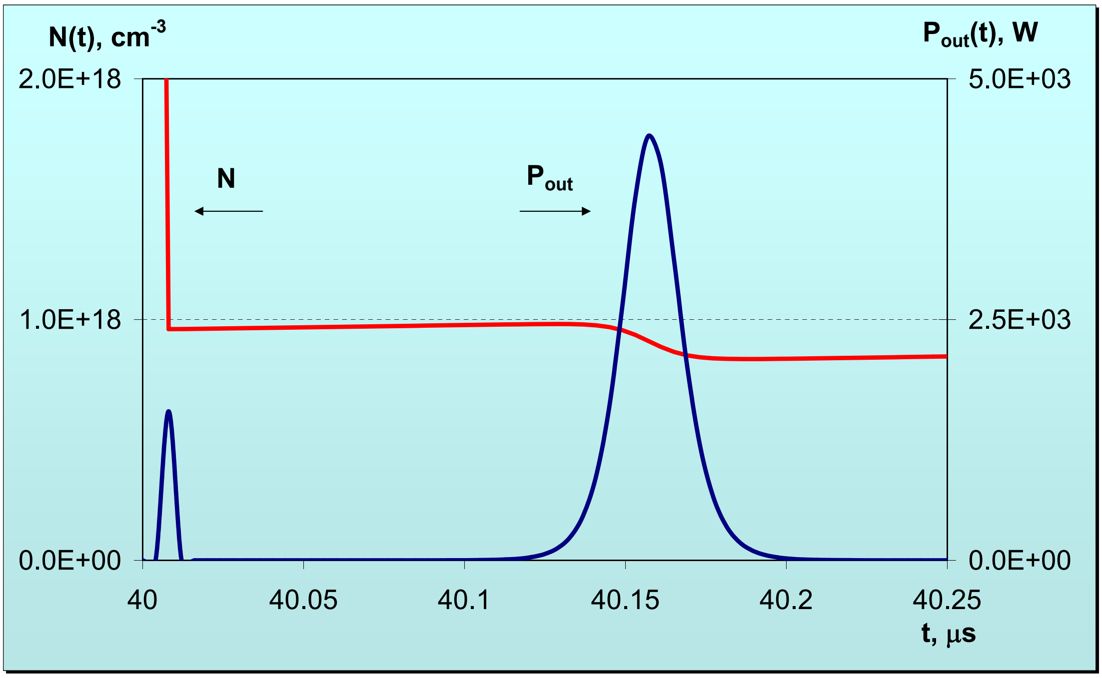

Figure 5.27: *One single pulse which is developed after opening of the Q-modulator.*

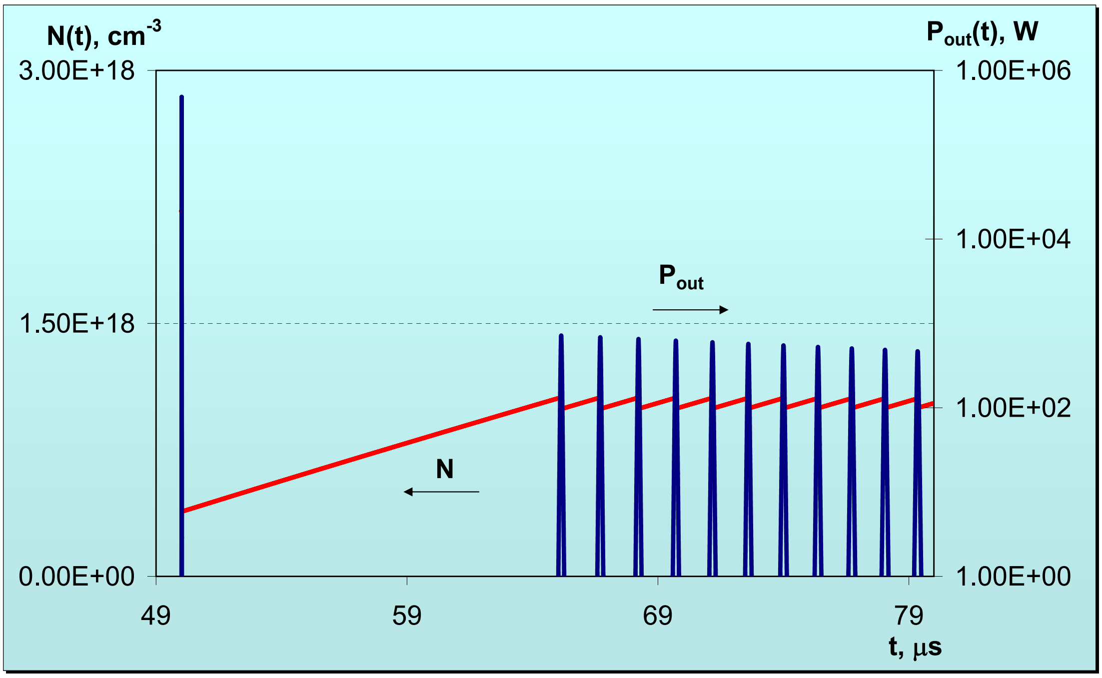

Figure 5.28: *Too early opening of the Q-switch leads to one single pulse and after this to the case of free lasing.*

In Figure 5.25, 5.26, 5.27, and 5.28 the Q-switch is opened too early to obtain one single giant pulse. The first developed pulse is in the range of several kW, but the inversion population increases again due to the introduced pump energy and after the treshold level is passed again, the next pulses are formed. This is the same situation like free lasing. The pulse length is $\approx 3\mu s$ compared to $\approx 4ns$ in the case of opening to Q-switch in the optimal time. The many developed pulses after the first strongest pulse are shown in Figure 5.28.

The possibility to choose the time for opening solves this problem. The result for proper moment of opening are displayed in the next two pictures.

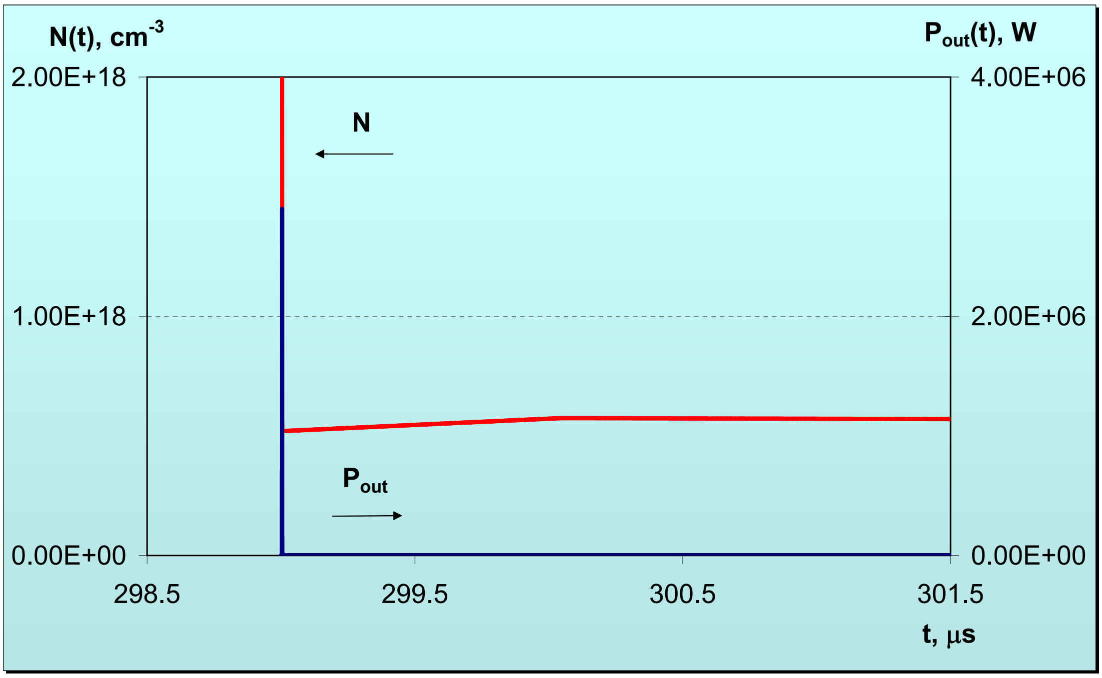

Figure 5.29: *One single giant pulse as a result of opening the Q-modulator at the end of the pump pulse.*

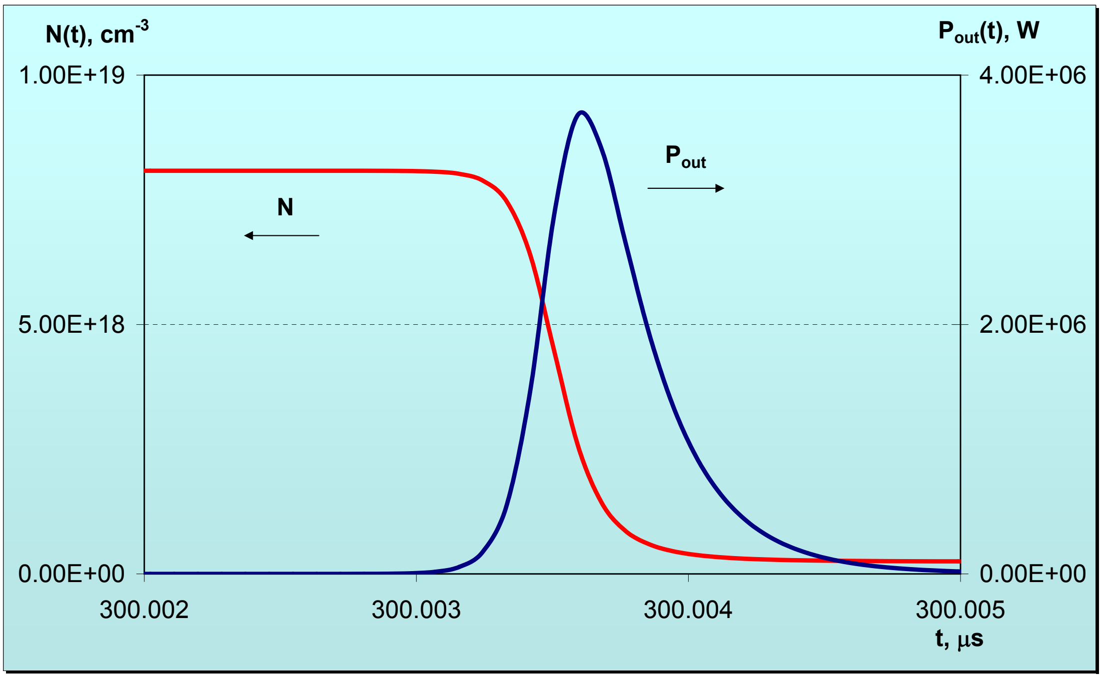

Figure 5.30: *Extension of Figure 5.29 for a better view of the obtained pulse.*

The desired single giant pulse which is necessary for laser ignition is presented in Figure 5.29. The best time for opening the Q-switch is at the end of the pump pulse, in this case one single pulse with a duration of ≈ 1 ns and a output power in the range of 4 MW is developed.

The calculation step-size h is also a very important parameter to recieve useful results. It has to be optimised for every single calculation dependent upon the aim of this calculation. If h is choosen too small, the abundance of obtained registered data points increases very quickly. On the other side, if h is choosen too large, there are not enough data points to approximate the obtained pulses satisfactorily. Two cases are presented as follows. In the first picture, Figure 5.31 every marked dot is one registered data point, so it is possible to approximate the giant pulse very well. In the second case, Figure 5.32 h is too large and it is not possible to recieve useful results regarding the important parameters of the laser system.

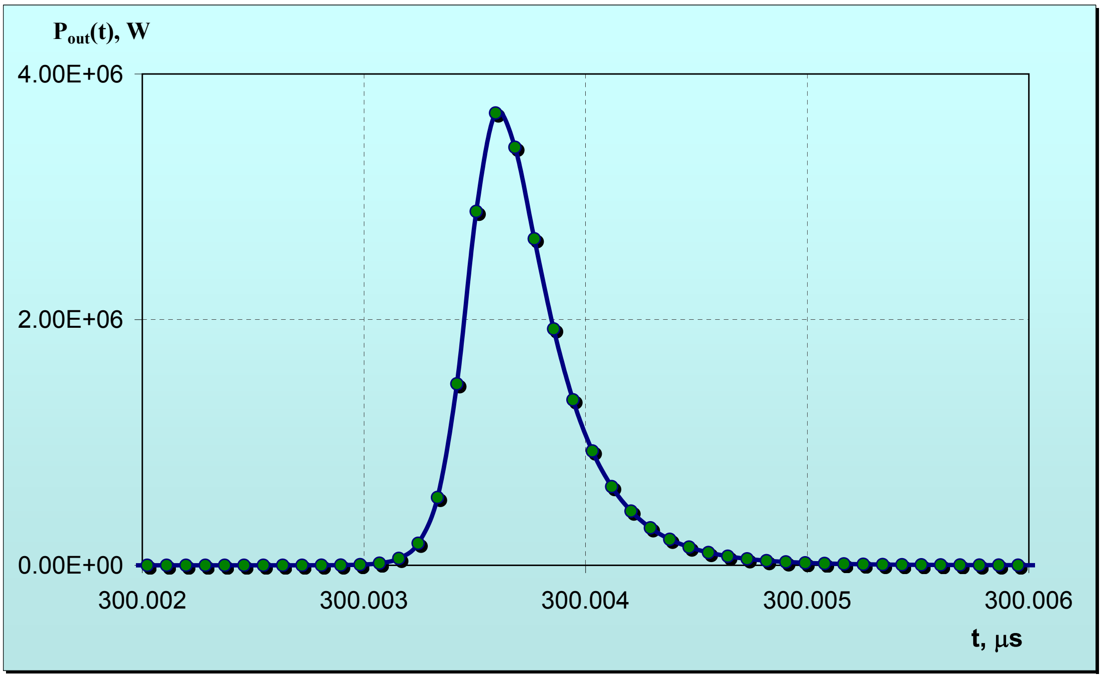

Figure 5.31: *The obtained pulse with very small calculation step-size h to recieve enough data points for best approximation of the pulse.*

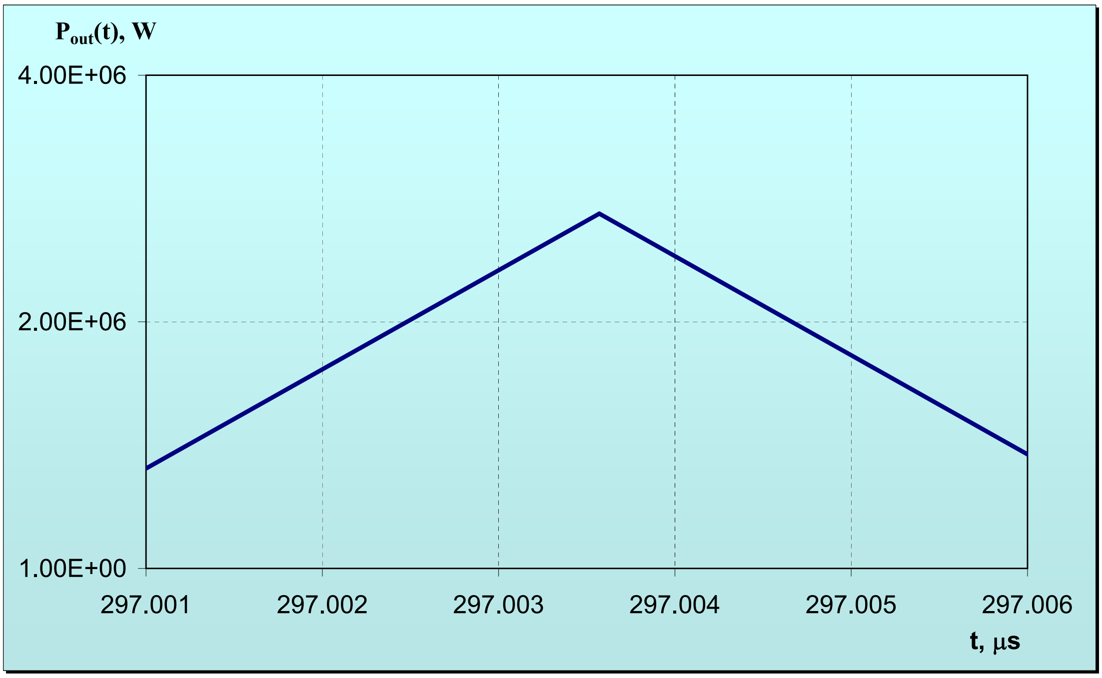

Figure 5.32: *The obtained pulse with a calculation step-size h being too large. There are not enough data points to approximate the pulse.*

5.2.1 Optimisation of the active Q-switched system

The next aim of the simulation was to find one best configuration for the laser system. In the case of active Q-switching it is possible to choose the time for opening the Q-modulator, the duration for opening the modulator can also be changed in order to increase the obtained giant pulse. Finally, the results for the best time for opening is fixed and the reflectivity of the output coupler is modified over the whole possible range. It is quite difficult to find one best configuration because changing of one parameter changes the whole laser system. Therefore, many calculations were necessary to find one configuration which was able to fulfill all the required parameters. Eventually, the simulations lead to the best configuration of the laser system and with this optimisation it is possible to obtain one single pulse with P_{out} over 4 MW and a pulse duration of $\approx$ 1 ns.

The obtained results of this optimisation are presented on the next three figures.

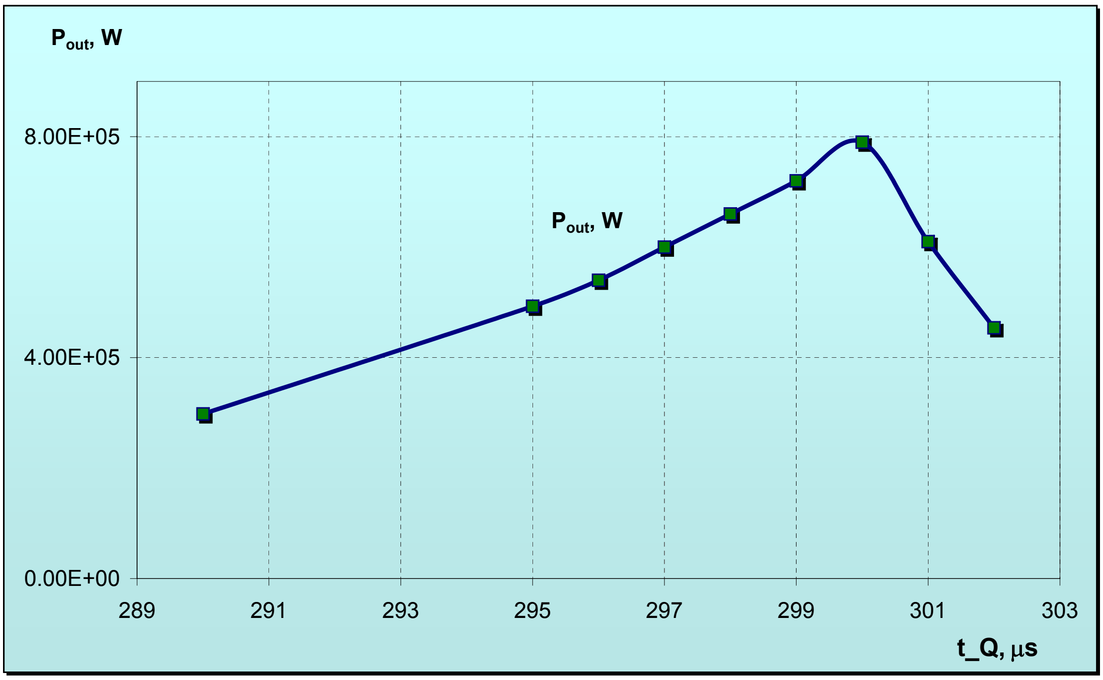

Figure 5.33: *P_{out} for different times of opening the Q-modulator. The pump duration was 300 μs.*

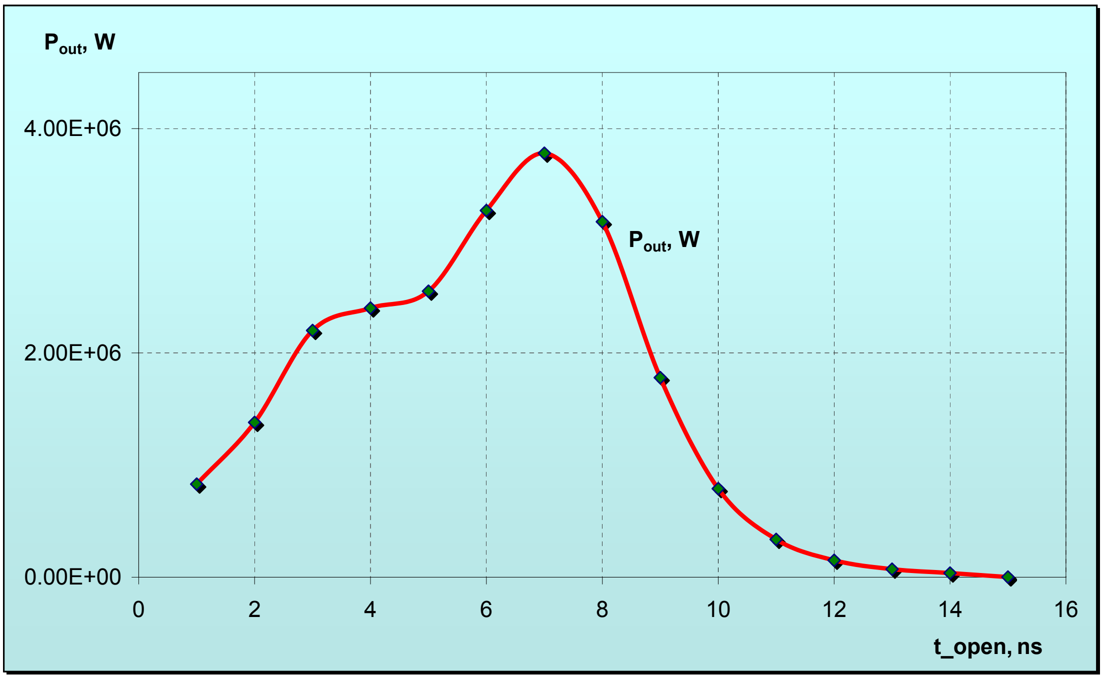

Figure 5.34: *P_{out} for different times untill the Q-modulator is completely opened. The best result from Figure 5.33 was fixed in the simulation.*

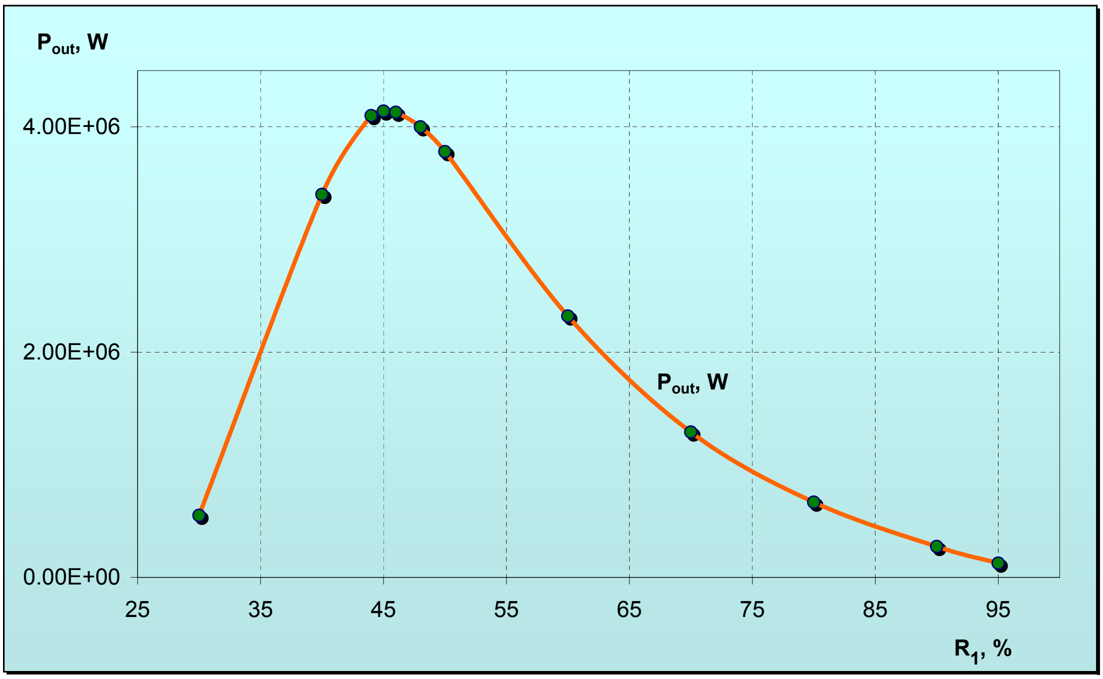

Figure 5.35: *P_{out} for different reflectivities of the output mirror. The best values from Figures 5.33 and 5.34 were fixed to find the best configuration.*

The best value was obtained for opening the Q-switch after 300 μs with a pump pulse duration of 300 μs. The time till the Q-switch is completely opened was set to 7 ns and the reflectivity of the output mirror was 45 % in the optimal case as shown in 5.35.

5.3 Computational variation of important parameters

In the last section of this chapter the results of the computational variation of the most important parameters are presented. The first part was a sensitivity analysis of the transmission T and the output energy E_{out}. The tranmission of the Q-switch was changed before and after opening it. The results of the energy E_{out} and the transmission T are displayed on the next four graphics.

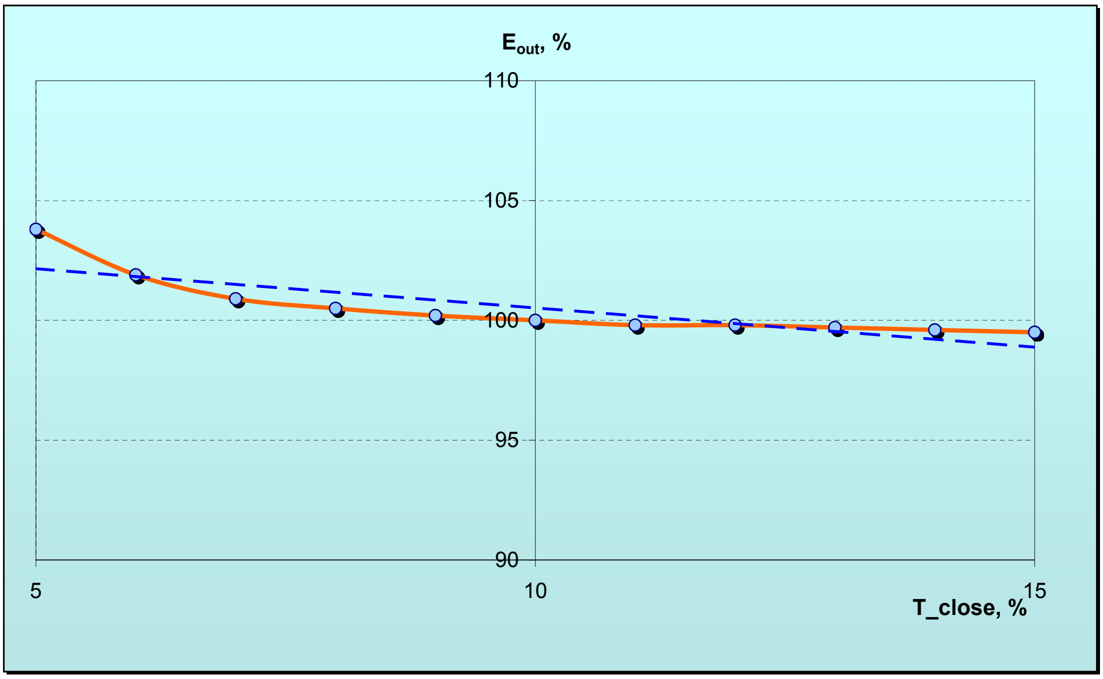

Figure 5.36: *Different values of the output energy E_{out} in the case of a changing transmission of the closed Q-switch. The blue-dashed line represents a regression line of the obtained results.*

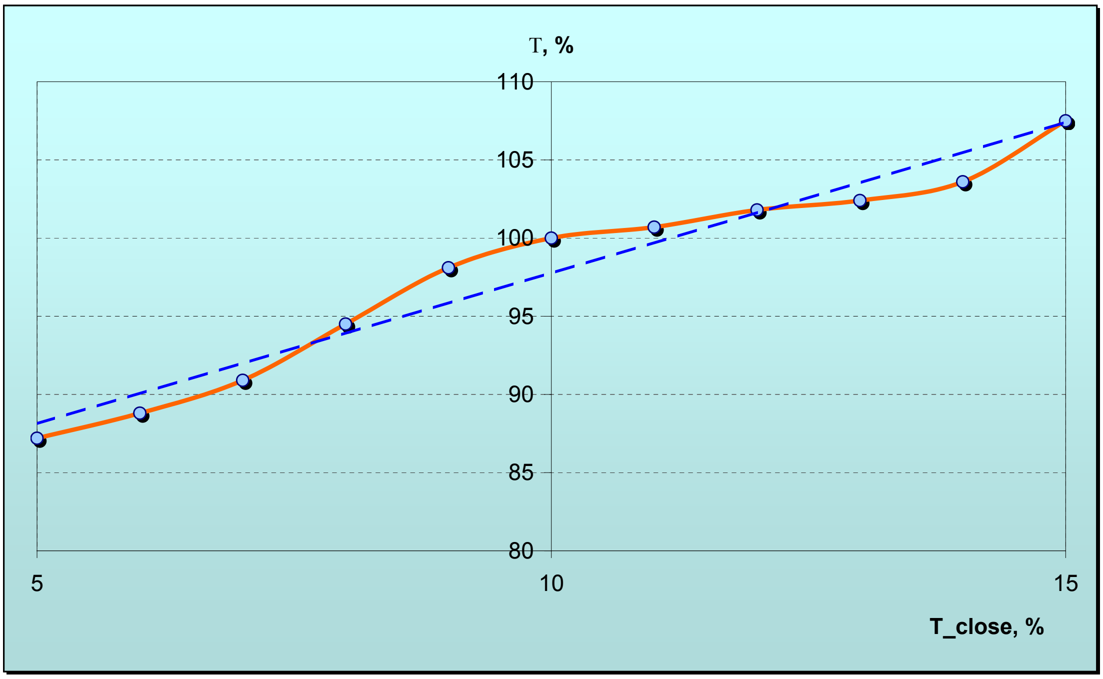

Figure 5.37: *Different values of the transmission T of the laser in the case of a changing transmission of the closed Q-switch.*

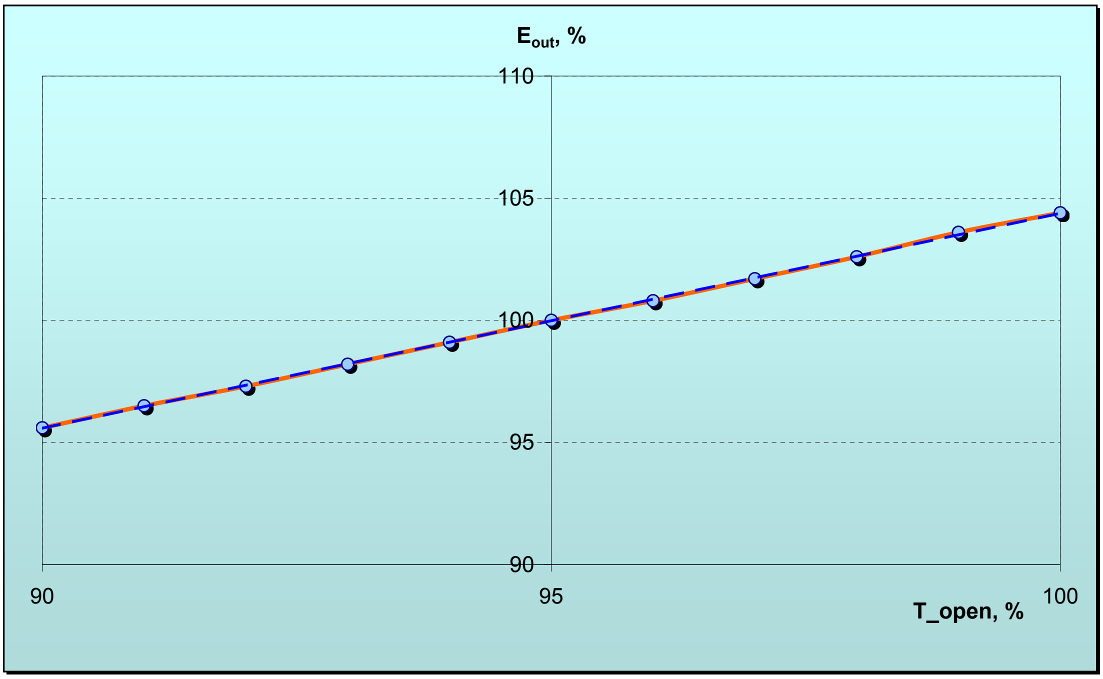

Figure 5.38: *Different values of the output energy E_{out} in the case of a changing transmission of the opened Q-switch.*

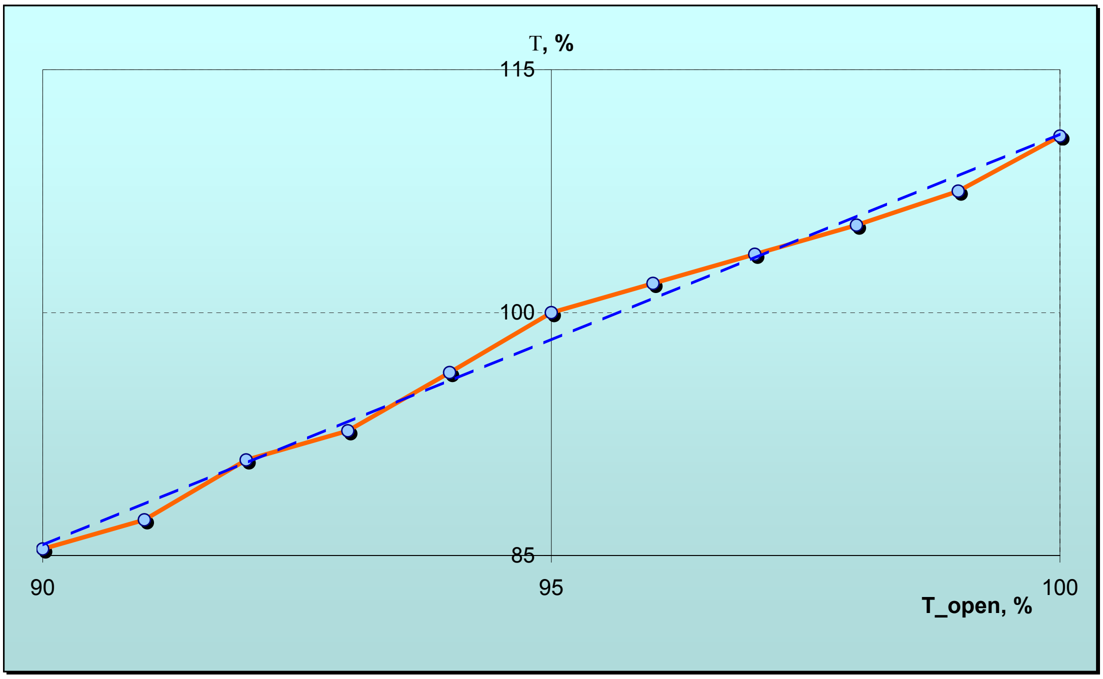

Figure 5.39: *Different values of the transmission T of the laser in the case of a changing transmission of the opened Q-switch.*

In Figure 5.36, and 5.37 the Q-switch is closed and 100 % in the sensitivity analysis correspond to 10 % transmission of the closed Q-switch. The transmission T is changing faster than the output energy E_{out}. In Figure 5.38, and 5.39 the Q-switch is opened and 100 % in the sensitivity analysis correspond to 95 % transmission of the opened Q-switch. A nearly linear changing can be seen in Figure 5.38. The variation of the transmission of the opened Q-switch leads to a bigger alteration of the transmission T compared to the closed Q-switch. That applies to the results of the output energy E_{out} too.

The last two groups of graphics in this chapter compare the maximum output power P_{out} for different cases. The simulation for 15, 25 and 40 mJ of introduced pump energy lead to the different results. In the last three graphics, the transmissions of the Q-switch are changed from 10 % and 90 % of the first case to 5 % and 95 % before and after opening of the Q-switch. The pump energies are the same to be able to compare the obtained results.

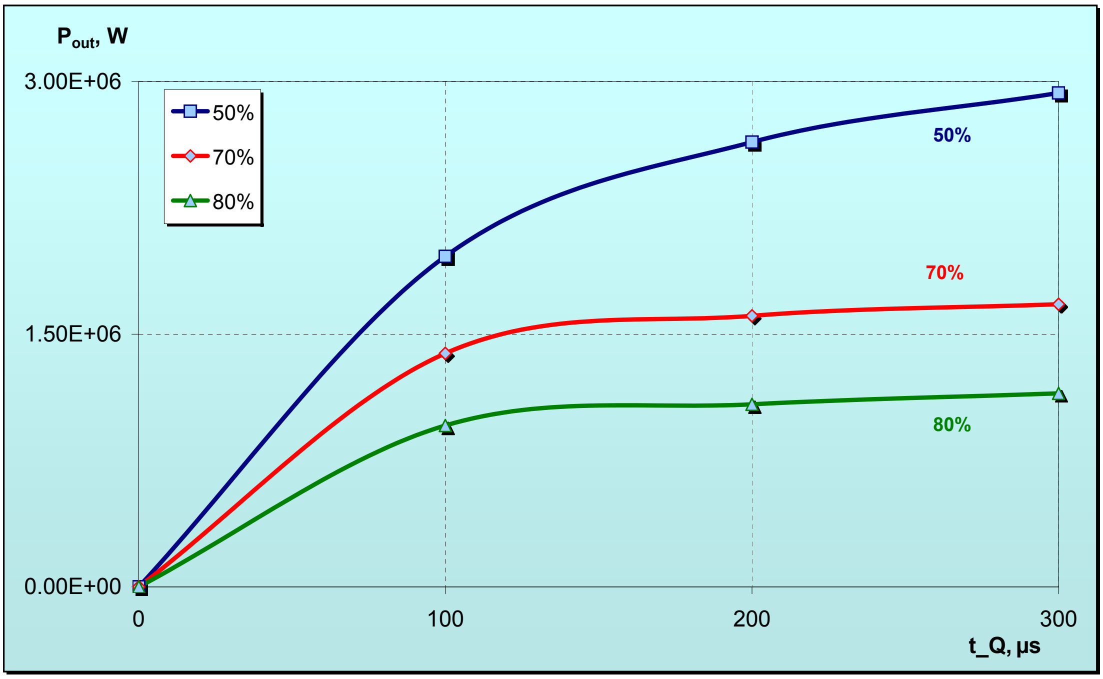

Figure 5.40: *Output power P_{out} in the case of 15 mJ of pump energy and 10 % and 90 % of transmission of the Q-switch. The three different presented curves correspond to three different reflectivities of the output coupler.*

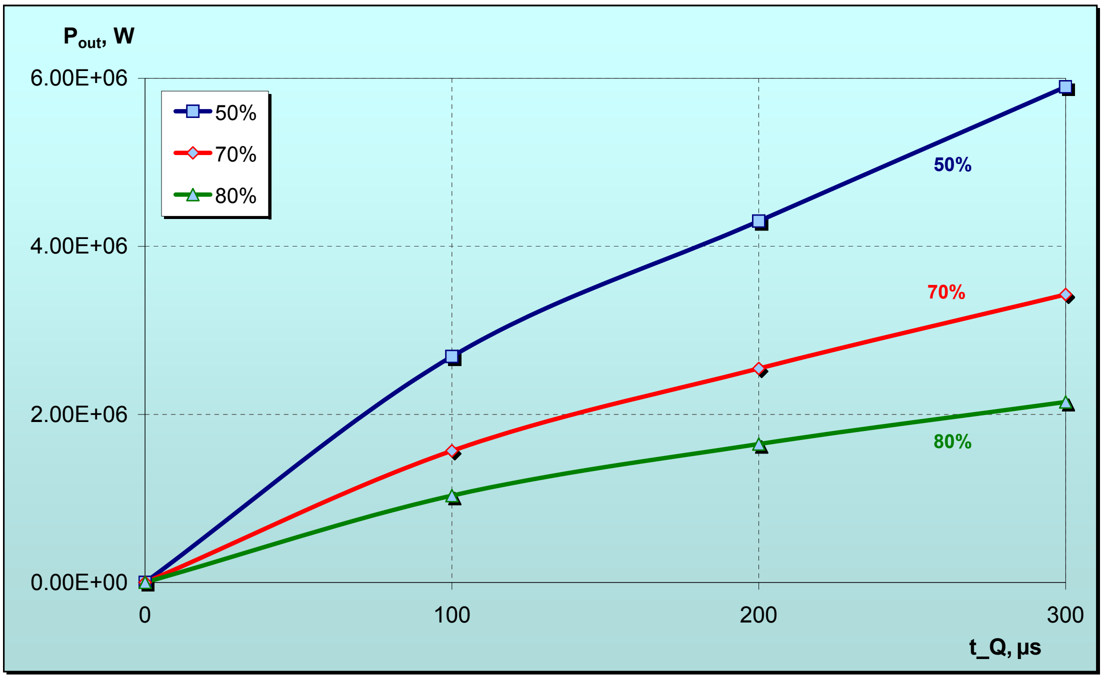

Figure 5.41: *Output power P_{out} in the case of 25 mJ of pump energy and 10 % and 90 % of transmission of the Q-switch.*

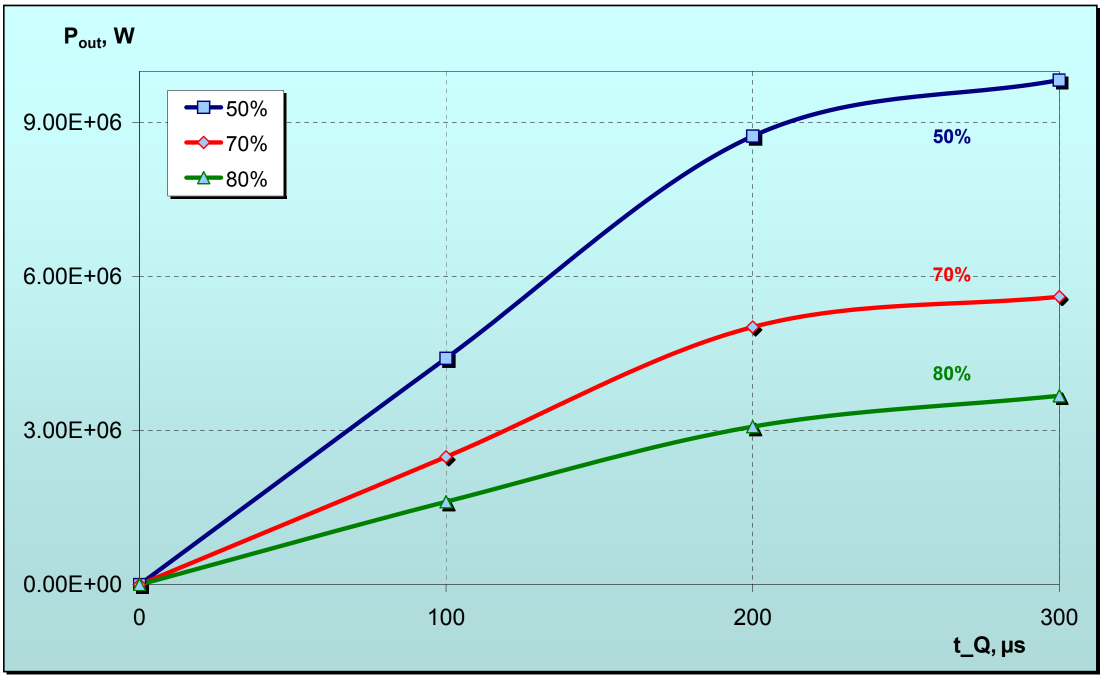

Figure 5.42: *Output power P_{out} in the case of 25 mJ of pump energy and 10 % and 90 % of transmission of the Q-switch.*

Figure 5.40, 5.41, and 5.42 show the different values for the output power P_{out} for the three chosen pump energies (15, 25, 40 mJ). This simulation was calculated for three different reflectivities of the output mirror (50, 70, 80 %). The highest values are obtained for 50 % reflectivity of the output coupler. The registered data points are 30 ns, 100, 200 and 300 μs at a pump pulse duration of 300 μs. The best values are at the end of the pump pulse after 300 μs. The values for the first data points after 30 ns are beneath 1 kW because the threshold level is not reached at this time. The next three graphics illustrate the same results but in the case of 5 % and 95 % of transmission of the Q-switch.

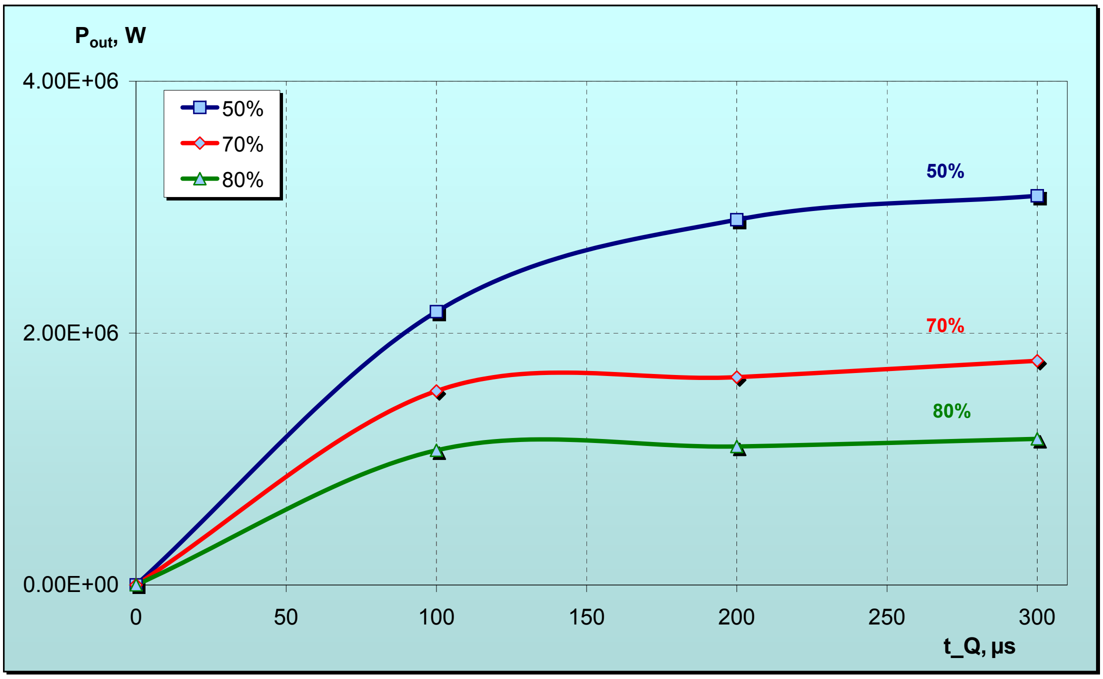

Figure 5.43: *Output power P_{out} in the case of 15 mJ of pump energy and 5 % and 95 % of transmission of the Q-switch.*

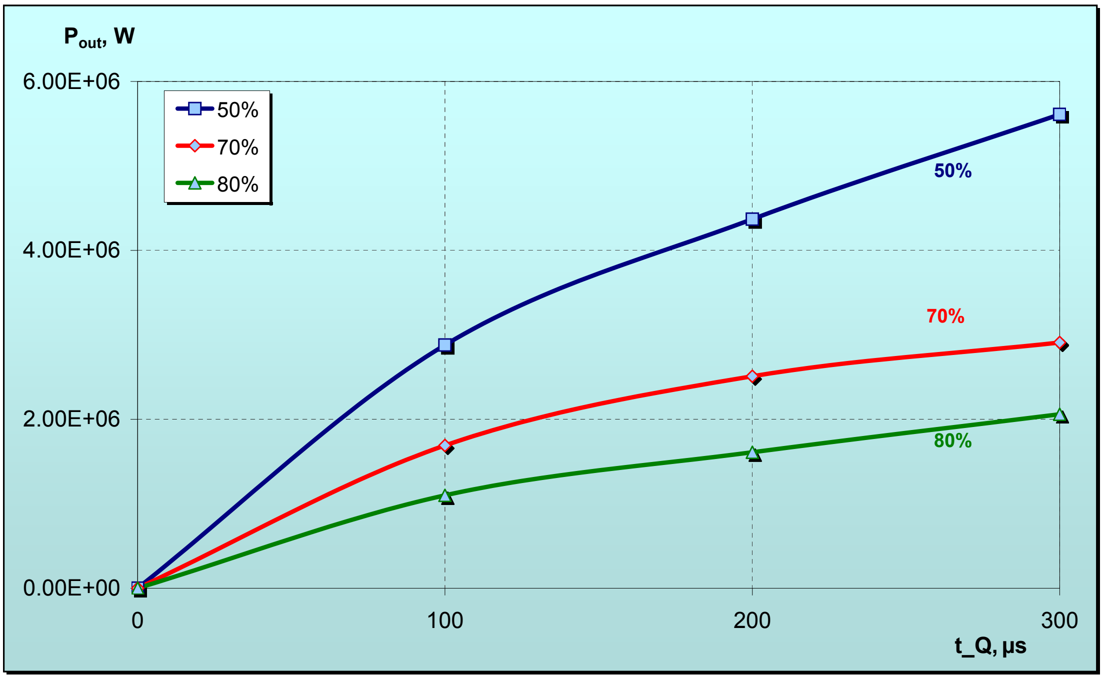

Figure 5.44: *Output power P_{out} in the case of 25 mJ of pump energy and 5 % and 95 % of transmission of the Q-switch.*

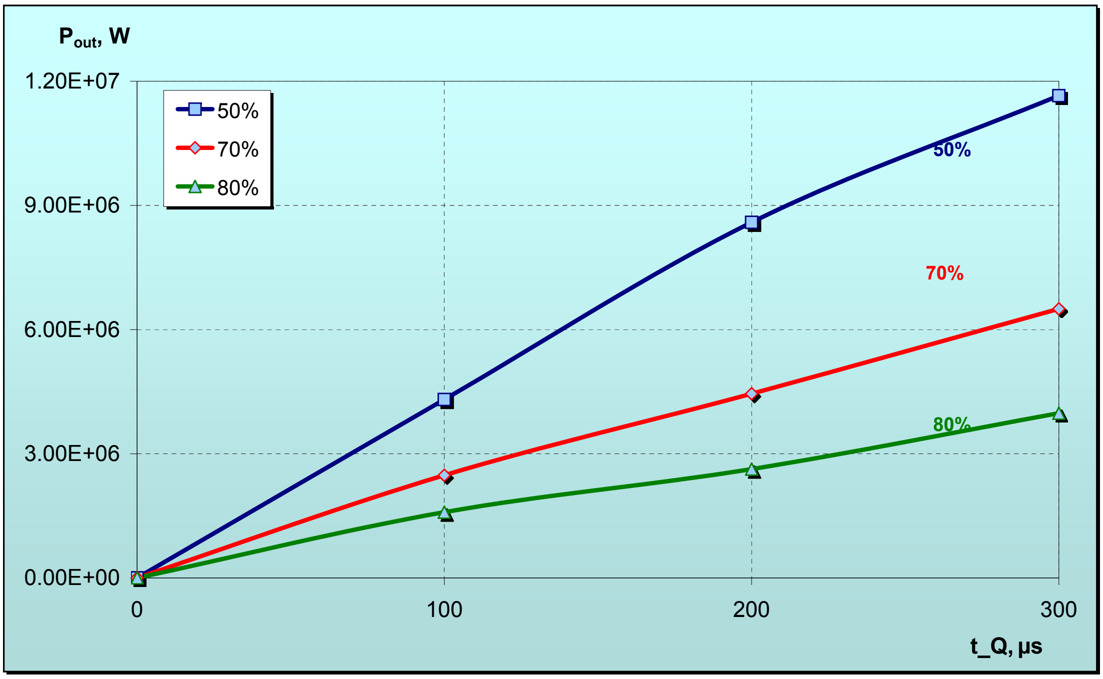

Figure 5.45: *Output power P_{out} in the case of 40 mJ of pump energy and 5 % and 95 % of transmission of the Q-switch.*

In Figure 5.43, 5.44, and 5.45 the results of 5 % and 95 % of transmission of the Q-switch are displayed. The temporal characteristics of the obtained curves are the same as in the first case. The highest values are at the end of the pump pulse, the first registered data points after 30 ns are beneath 1 kW due to the same reasons as in the first case and the maximum output power P_{out} is approximately the same for 15 and 25 mJ of pump energy. In the case of 40 mJ, the obtained values for the output power P_{out} are higher compared to the first case with 10 % and 90 % of transmission of the Q-switch.

6 Summary and Outlook

6.1 Summary

This work presents the calculation and simulation of a Q-switched laser system in order to develop an ignition spark plug. The basics of laser ignition are explained to understand the advantages of such an ignition system. Afterwards, the fundamentals of lasers are elucidated to establish better understanding for the basics of laser physics and laser systems. Both, the key elements of lasers and the main parameters of laser systems for ignition are explained in this chapter.

The theoretical description of Q-switched lasers is the background to understand the simulation and the results which are shown after this theoretical chapter. The calculation of one single roundtrip through the laser system is as important as the calculation of the treshold conditions or the output power. The last chapter includes some selected results of the many simulations of this laser system.

Summing up all the different simulations and calculations, the case of an active Q-switched solid-state laser system for ignition is a possible solution for the development of an ignition spark plug. Nevertheless, such a system has some disadvantages compared to a passive Q-switched laser system. The different simulations delivered the necessary results for the used laser system. The behaviour of the losses γ in the optical resonator, the transmission T, the developed pulses after opening of the Q-switch and the gain coefficient g were studied in the simulation.

Some of the simulations regard the case of free lasing, where no Q-switch is introduced into the laser system. The obtained pulses were analysed very detailed to compare the length of the pulses, the distance between two pulses, the starting time of the first formed pulse and the output power which is in the range of several kW. In order to increase the output power and to collect all the energy to one single giant pulse, a Q-switch is placed in the optical cavity. This leads to a higher level of the losses γ in the resonator but after switching on the Q-modulator these losses fall to a very low level and the giant pulse with an output power in the range of some MW is formed. There are several important parameters which influence the obtained results decisively. Changing one of these parameters may lead to completely different results. For that reason, the optimization of the laser system was very difficult. The proper time for opening the Q-switch which can be chosen freely in the case of active Q-switching, the duration till the Q-switch is completely opened and the reflectivity of the output mirror were changed to find the best condition.

The best value was obtained for opening the Q-switch after 300 μs with a pump pulse duration of 300 μs. The time till the Q-switch is completely opened was set to 7 ns and the reflectivity of the output mirror was 45 % in the optimal case as shown in Figure 6.1.

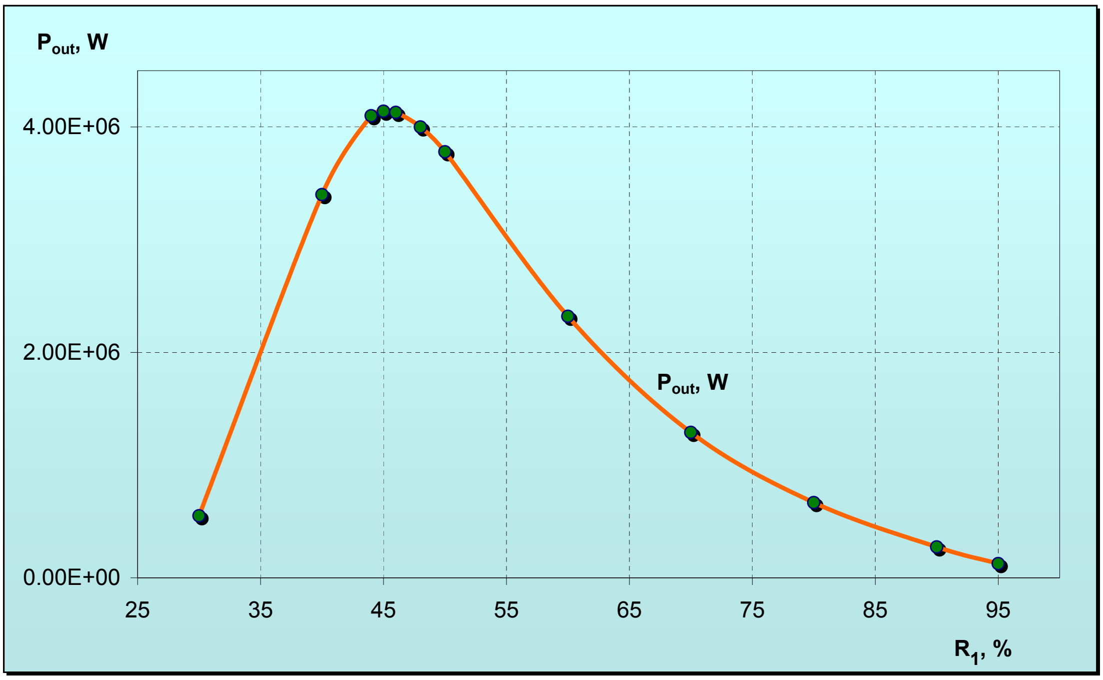

Figure 6.1: *P_{out} for different reflectivities of the output mirror. The best values for the time of opening of the Q-switch and the optimal duration till the Q-switch is opened were fixed before.*

In this best configuration for a duration of the pump pulse of 300 μs the maxiumum output power P_{out} reaches 4.2 MW, the duration of the single giant pulse is $\approx$ 1.5 ns, and the output energy E_{out} of the pulse is $\approx$ 2.5 mJ. The Q-switch is opened after 300 μs and the time for opening is set to 7 ns in this case.

Finally, a sensitivity analysis is presented to compare the output energy E_{out} and the transmission T of the laser system after while the starting and the end transmission of the Q-switch are changed slightly. The output power P_{out} was also calculated for three different introduced pump energies between 15 and 40 mJ, three different reflectivities of the output mirror between 50 and 80 % and two different transmissions of the Q-switch (10 % closed, 90 % opened and 5 % closed, 95 % opened). These results are also displayed in this diploma thesis.

6.2 Outlook

The next important steps after finishing all these simulations of an actively Q-switched solid-state laser system are the development of a passively Q-switched solid-state laser system which is even more useful for the application in a laser spark plug. The prototype of the laser spark plug contains such a passively Q-switched laser system. The complete simulation of a passively Q-switched laser system is necessary to obtain more results which are important for the development of the laser spark plug. The actively Q-switched laser system is not economically feasible due to mechanical and constructional restrictions. Most of the active Q-switched systems require high voltage and this can be avoided in the case of passive Q-switching.

The laser spark plug as realised in the laser ignition group at the Vienna University of Technology is displayed in Figure 6.2.

Figure 6.2: *Laser spark plug with a one euro coin to assess the size of the prototype.*

The simulation of the passively Q-switched system is very complicated because it is not possible to choose the time for opening of the Q-switch. In this case, the function of the transmission of the Q-switch is not depending on the time but is a function depending on the intensity. The time till the saturable absorber is bleached enough is difficult to assess. The intensity of the light is radial distributed according to a Gaussian profile and this is also indispensable to incorporate for the simulation of such a laser system.

The compromise of all the results of the simulations with the experimental conditions of the laboratory is also not finished yet.

Potential applications for the future of the vision of laser ignition are large stationary gas engines, direct fuel injection engines and rocket ignition systems. The possible applications of large stationary gas engines and direct fuel injection engines are displayed in Figure 6.3, 6.4.

Figure 6.3: *Large stationary gas engine from GE Jenbacher as a possible application for a laser ignition system.*

The application in large stationary gas engines requires both, the optimisation of the ignition processes and the adaption of the combustion processes. This is essential to ensure the advantages of the laser induced ignition concept. Testing the prototypes with conventional engines is difficult because the used engines are optimised for conventinal electic ignition.

The laser-induced ignition concept will be very important and indispensable for the future, because it won‘t be impossible to satisfy the exhaust emission standards without a new ignition concept in the future. It is also necessary to optimise the different components of the laser ignition system like the pump energy maintenance, the pump fibers, the incoupling optics and the coatings.

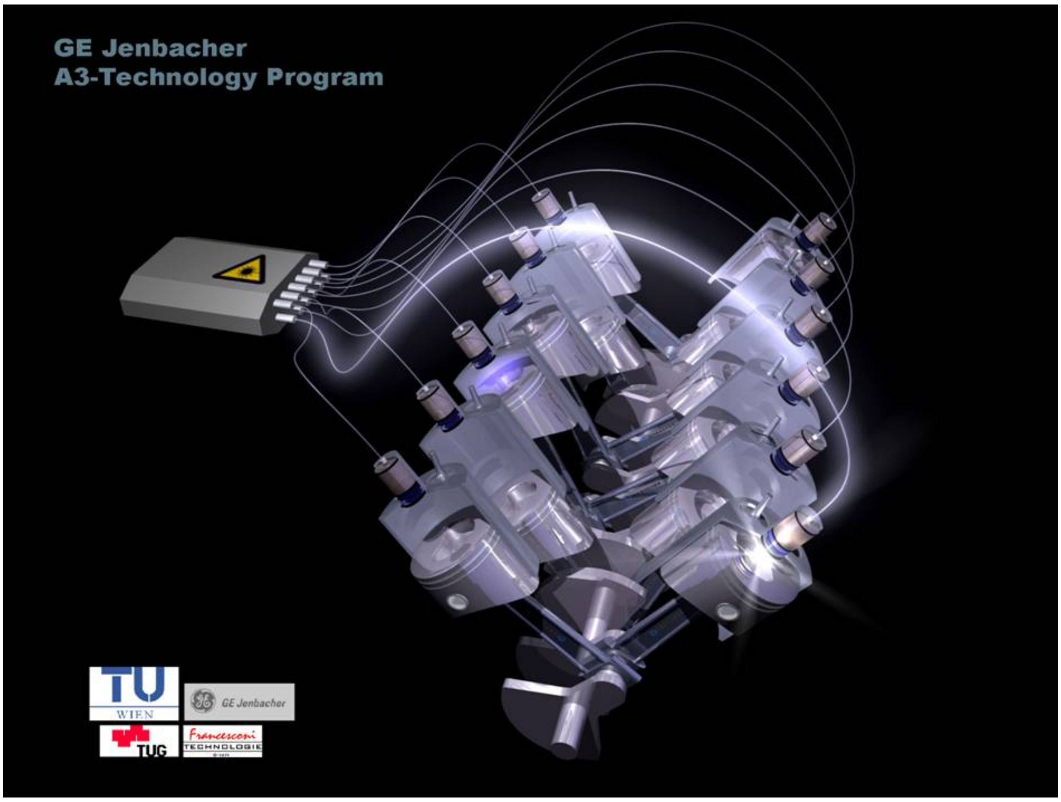

Figure 6.4: *Vision of a future laser ignition system applied in a direct fuel injection engine.*

The development of this promising new ignition concept is not finished yet. Many obstacles have been removed after several years of development, however only the next steps in the future may solve the last problems and difficulties of this concept.

7 Nomenclature

Parameters of the simulation

c_0	......	speed of the light
h_{Planck}	......	Planck's constant
PI	......	π
E_{pump}	......	pump energy introduced into the laser system
σ_{21}	......	emission cross section
N_{tot}	......	total number of particles
Tau	......	lifetime of the upper laser level
V_{am}	......	active volume
l	......	length of the resonator
n	......	factor of refraction
r	......	radius of the Nd crystal
s	......	area of the cross section
T_p	......	approximation of the rising edge of the pump function
T_{pto}	......	approximation of the plateau of the pump function
T_z	......	approximation of the falling edge of the pump function
P_{out}	......	output power
E_{out}	......	output energy
P_{outmax}	......	peak power
T_i	......	losses in the active medium due to scattering, absorption
L'	......	optical length of the resonator
h	......	step-size of the calculation
L	......	physical length of the resonator
q_{max}	......	maximum value of photons
a, c, k	......	coefficients for the approximation of Q-switch transmission curve
T	......	value of transmission which is saved for the next calculation step
F_1, F_2, F_3, F_4	......	variables of the Runge Kutta calculation
G_1, G_2, G_3, G_4	......	variables of the Runge Kutta calculation
Δ_t	......	duration of the pump pulse
V_{am}	......	cylindrical approximation of the active volume
l	......	length of the active medium
T_m	......	additional losses due to the Q-modulator
γ	......	total losses of the laser system

Specific laser parameters

σ	......	emission cross section
τ	......	lifetime of the upper laser level
ϕ	......	photon flux
α	......	absorption coefficient
λ	......	wavelength of light
ω	......	angular frequency of light
$\hbar$	......	Planck's constant
I_0	......	initial intensity
I_{rt}	......	intensity after one roundtrip
α	......	coefficient for absorption loss
β	......	coefficient for scattering loss
g	......	coefficient of amplification
Q	......	quality factor of the optical resonator
A_{21}, B_{12}, B_{21}	......	Einstein coefficients
N_i	......	number of particles in the different energetic levels
N_t	......	total number of particles in the laser system
$R_p(t)$	......	pump function
V_a	......	active volume of the laser system
γ	......	coefficient of total losses of the laser system
g_{th}	......	threshold coefficient of amplification
η_s	......	laser slope efficiency
$P(t)$	......	pump pulse
R	......	reflectivity of the output mirror
$T_{Qmodclosed}$	......	transmission before opening the Q-modulator
$T_{Qmodopened}$	......	transmission after opening the Q-modulator
T_0	......	initial transmission of the passive absorber
T_S	......	saturated transmission of the passive absorber
$\Delta\tau$	......	length of the laser pulse
E_{out}	......	energy of the laser pulse
Δt	......	duration of the pump pulse
P_{out}	......	power of the laser pulse
L	......	physical length of the resonator
L'	......	optical length of the resonator
l	......	length of the active medium
λ	......	air/fuel equivalence ratio
ϵ	......	compression ratio

Bibliography

[1] Dale, J.D., Edwards C.F., Oppenheim A.K.: *A Comparative Study of Plasma Ignition Systems.* SAE Technical Paper Series, 2004

[2] Ast, G.: *Vergleich Laserzündung mit Zündkerzenzündung.* Diploma Thesis TU Wien, 2004

[3] Kopecek, H.: *Laser Ignition of Gas Engines.* Dissertation TU Wien, 2004

[4] Weinrotter, M.: *Laser Ignition of Internal Combustion Engines- Basic Laser and Ignition Optics Developments, Engine Application and Optical Diagnostics.* Dissertation TU Wien, 2006

[5] Tauer, H.: *Development of an Ignition Laser.* Diploma Thesis TU Wien, 2006

[6] Schwarz, E.: *Laserentwicklung und -testung für Motorenzündung.* Diploma Thesis TU Wien, 2008

[7] Kofler, H.: *Brennraumfenster - eine Schlüsselkomponente der laserinduzierten Zündung von Verbrennungsmotoren.* Diploma Thesis TU Wien, 2005

[8] Puhl, M.: *Corona and Laser Ignition in Internal Combustion Engines - A Comparison to conventional spark plug ignition.* Diploma Thesis TU Wien, 2007

[9] Kofler, H., Tauer, H., Tartar, G., Iskra, K., Klausner, J., Herding, G., Wintner, E.: *An innovative solid-state laser for engine ignition.* Laser Phys. Lett. 4, 2007

[10] Pischinger, R., Kraßnig, G., Taucar, G., Sams, Th.: *Thermodynamik der Verbrennungskraftmaschine.* Neue Folge, Band 5, Springer Verlag, Wien, 1989

[11] Zacharias, F.: *Gasmotoren* Würzburg: Vogel, 2001

[12] Weinrotter, M., Kopecek, Wintner, E.: *Laser Ignition of Engines.* Laser Physics, No.7, 2005

[13] *Wikipedia, the free encyclopedia.*, 2006

[14] Wintner, E.: *Oral Laser Application* Buchkapitel Basic Infomation on Lasers Quintessenz Verlags-GmbH, Berlin 2006

[15] Aldrich, R.: *Laser Fundamentals* Buchkapitel, 2005

[16] Deneva, M.: *Solid-State Laser Engineering* Skriptum, Vienna University of Technology, 2008

[17] Reider, G.: *Photonik– Eine Einführung in die Grundlagen.* 2nd Edition, Wien, New York: Springer-Verlag, 2005

[18] Svelto, O.: *Principles of Lasers.* 4th Edition, New York: Springer-Verlag, 1998

[19] Koechner, W.: *Solid-State Laser Engineering.* 5th Edition, New York, Berlin, Heindlberg: Springer-Verlag, 1999

[20] Koechner, W. and Bass, M.: *Solid-State Laser Engineering. A graduade text.* 1st Edition, New York, Berlin, Heindlberg: Springer-Verlag, 2003

[21] *Encyclopedia of Laser Physics and Technology.* Available from: http://www.rp-photonics.com

[22] Slavov, D., Deneva, M., Stoykova, E., Nenchev, M.: *Tunable subnanosecond pulse generation in a ring dye laser bi-directionally pumped by overlapped nanosecond pulses.* Proceedings of SPIE - The International Society for Optical Engineering Volume 3571, 1999

[23] Taira, T., Kobayashi, T.: *Q-switching and frequency doubling of solid-state lasers by a single intracavity KTP crystal.* IEEE Journal of Quantum Electronics Volume 30, Issue 3, 1994

[24] Tsunekane, M., Inohara, T., Ando, A , Kanehara, K., Taira, T.: *Compact, high peak power, passively Q-switched micro-laser for ignition of engines* Conference on Quantum Electronics and Laser Science Conference on Lasers and Electro-Optics, 2008

[25] Liedl, G., Schuöcker, D., Geringer, B., Graf, J., Klawatsch, D., Lenz, H., Piock, W., Jetzinger, M., Kapus, P.: *Laser induced ignition.* Proceedings of SPIE - The International Society for Optical Engineering Volume 6346 PART 1, 2007

[26] Sali, E., Ignesti, E., Cavalieri, S., Fini, L., Tognetti, M., Buffa, R.: *A tuneable, single-mode titanium-doped-sapphire laser source with variable pulse duration in the nanosecond regime.* Optics Communications Volume 282, Issue 16, 2009

[27] Lange W.: *Einführung in die Laserphysik.* 2. Auflage, Darmstadt, 1994

[28] Kneubühl, F., Sigrist, M.: *Laser.* 6. Auflage Teubner Verlag, Wiesbaden, 2005

[29] Hering, E., Martin, R.: *Photonik Grundlagen, Technologie und Anwendung.* 1. Auflage, Springer Verlag Berlin Heidelberg, 2006

[30] Bahaa, E., Saleh, A., Teich, M.: *Grundlagen der Photonik.* 2. überarbeitete und erweiterte Auflage, Wiley-VCH Verlag Weinheim, 2008

[31] Geusic, J.: *Laser oscillations in Nd-doped yttrium aluminum, yttrium gallium and gadolinium garnets* Appl. Phys. Lett. 4, 1964

[32] Berry, A., Hanna, D., Sawyers, G.: *High power, single frequency operation of a Q-switched TEM00 Mode NdYAG laser*Optics Communications Volume 40, 1981

[33] Dubrov, V., Grishaev, R., Homenko, M., Zavalov, Y.: *Estimation of output beam characteristics of laser with unstable resonator and turbulent active medium* Laser Physics Volume 19, 2009

[34] Cui, Z., Li, D., Zhao, S., An, J., Li, M., Liang, J., Wang, W.: *Optimization of the peak power of doubly Q-switched lasers with both an acousto-optic modulator and a GaAs saturable absorber* Optics and Laser Technology, Volume 41, 2009

[35] Zayhowski, J., Kelley, P.: *Optimization of Q-switched lasers* IEEE Journal of Quantum Electronics, Volume 27, 1991

[36] Butcher, J.: *The numerical analysis of ordinary differential equations: Runge Kutta and General linear methods*, 1987

[37] Fehlberg, E.: *Klassische Runge Kutta Formeln 5. und 7. Ordnung mit Schrittweitenkontrolle* Computing, 4 (2), 1969

[38] Lambert, H.: *Numerical methods for ordinary differential systems, the initial value problem*, 1991

[39] Wu, X., Xia, J.: *Extended Runge Kutta like formulae* Applied Numerical Mathematics Volume 56, Issue 12, 2006

[40] Goeken, D., Johnson, O.: *Runge Kutta with higher order derivative approximations* Applied Numerical Mathematics Volume 34, Issue 2, 2000

[41] Schranz-Kirlinger, G.: *Numerische Mathematik* Skriptum zur Vorlesung an der Technischen Univerisät Wien, 2006

[42] Taschner, R.: *Höhere Analysis und Differentialgleichungen* Skriptum zur Vorlesung an der Technischen Univerisät Wien, 2005

[43] Taschner, R.: *Analysis 2* Skriptum zur Vorlesung an der Technischen Univerisät Wien, 2004

[44] Taschner, R.: *Funktionentheorie* Skriptum zur Vorlesung an der Technischen Univerisät Wien, 2006

Simulation

This section presents the used code for the simulation of the laser system, written in Borland PASCAL:

```
Program NdYAG_Q_switch;
Uses wincrt;
Label End_0, End_1, End_2 ;

Const Co = 3E+10;                {cm/s}
Const h_Plank = 6.626*1E-34;     {J*s}
Const PI = 3.1415;

   Var max_N  :  Single;
   Var Epump_Nd, E1, E2  :  Single;
   Var Lambda, Sigma21  :  Single;
   Var time, time_Q, t_open, T_Qmod_open, T_Qmod_close, T  :  Single;
   Var FileVar1, FileVar2  :  text;
   Var Ntot, Tau, Vam_Nd, Vam, l, n, r_Nd  :  Single;
   Var Tp, Tpto, Tz, time_for_registration  :  Single;
   Var Pout, Eout, Pout_max_Nd  :  Single;
   Var R1, R2, Re, Ti, gamai, gama1, gama2, gama  :  Single;
   Var Lprim, Lres_Nd  :  Single;
   Var h  :  Single;
   Var B  :  Single;
   Var Tau_c  :  Single;
   Var delta_t, Pp_max, R_p_max, Rpp, Rpump, Rp  :  Single;
   Var N_t_h, N_t  :  Single;
   Var Ng_t_h, Ng_t  :  Single;
   Var q_t_h, q_t  :  Single;
   Var F1, F2, F3, F4  :  Single;
   Var G01, G02, G03, G04  :  Single;
   Var H01, H02, H03, H04  :  Single;
```

```
Function R_p(time  :  Single)  :  Single;
  Begin
        If (time <= Tp) Then
            R_p := R_p_max * time / Tp
            Else If ((time <= (Tp + Tpto)) And (time > Tp)) Then
            R_p := R_p_max
                  Else If (time > (Tp + Tpto)) And
                  (time <= (Tp + Tpto + Tz))
                  Then
                  R_p := R_p_max * (1 + (Tp + Tpto - time) / Tz)
                  Else R_p := 0;
  End;  {R_p}

Function Q_modulator_open (time  :  Single)  :  Single;
 Begin
    if ((time>=time_Q) and (time < (time_Q+t_open))) then
     Q_modulator_open := ((T_Qmod_open-T_Qmod_close)/t_open)*time +
     (T_Qmod_close-((T_Qmod_open-T_Qmod_close)/t_open)*time_Q)
       else Q_modulator_open := T_Qmod_open;
  End;  {Q_modulator_open}

{---------  for Nd:YAG laser -----------}
Function f_t(N_t, q_t, time  :  Single)  :  Single;
Begin
   f_t := R_p(time) - B * q_t * N_t -  (1 / Tau) * N_t;
End; {f_t -> dN2/dt - opened Q_modulator}

Function f_t1(N_t, time  :  Single)  :  Single;
Begin
   f_t1 := R_p(time) - (1 / Tau) * N_t;
End; {f_t1 -> dN2/dt - closed Q_modulator}

Function g_t(N_t, q_t : Single)  :  Single;
Begin
   g_t := (B * Vam * N_t - (1 / Tau_c)) * q_t ;
End; {g_t -> dq/dt - opened modulator}
{------------- end Nd:YAG -------------}
```

```
BEGIN{--- --- }
    Tp := 30*1E-9;          {s}
    Tpto := 300*1E-6;       {s}
    Tz := 30*1E-9;          {s}
    time_Q := 300*1E-6;     {s}  {time for opening of the Q-modulator}
    t_open := 7*1E-9;       {s}  {time till Q-modulator is opened}
    T_Qmod_open := 0.9;          {Transmission of the opened Q-modulator}
    T_Qmod_close := 0.1;         {Transmission of the closed Q-modulator}
    delta_t := (Tp + 2*Tpto + Tz)/2; {s} {duration of pump pulse}
    l := 1.5 ;                 {cm}
    r_Nd:= 0.03 ;              {cm}
    Vam_Nd := PI*l*(sqr(r_Nd)); {cm^3}
    Epump_Nd := 15*1e-3 ;      {J}  {pump energy}
    Lres_Nd := 5 ;             {cm}

   { calculation of Nd:YAG }
    Vam := Vam_Nd;
    Ntot := 3E+19;            {cm^-3}
    Tau := 0.23E-3;           {s}
    n := 1.83;
    Ti := 0.01;
    gamai := -ln(1-Ti);
    Lprim := Lres_Nd+(n-1)*l;
    R1 := 0.50 ;              {output mirror}
    R2 := 0.99999 ;           {signal mirror}
    gama1 :=-ln(R1);
    Sigma21 := 3*1E-19 ;      {cm^2}
    B := (Sigma21*l*Co)/(Vam*Lprim);
    Lambda:= 1064*1E-7;       {cm}
    Pp_max := Epump_Nd / delta_t ;
    R_p_max := Pp_max/((h_Plank*Co/(808*1E-7))*Vam) ;
    h := 1*1E-10 ;            {s}
    time_for_registration := 0 ;


{before opening of the Q-modulator}

  Assign(FileVar1,'C:\franz\Q_closed.txt');
  Rewrite(FileVar1);
```

```
    N_t := 0;
    time:= 0;
    Re := sqr(T_Qmod_close)*R2;
    gama2 :=-ln(Re);
    gama := 0.5*(gama1+gama2) + gamai;
    Write(FileVar1,(time*1E+6));  {microseconds}
    Write(FileVar1,R_p(time));
    Write(FileVar1,(N_t));
    Write(FileVar1,gama);
    Write(FileVar1,q_t);
    Write(FileVar1,T_Qmod_close);
    Writeln (FileVar1,N_t*sigma21);

  repeat
      If KeyPressed Then GoTo End_1;

    If (time_for_registration >= 5000*h)  Then
      Begin
      Re := sqr(T_Qmod_close)*R2;
      gama2 :=-ln(Re);
      gama := 0.5*(gama1+gama2) + gamai;
      Writeln(time*1E+6:5:5, '    ', N_t);
      Write(FileVar1,(time*1E+6));  {microseconds }
      Write(FileVar1,R_p(time));
      Write(FileVar1,(N_t));
      Write(FileVar1,gama);
      Write(FileVar1,q_t);
      Write(FileVar1,T_Qmod_close);
      Writeln (FileVar1,N_t*sigma21);
      time_for_registration := 0;
    End;

        F1 := h * f_t1(N_t, time);
        F2 := h * f_t1(N_t + 0.5 * F1, time + 0.5*h);
        F3 := h * f_t1(N_t + 0.5 * F2, time + 0.5*h);
        F4 := h * f_t1(N_t + F3, time + h);

        N_t_h := N_t + (1 / 6) * (F1 + 2 * F2 + 2 * F3 + F4);
        N_t := N_t_h;
        time := time + h ;
        time_for_registration := time_for_registration + h ;

   until (time > time_Q) ;

End_1:
     Close(FileVar1);
```

```
{after opening of the Q-modulator}

  h := 1*1E-10 ;    {s}

   Assign(FileVar1,'C:\franz\Q_opened.txt');
   Rewrite(FileVar1);
   Assign(FileVar2,'C:\franz\Eout.txt');
   Rewrite(FileVar2);

    N_t := N_t_h;
    q_t := 1;
    time:= time_Q;
    Eout := 0; Pout := 0; Pout_max_Nd := 0;
    T := Q_modulator_open(time);
    Re := sqr(T)*R2;
    gama2 :=-ln(Re);
    gama := 0.5*(gama1+gama2) + gamai;
    Tau_c := Lprim/(Co*gama);
    Write(FileVar1,(time*1E+6));  {microseconds }
    Write(FileVar1,R_p(time));
    Write(FileVar1,N_t);
    Write(FileVar1,gama);
    Write(FileVar1,Pout);
    Write(FileVar1,T);
    Writeln(FileVar1,N_t*sigma21);
  repeat
      If KeyPressed Then GoTo End_2;
      Re := sqr(Q_modulator_open(time))*R2;
      gama2 :=-ln(Re);
      gama := 0.5*(gama1+gama2) + gamai;
      Tau_c := Lprim/(Co*gama);

   If (time_for_registration >= 1*h)  Then
      Begin
        Writeln(time*1E+6:5:5, '    ', q_t,'    ', N_t);
        Write(FileVar1,(time*1E+6));  {microseconds}
        Write(FileVar1,R_p(time));
        Write(FileVar1,(N_t));
        Write(FileVar1,gama);
        Write(FileVar1,Pout);
        Write(FileVar1,Q_modulator_open(time));
        Writeln(FileVar1,N_t*sigma21);
        time_for_registration := 0;
      End;
```

```
        F1 := h * f_t(N_t, q_t, time);
        G01 := h * g_t(N_t, q_t);

        F2 := h * f_t(N_t + 0.5 * F1, q_t + 0.5* G01, time + 0.5*h);
        G02 := h * g_t(N_t + 0.5 * F1, q_t + 0.5 * G01);

        F3 := h * f_t(N_t + 0.5 * F2, q_t + 0.5* G02, time + 0.5*h);
        G03 := h * g_t(N_t + 0.5 * F2, q_t + 0.5 * G02);

        F4 := h * f_t(N_t + F3, q_t + G03, time + h);
        G04 := h * g_t(N_t + F3, q_t + G03);

        N_t_h := N_t + (1 / 6) * (F1 + 2 * F2 + 2 * F3 + F4);
        q_t_h := q_t + (1 / 6)*(G01 + 2 * G02 + 2 * G03 + G04);

        If q_t_h < 1 Then
        q_t_h := 1;

        Pout := (h_Plank*Co/Lambda) * (Co*gama1)/(2*Lprim) * q_t_h;  {W}
        if (Pout_max_Nd < Pout) Then  Pout_max_Nd := Pout;
        Eout := Eout + Pout * h;                                     {J}

        N_t := N_t_h;
        q_t := q_t_h;
        time := time + h ;
        time_for_registration := time_for_registration + h;

  until (time > ( time_Q + 70*1E-9));

End_2:
      Close(FileVar1);
      {end of the calculation for Nd:YAG}
      Writeln(FileVar2, Eout, Pout_max_Nd);
      Close(FileVar2);
End_0:
      Writeln;
      Repeat
      Until Keypressed;
END.
```